การจำลองระบบผลิตไฟฟ้าจากเซลล์แสงอาทิตย์
สำหรับการวิเคราะห์ผลกระทบจากการบังแสงอาทิตย์

นายสันติสุข ผิวท่อนคำ

วิทยานิพนธ์นี้เป็นส่วนหนึ่งของการศึกษาตามหลักสูตรปริญญาวิศวกรรมศาสตรมหาบัณฑิต
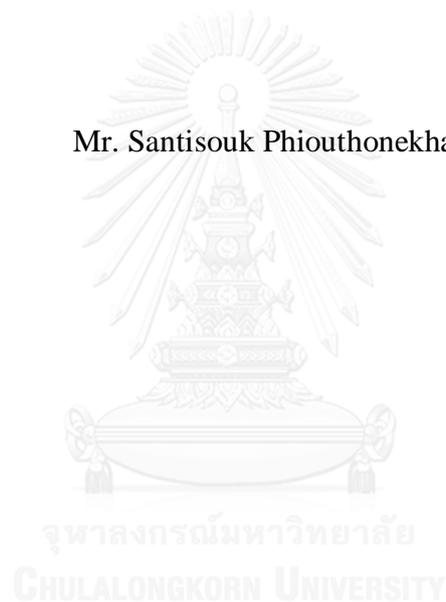สาขาวิชาวิศวกรรมไฟฟ้า ภาควิชาวิศวกรรมไฟฟ้า
คณะวิศวกรรมศาสตร์ จุฬาลงกรณ์มหาวิทยาลัย
ปีการศึกษา 2557
ลิขสิทธิ์ของจุฬาลงกรณ์มหาวิทยาลัย

MODELING OF PHOTOVOLTAIC GENERATION SYSTEM
FOR SHADING IMPACT ANALYSIS

Mr. Santisouk Phiouthonekham

A Thesis Submitted in Partial Fulfillment of the Requirements

for the Degree of Master of Engineering Program in Electrical Engineering

Department of Electrical Engineering

Faculty of Engineering

Chulalongkorn University

Academic Year 2014

Thesis Title	MODELING OF PHOTOVOLTAIC GENERATION SYSTEM FOR SHADING IMPACT ANALYSIS
By	Mr. Santisouk Phiouthonekham
Field of Study	Electrical Engineering
Thesis Advisor	Assistant Professor Surachai Chaitusaney, Ph.D.

Accepted by the Faculty of Engineering, Chulalongkorn University in Partial Fulfillment of the Requirements for the Master's Degree

.... Dean of the Faculty of Engineering
(Professor Bundhit Eua-arporn, Ph.D.)

THESIS COMMITTEE

.... Chairman
(Assistant Professor Thavatchai Tayjasanant, Ph.D.)
.... Thesis Advisor
(Assistant Professor Surachai Chaitusaney, Ph.D.)
.... Examiner
(Assistant Professor Sotdhipong Phichaisawat, Ph.D.)
.... External Examiner
(Chakphed Madtharad, Ph.D.)

สันติสุข ผิวท่อนคำ : การจำลองระบบผลิตไฟฟ้าจากเซลล์แสงอาทิตย์สำหรับการวิเคราะห์ผลกระทบจากการบังแสงอาทิตย์ (MODELING OF PHOTOVOLTAIC GENERATION SYSTEM FOR SHADING IMPACT ANALYSIS) อ.ที่ปรึกษาวิทยานิพนธ์หลัก: ผศ. ดร.สุรชัย ชัยทัศนีย์, 106 หน้า.

ปัจจุบันพลังงานไฟฟ้าเป็นหนึ่งในปัจจัยสำคัญต่อการพัฒนาต่างๆ เช่น เศรษฐกิจ, การศึกษา, การขนส่ง, การสื่อสาร เป็นต้น ส่งผลให้ความต้องการพลังงานไฟฟ้าทั่วโลกเพิ่มสูงขึ้นอย่างต่อเนื่อง และถึงแม้ว่าแหล่งพลังงานไฟฟ้าจะมีอยู่มากมายหลากหลายรูปแบบ แต่ก็ยังเป็นแหล่งพลังงานที่ไม่ปลอดภัยและเป็นอันตรายต่อสิ่งมีชีวิตและสิ่งแวดล้อม เช่น พลังงานนิวเคลียร์ เป็นต้น อีกทั้งยังเป็นแหล่งพลังงานที่ไม่ยั่งยืน ไม่เหมาะที่จะนำมาใช้เป็นแหล่งพลังงานในอนาคต เช่น พลังงานฟอซซิล เป็นต้น

แต่ในทางตรงข้าม พลังงานทางเลือก เช่น พลังงานลม พลังงานชีวมวล และพลังงานแสงอาทิตย์ จึงเป็นอีกตัวเลือกหนึ่งที่เหมาะสมที่จะนำใช้สำหรับแหล่งพลังงานในอนาคต จากแหล่งพลังงานทางเลือกทั้งหมด พลังงานแสงอาทิตย์เป็นแหล่งพลังงานที่นิยมมากที่สุด เพราะว่าเป็นแหล่งพลังงานที่มีอยู่อย่างไม่จำกัด และเป็นมิตรต่อสิ่งแวดล้อมมากที่สุดเมื่อเปรียบเทียบกับแหล่งพลังงานทางเลือกอื่นๆ นอกจากนี้ เซลล์แสงอาทิตย์ที่ใช้สำหรับการเปลี่ยนแปลงพลังงานแสงไปเป็นพลังงานไฟฟ้ายังสามารถติดตั้งได้ง่ายและหลากหลายพื้นที่ ตราบใดก็ตามที่พื้นที่นั้นๆ มีแสงอาทิตย์ที่เพียงพอ เช่น หลังคาบ้านเรือน และที่อยู่อาศัย หรือแม้กระทั่งผนังอาคารต่างๆ

ดังนั้นวิทยานิพนธ์นี้จึงนำเสนอเกี่ยวกับแบบจำลองเซลล์แสงอาทิตย์ ผลกระทบการบังแสงแดดที่มีผลต่อระบบผลิตไฟฟ้าจากเซลล์แสงอาทิตย์ และนำเสนอแนวคิดการจัดเรียงโมดูลเซลล์แสงอาทิตย์ และการปรับตั้งมุมเอียงและมุมทิศที่เหมาะสม เพื่อลดผลกระทบจากการบังแสงแดดที่เกิดขึ้นบนระบบผลิตไฟฟ้าจากเซลล์แสงอาทิตย์

ภาควิชา	วิศวกรรมไฟฟ้า	ลายมือชื่อนิสิต
สาขาวิชา	วิศวกรรมไฟฟ้า	ลายมือชื่อ อ.ที่ปรึกษาหลัก
ปีการศึกษา	2557	

5670516021 : MAJOR ELECTRICAL ENGINEERING

KEYWORDS: PHOTOVOLTAIC MODEL / PHOTOVOLTAIC ARRAY CONFIGURATION / PARTIAL SHADING / MULTIPLE MAXIMUM POWER POINT / MAXIMUM POWER POINT TRACKING / REARRANGEMENT / APPROXIMATE TILTED AND AZIMUTH ANGLE

SANTISOUK PHIOUTHONEKHAM: MODELING OF PHOTOVOLTAIC GENERATION SYSTEM FOR SHADING IMPACT ANALYSIS. ADVISOR: ASST. PROF. SURACHAI CHAITUSANEY, Ph.D., 106 pp.

At present, electrical energy is very important for the development of economy and living, such as education, transportation, communication, etc. The demand for electrical energy worldwide is increasing year by year. Although there are a variety of electrical energy sources, some of them are unsafe for humans and environment (nuclear power), not sustainable for the long future (fossil thermal power).

In contrast, renewable energy sources, such as wind, biomass, photovoltaic, etc., are sustainable and environment-friendly. Among these sources, solar energy has been intensively promoted because it is prevailing wherever the sun is shining and it is the most environmentally friendly compared with other energy sources. Additionally, photovoltaic modules and plants for converting solar energy into electrical energy are easily installed at various places where the sunlight is available such as roof tops and wall sides of buildings, and farms.

This research examines the decrease of solar power caused by various shading patterns. Then, the arrangement of PV modules in order to mitigate the impact of shading and to optimize the maximum power point tracking is proposed. After that, shading patterns with appropriate tilted angle and azimuth are simulated to show the improvement in power generation.

Department:	Electrical Engineering	Student's Signature _____
Field of Study:	Electrical Engineering	Advisor's Signature _____
Academic Year:	2014	

ACKNOWLEDGEMENTS

CONTENTS

LIST OF TABLES

LIST OF FIGURES

Chapter 1

Introduction

1.1 Problem Statement

At present, electrical energy is very important for the development of economy and living, such as education, transportation, communication, etc. The demand for electrical energy worldwide has increased steadily. Although there are a variety of electrical energy sources, some of them are unsafe for humans and environment (nuclear power), not last for the long future (fossil thermal power), or being exploited (hydro power).

In contrast, renewable energy sources, such as wind, biomass, photovoltaic, etc., can be utilized longer because they can be replaced whenever they are used up. Among these renewable energy resources, the photovoltaic (PV) energy has been intensively promoted because it is prevailing wherever the sun is shining and it is the most environmental friendly compared with other energy sources[1]. Additionally, PV energy is easily to install at various places which can receive the sunlight such as roof tops, building wall sides, and farms. According to the Energy Information Administration (EIA) for world market energy consumption, Figure 1.1 demonstrates an increase in the PV energy supplies project over the period 1980-2030. In addition, Figure 1.2 presents the evolution of world production of PV cells. It can be seen that the number of production in megawatt peak (MWp) has been increasing. This means the number of the PV installation will be higher for generating energy to meet the electrical load demand.
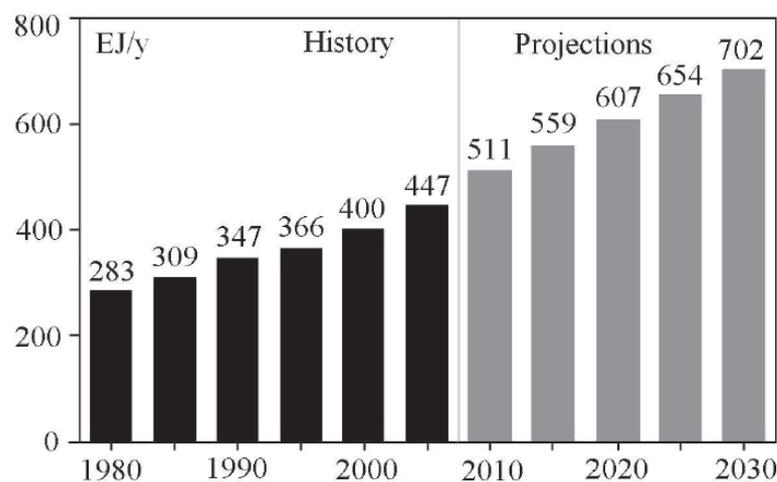
Figure 1.1.World marketed energy consumption, 1980–2030

(*Source:* Energy Information Administration (EIA), official energy statistics from U.S. government. History: *International Energy Annual 2004* (May–July 2006), website www.eia.doe.gov/iea. Projections: EIA, *International Information Outlook 2007*).
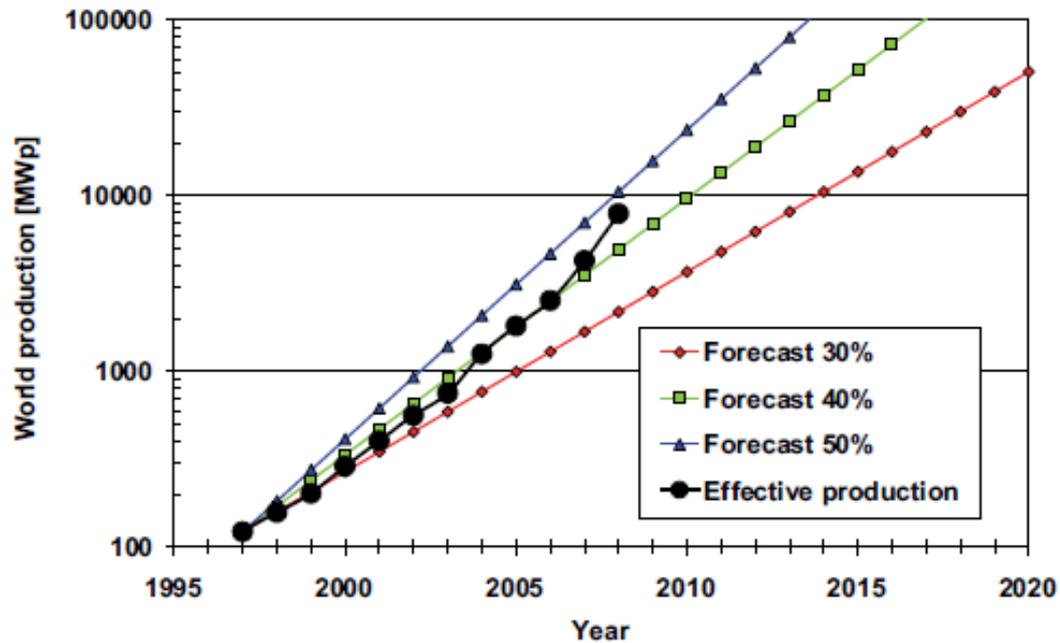
Figure 1.2. Evolution of World Production of Solar Cells

Indeed, PV modules generate electrical power by receiving the sunlight that contains solar energy [2]. Then, it is converted into electrical energy as direct current (DC). This current is inverted to alternative current (AC) by using inverter technologies [3]. Finally, the power is delivered from the inverter through electrical wires to supply power consumers.

Generally, many factors can affect the power production of PV modules including the intensity of sunlight, the environmental weather such as a temperature, the shading on PV modules such as from building, trees, moving clouds, and PV modules (panels) themselves. These shading types will decrease the power produced from the PV system. The final factor is the tilted angle and azimuth of installation. An appropriate tiled angle and azimuth can help PV modules receive more solar irradiation. Subsequently, more power could be generated [4]-[5]. Sometimes, the decrease of power may be caused by dust covering the PV modules. Basically, the power generated from PV modules is characterized to have a single maximum power point (MPP) [6] as shown in Figure 1.3 that is from a simulation of 15° of tilted angle and 40° of azimuth. For 15°, PV modules are installed by tiled surface. For 40°, PV modules are installed to direct in the southwest. However, with the shading effects, the power generated from PV modules may be characterized to have multiple maximum power point (MPPs) as shown in Figure 1.4 [7]. The characterization is dependent on the shading pattern over the PV modules.
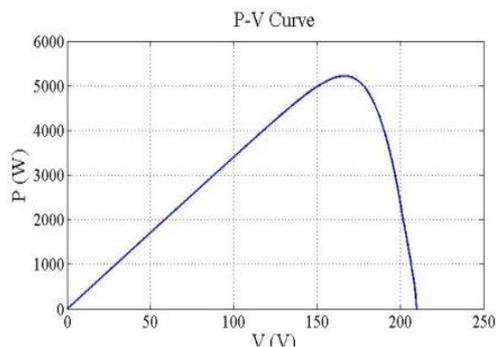
Figure 1.3. The relation between voltage and power without shading effect
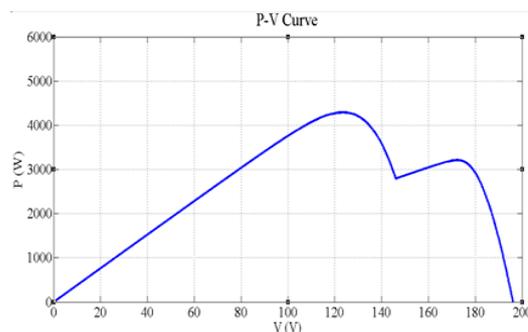
Figure 1.4. The relation between voltage and power with shading effect

The relationship between voltage and power in Figure 1.3 is characterized to have single maximum power point (MPP) at 5,219 W. Whereas, the relationship in Figure 1.4 is characterized to have the multiple maximum power point (MPPs) at 4,627 W and 3,425 W, which is resulted from the shading effect. The controlling system of the inverter will optimize (maximize) the power generation at 4,627 W. Moreover, PV modules are installed at appropriate tilted angle and azimuth. The tiled angle and azimuth are installed at 13.48° and 0°, respectively. For 13.48°, PV modules are installed by tiled surfaced. For 0° PV modules are installed to direct in the south. The PV modules can generate more power as shown in Figure 1.5, which is characterized to have multiple maximum power point (MPPs) at 5,232 W and 4,874 W.
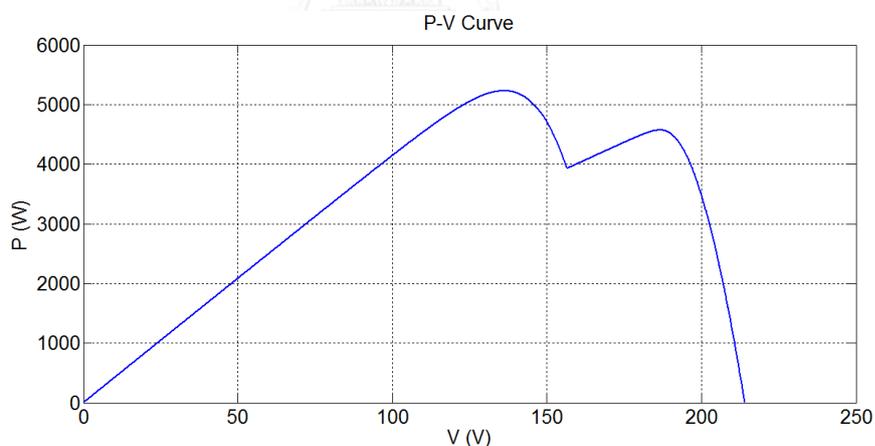
Figure 1.5. The relation between voltage and power for appropriate angle with shading effect

In conclusion, the shading pattern can impact the power generation, system operation, and efficiency. Therefore, an approach to mitigate the shading impact on PV modules is proposed in the next chapters. This research examines the decreasing characteristic of power from other shading patterns. Then, the arrangement of PV modules in order to mitigate the impact of shading and optimize the maximum power point tracking (MPPT) is proposed. After that, shading patterns with appropriate tilted angle and azimuth are simulated to show an increase in generated power. Furthermore, this research determines the advantage of bypass diode for preventing the reverse power flow.

1.2 Objective

Two objectives of this research are to mitigate the impact of partial shading on PV modules and to change the multiple maximum power points (MPPs) to single maximum power point (MPP).

1.3 Scope of Works

This research is limited by the following scopes:

1) The work focuses on the partial shading of PV array, the effect of temperature, and irradiation on PV modules.

2) The work focuses on the PV module arrangement so that the multiple maximum power points (MPPs) are reduced to be single maximum power point (MPP).

3) The conditions of shading are considered as follows:

The cloud size: to consider the cloud shapes and dimensions.

The moving cloud: to consider the speed of moving cloud.

4) An appropriate tiled angle and azimuth can help PV modules receive the amount of solar irradiance and increase power generation.

5) The approach and step examine on the real experiment at PV farm.

6) The experiment from real farm with shading on PV array: the results will be compared with Matlab simulation.

1.4 Methodology

1) To review literatures on the fundamental below:

o Photovoltaic generation technologies and modeling.

o The impact of the temperature and irradiation to the PV generation.

o Photovoltaic array with the effect of shading and efficiency.

o The advantage of shading on string of PV array configuration.

o The effect of the bypass diode on prevention the reverse power flow on PV module shading.

2) To identify the specific objectives and scope of study.

3) To determine the proper solution method.

4) To collect the relevant historical data.

5) To establish and test the mathematical models of system components.

6) To develop computer programs to analyze the problem.

7) To simulate, evaluate, and verify the results.

8) To draw conclusions and complete relevant documents for publication and thesis report.

1.5 Expected Benefits

This thesis is aimed to provide a background understanding as the impacts of partial shading on the PV array generation and the appropriate tiled angle and azimuth angle surface for PV module installation. The utilities and the PV owners can consider this approach to practice on their works. It is expected that the installation and mobilization of PV transaction will become more efficient. Especially, the PV farms should be integrated to gain the maximum benefits because this study focuses on the PV farm where the research can help make the right decision in choosing the location and correcting tiled angle and azimuth angle surface of the PV farm.

In addition, the PV array shading generation is established through the research. Hence, this approach can be practiced to other studies related to the PV array arrangement.

Chapter 2

Fundamental of Photovoltaic (PV)

2.1 Literature Review

This literature review can be categorized into 4 parts. Firstly, model of photovoltaic is studied. Secondly, the factors such as temperature and sunlight which impact on PV modules are considered. Thirdly, effects of shading on PV generation are analyzed. Finally, impacts of shading on PV array configuration are studied along with some proposals.

2.1.1 Model of Photovoltaic Cell

There have been lots of research on modeling photovoltaic cell based on differently desired objectives. The authors of [8]-[9] proposed a single-diode model with the consideration of shunt resistance. This model caused some mistakes because it did not concern the series resistance inside. To fulfil this lack, this thesis considers a model of PV cell with shunt and series resistance to improve the accuracy. In addition, such model is not complex and is comfortable to compare with the double diode model that has been proposed by other researchers [10]-[11].

2.1.2 Impacts of Temperature and Sunlight Intensity on PV Panels

Impacts of temperature and sunlight intensity on the PV panels were considered in [12]-[13] for maximum power point tracking (MPPT). These papers revealed the relation among voltage, current and power generation with various sizes of shunt and series resistance. By studying on a mathematical model, authors in [14] found out the impact of light intensity and temperature on the relationships among voltage, current and power. Moreover, the principle of how to model PV cells in order to generate the maximum power output was discussed in [15].

2.1.3 Effects of Shading on PV Generation

The effect of sunlight on PV cells, which consisted of series and parallel modules in connection [16] was considered. Generally, the PV system can process finding the maximum power point (MPP) without shading. But, the processing system cannot find the MPP under shading condition because the shading on PV cells causes multiple maximum power point (MPPs). Obviously, solar photovoltaic array has the non-linear V-I and V-P characteristics when using the uniform solar irradiance [17]. The relationship between voltage (V) and power (W) characteristics becomes more complex with MPPs when the PV array is operated under partial shaded condition [18]. For example, the MPP is trapped when tracking power. Otherwise, [19] studied the relation between voltage and current on shading and mitigated the power reduction by using across bypass diode. Other researchers used simulation to obtain results for comparing with results of real experiments [20]-[21]. They included cases of shaded and unshaded conditions which were the environmental factors.

2.1.4 Impacts of Shading on PV Array Configuration

It was found that the arrangement of a new structure could reduce the effects of partial shading. There have been a number of approaches to decrease the effects from shading [22]-[23]. Authors of [24] presented method of reducing the sunlight effect on PV module by using shunt-series compensation. PV array connection (series and parallel connection configuration) was studied in [25] with consideration of voltage and current to produce the highest power generation or MPP. A method to mitigate effects of shading by installing the across bypass diode on PV modules connection was proposed in [26]. Using a centralized inverter [27] is another option to arrange a new structure for maximizing power.

2.2. Photovoltaic Generation

2.2.1. Overview of Solar Photovoltaic Technology

Solar photovoltaic technology is used to generate electricity from sunlight by using semiconductors that exhibit the PV effects and DC-AC inverter systems. PV panels are composed of a high quantity of solar cells which play an important role in converting solar radiation into direct electrical current. The main materials utilized for manufacturing PV cells contain polycrystalline silicon, mono crystalline silicon, cadmium telluride, amorphous silicon, and copper indium gallium selenite as shown in Figure 2.1. When these special materials are under the sunlight, photons of light with suitable wavelength and energy can cause some electrons in covalent bonds to break of their atoms and they move freely throughout the crystal. If an electric field is supplied, those electrons can move in a certain direction, i.e. generating a direct electric current. Then, DC-AC inverters transform the generated DC power into standard AC power before delivering to utility grids. PV arrays can be dispersedly integrated on the roofs or walls of buildings, or they can be constructed as a small power plant. By the end of 2014, the 100 GW solar power capacity had been installed around the world, in more than 100 countries [28]. With the efficient development of PV technologies demonstrated in Figure 2.2, the competition between manufacturers and the financial incentives from responsible organizations, the cost of PV panels has decreased steadily leading to the increasing penetration of PV in power systems. Due to many global problems such as climate changes, greenhouse effects and the depletion of fossil fuels, this renewable energy source is being expected to become an efficient solution for power industry in the near future.

The PV generated electrical power strongly depends on solar irradiance and ambient temperature, which are intermittent variables. As a result, the PV system delivers an uncertain amount of power into the grid causing some troubles of maximum power point tracking (MPPT). For instance, the shading reduces the amount of power generation. However, a new arrangement of PV strings can alleviate that reduction. For example, when a PV array is shaded on some modules, strings can be rearranged to escape the shade. Therefore, many researches have been conducted to explore the impacts of PV shading on power systems; from that, the positive effects are exploited absolutely while the negative ones are limited.

Figure 2.1. Semiconductor solar cells

(Ref: Google.co.th: Silicon solar module picture)
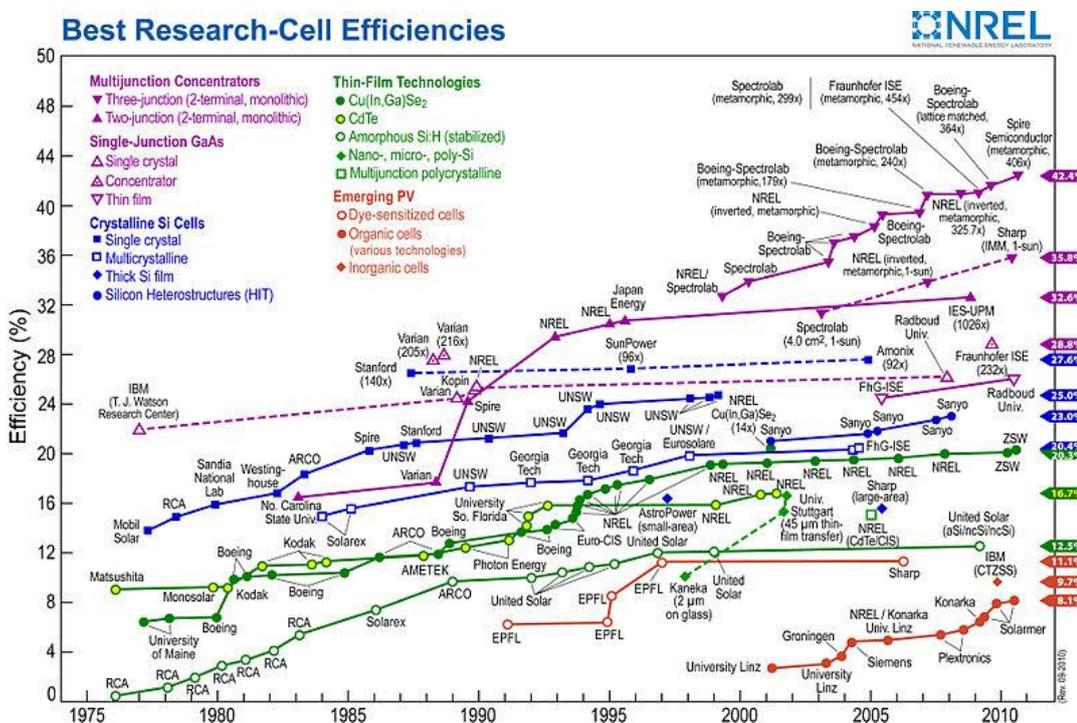
Figure 2.2. The solar cell efficiency for each material

(Ref: http://www.nrel.gov/ncpv/images/efficiency_chart.jpg)

2.2.2 PV Generation Model

For analyzing a power system with PV generations, it is necessary to formulate a mathematical model of solar cells to reflect their electrical behavior. Over the years, the PV model has been established by using the circuit-based method [29]. The simplest equivalent circuit consists of an ideal current source, a series resistance R_s, a shunt resistance R_{sh} and a real diode connected in parallel. The current source is assumed to generate a current in proportion to the solar intensity so that the relationship between solar energy and electricity is depicted. On the other hand, the diode represents a physical essence of a PV cell that is a p-n junction.

To study the PV generation, the model of a PV module is illustrated by an equivalent circuit containing a diode as shown in Figure 2.3 ("single-diode model") [30].
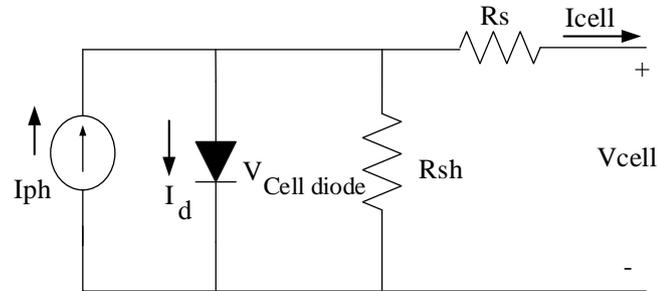
Figure 2.3. The equivalent circuit of a single diode on cell

Because the equivalent circuit of a single diode uses the Kirchhoff's current and voltage Laws (KCL, KVL), the cell current can be calculated by (2.1) [31].

$$I_{cell} = I_{ph} - I_D - I_{Rsh} \tag{2.1}$$

In (2.1):

I_{cell} Cell current (A)
I_{ph} Photoelectric current (A)
I_D Current flowing through diode (A) defined by (2.2)
I_{Rsh} Current flowing through the shunt resistance (R_{sh}) of solar cell (A) defined by (2.3)
V_{cell} Cell voltage

$$I_D = I_o[\exp(\frac{V_D}{aV_{th}}) - 1] \tag{2.2}$$

$$I_{Rsh} = \frac{V_D}{R_{sh}} \tag{2.3}$$

Where:

I_0 Saturation current of the single diode (A)
V_D Diode voltage (V)
a Factor of diode which depend on material production $a = 1.025$
V_{th} Threshold voltage for cell in single diode (V) defined by (2.4)
R_{sh} Shunt resistance of a single diode (Ω)

$$V_{th} = \frac{KT}{q} \tag{2.4}$$

Where:

K Boltzmann constant, $K = 1.38 \times 10^{-23}$ (J/K)
T Cell temperature (K)
q Elementary electric charge $q = 1.6 \times 10^{-19}$ (C)

Substituting (2.2) for I_D and (2.3) for I_{Rsh} in (2.1) yields (2.5).

$$I_{cell} = I_{ph} - I_o[\exp(\frac{V_D}{aV_{th}}) - 1] - \frac{V_D}{R_{sh}} \qquad (2.5)$$

The diode voltage V_D in Figure 2.1 can be given by (2.6) according to the KCL and KVL.

$$V_D = V_{cell} + I_{cell}R_s \qquad (2.6)$$

where R_s is the series resistance (Ω).

Replacing V_D in (2.5) by the term in (2.6) produces a new equation of the cell current given by (2.7).

$$I_{cell} = I_{ph} - I_o[\exp(\frac{V_{cell} + I_{cell}R_s}{aV_{th}}) - 1] - \frac{V_{cell} + I_{cell}R_s}{R_{sh}} \qquad (2.7)$$

2.2.3 The Effect of Temperature and Light Intensity

Because voltage and power of a PV cell can be affected by temperature and sunlight intensity (irradiation), both these two factors are significant to efficiency of a PV cell.

2.2.3.1 Temperature of Cell

Generally, the solar photovoltaic cells are sensitive to changes in temperature. When temperature increases, the band gap of the semiconductor decreases. Hence the increasing temperature affects the I-V curve of a solar cell. The open-circuit voltage (V_{OC}) is the parameter which is most affected by the temperature variation. When a photovoltaic cell is exposed to a higher temperature, the current short-circuit (Isc) increases slightly, while V_{OC} decreases more significantly.

Higher temperatures lead to a decrease in the maximum power point (MPP) of a solar cell. Since the I-V curve is sensitive to temperature variations, it is necessary to mention the parameters under the I-V curve of a solar cell.

The temperature affects the variation of the open-circuit voltage and the photoelectric current can be expressed by (2.8) and (2.9), respectively.

$$V_{OC} = V_{OC,Tref} + K_V\left(T - T_{ref}\right) \qquad (2.8)$$

$$I_{ph} = I_{ph,Tref} + K_i\left(T - T_{ref}\right) \qquad (2.9)$$

Where:

$I_{ph,Tref}$ Photoelectric current at standard test condition (25˚C) (A)
$V_{oc,Tref}$ Open-circuit voltage at standard test condition (V)
K_i The current temperature coefficient (A/°C)
K_v The voltage temperature coefficient (V/°C)
T_{ref} The reference temperature 25°C and T is temperature (˚C)

For example, parameters of a PV module type SP120 with $V_{oc,Tref}$ = 21.7 V, $I_{ph,Tref}$ = 7.617 A, K_i = 0.003 A/K, K_v = -0.074 V/K, T_{ref} = 25 °C, T = 47.5 °C can be specified as follows.

$$V_{OC,T} = 21.7 + (-0.074)(47.5 - 25) = 20.035V$$

$$I_{ph} = (7.617 + (0.003)(47.5 - 25)) = 7.6845A$$

2.2.3.2 Sunlight Intensity

The irradiance of sunlight is a term used in radiometry; it measures the power of electromagnetic radiation per unit area. It is measured in watt per square meter (W/m^2). In the solar energy, irradiance is referred to as insolation.

The irradiance affects the variation of the photoelectric current and the shunt resistance as shown in (2.10) and (2.11), respectively.

$$I_{ph,G} = I_{ph,Gref} \left(\frac{G}{G_{ref}} \right) \qquad (2.10)$$

$$R_{sh,G} = R_{P,Gref} \left(\frac{G_{ref}}{G} \right) \qquad (2.11)$$

Where:

$I_{ph,G}$ Photoelectric current at irradiance G W/m^2 (A)

$I_{ph,Gref}$ Photoelectric current at standard test condition (1,000 W/m^2) (A)

G_{ref} The reference irradiation of 1,000 (W/m^2)

$R_{P,G}$ Shunt resistance of solar cell at irradiation G W/m^2 (Ω)

$R_{P,Gref}$ Shunt resistance of solar cell at standard test condition (Ω).

For example, at given parameters of $I_{ph,Gref}$ = 7.6845A, $R_{sh,Gref}$ = 198.09Ω, G_{ref} = 1000 W/m^2, and G = 929.25 W/m^2, the photoelectric current and the shunt resistance can be calculated as follows.

$$I_{ph,G} = 7.6845 \times (\frac{929.25}{1000}) = 7.104A$$

$$R_{sh,G} = 198.09 \times (\frac{1000}{929.25}) = 213.171\Omega$$

2.3 Technical Data of Solar Cells

Technical specification of photovoltaic (Commercial data sheet) provides parameters of the solar cell of a manufacturer. These parameters are obtained from laboratory experiments performed by the manufacturer. There are 8 parameters of the basic measurements of the solar cell module. These parameters should be used in the model of a solar cell module to accurately reflect its operation.

The production varies over primary technologies used by each manufacturer. However, the technical data of the individual solar cells are defined similarly in general. Since the parameters derived from the manufacturer are determined by the temperature and sunlight intensity at the Standard Test Condition (STC) which has temperature of 25 °C or 278 K and the sunlight intensity of 1,000 W / m^2. Essential parameters are usually listed as:

1) Maximum power P_{MPP} (W)
2) Maximum power voltage: V_{MPP} (V)
3) Maximum power current: I_{MPP} (A)

4) Open circuit voltage: V_{OC} (V)
5) Short circuit current: I_{SC} (A)
6) Temperature coefficient short circuit: K_i (A/K)
7) Temperature coefficient open circuit: K_v (V/K)
8) Number of cell per module: N_s

Some examples of the technical information are adopted from Solartron Public Company Limited (Poly-crystalline) [32] and Suntech Co., Ltd. (Single-crystalline) [33] as shown in Table 2.1 and Table 2.2, respectively.

Table 2.1. SP120 solar panel from Solartron public company limited

Parameters	Units
Maximum power(P_{MPP})	120 W
Maximum power voltage (V_{MPP})	17.28 V
Maximum power current (I_{MPP})	7 A
Open circuit voltage (V_{OC})	21.7 V
Shot circuit current (I_{SC})	7.45 A
Temperature coefficient of short circuit current (K_i)	0.003 A/K
Temperature coefficient of open circuit voltage (K_v)	-0.074 V/K
Number cell per module (N_s)	36 Cells

Table 2.2.STP 295-24/Ve solar panel from Suntech Power Company limited

Parameters	Unit
Maximum power(P_{MPP})	285 W
Maximum power voltage (V_{MPP})	35.4 V
Maximum power current (I_{MPP})	8.06 A
Open circuit voltage (V_{OC})	44.9 V
Shot circuit current (I_{SC})	8.37 A
Temperature coefficient of short circuit current (K_i)	0.055 A/°C
Temperature coefficient of open circuit voltage (K_v)	-0.33 V/°C
Number cell per module (N_s)	72 Cells

Table 2.1 provides many parameters for SP120. Additionally, these values can be used to illustrate the relation among the current, voltage and power as shown in Figure 2.4.
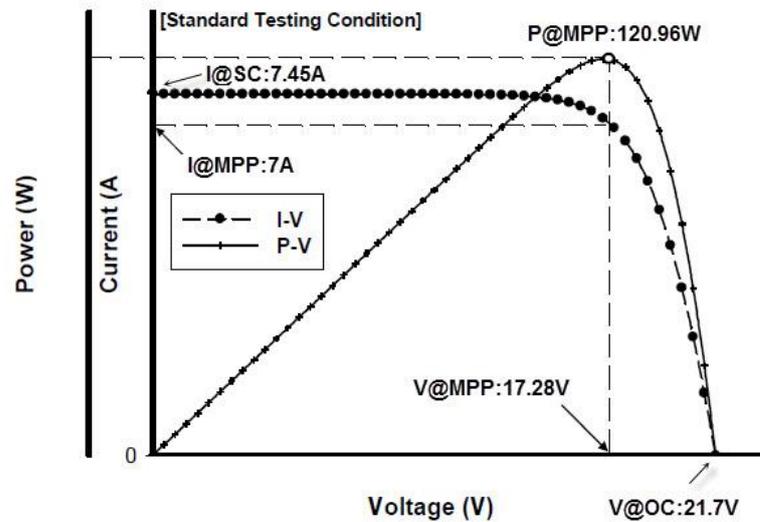
Figure 2.4. Relationship among I, V and P for SP120

Generally, a PV module consists of a number of individual solar cells connected together. Therefore, the parameters listed in Tables 2.1 and 2.2 are supposed to characterize a PV module as well. The equivalent circuit of a solar PV cell in Figure 2.3 can represent a PV module with some adaptations as shown in Figure 2.5.
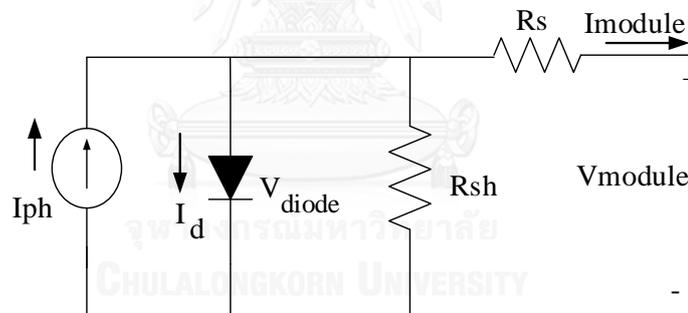
Figure 2.5. The equivalent circuit of a PV module

The relationship between current and voltage for a PV module can be expressed as (2.12).

$$I_{module} = I_{ph} - I_0 \left[\exp\left(\frac{V_{module} + I_{module}R_S}{aN_SV_{th}} \right) - 1 \right] - \frac{V_{module} + I_{module}R_S}{R_{sh}} \qquad (2.12)$$

Where:

I_{module} Module current (A)
V_{module} Module voltage (V)
V_{th} Threshold voltage for cell in single diode (V) defined by (2.4)
I_o Saturation current (A)
R_S Series resistance in module (Ω)
N_s Number of cells in series connection of a module
a Diode Factor (depending on material), $a = 1.025$

For example, if I_{ph} = 7.104 A, I_0 = 8.66x10^{-6} A, a = 1.02, V_{th} = 0.0276 V, R_{sh} = 213.182 Ω, R_s = 0.158 Ω, Ns = 36 cells, G = 929.25 W/m^2, and the temperature is 47.5 °C, some operation points of a PV module are calculated and listed in Table 2.3.

Table 2.3. The current, voltage and power of a PV module

I_{module} (A)	V_{module} (V)	P_{module} (W)
7.14	0.00	0.00
7.14	0.05	0.36
7.14	0.10	0.71
7.14	0.20	1.43
7.14	0.30	2.14
7.14	0.40	2.86
7.14	0.50	3.57
7.14	0.60	4.28
7.14	0.70	5.00
7.14	0.80	5.71
7.14	0.90	6.42
7.14	1.00	7.14
7.13	2.00	14.26
7.13	3.00	21.38
7.12	4.00	28.49
7.12	5.00	35.59
7.11	6.00	42.68
7.11	7.00	49.75
7.10	8.00	56.80
7.09	9.00	63.83
7.08	10.00	70.80
7.06	11.00	77.65
7.02	12.00	84.23
6.94	13.00	90.25
6.79	14.00	94.99
6.76	14.10	95.35
6.74	14.20	95.67
6.71	14.30	95.97
6.68	14.40	96.23
6.65	14.50	96.45
6.62	14.60	96.63
6.58	14.70	96.77
6.54	14.80	96.86
6.50	14.90	96.90

I_{module} (A)	V_{module} (V)	P_{module} (W)
6.46	14.99	96.89
6.46	15.00	96.89
5.78	16.00	92.45
4.35	17.00	73.95
1.35	18.00	24.29
0.91	18.10	16.43
0.43	18.20	7.86
0.00	18.29	0.00

In Table 2.3, when temperature and irradiance change, the PV module generates new values of current, voltage, and power (e.g., I_{module} = 6.50 A, V_{module} = 14.9 V and P_{module} = 96.90 W). The relationship among them have been demonstrated in Figures 2.6 and 2.7, respectively.
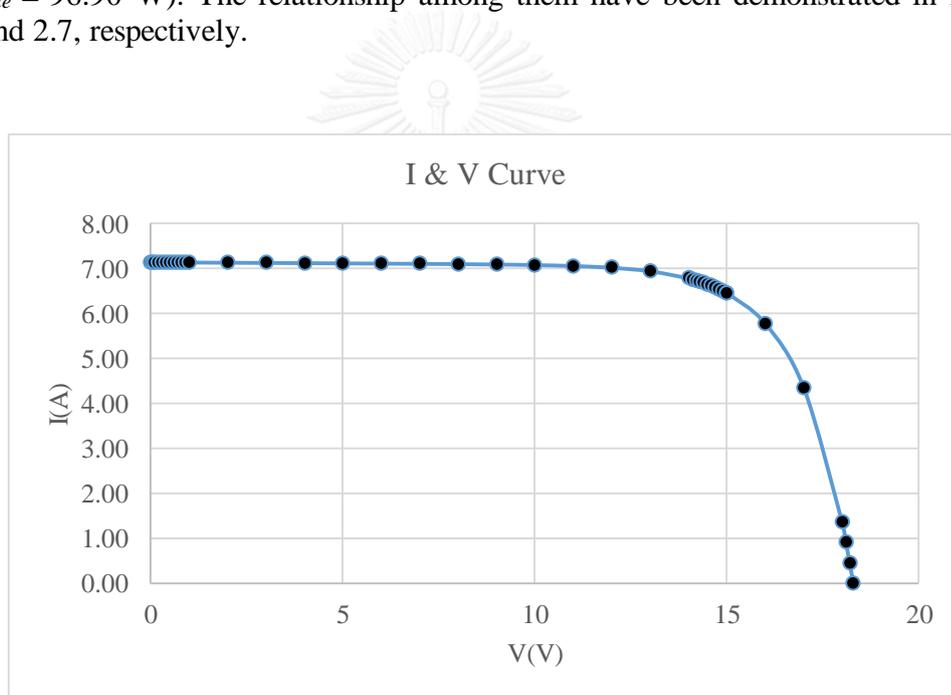
Figure 2.6. The relation between voltage and current of a PV module
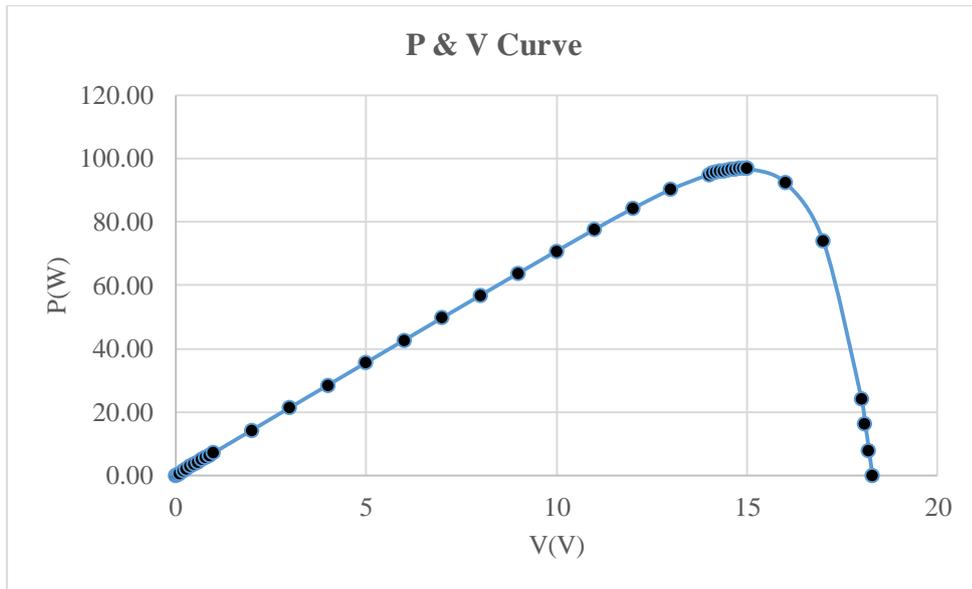
Figure 2.7. The relation between voltage and power of a PV module

2.4 Configurations of PV cell, PV Module and PV Array

A solar cell can produce voltage up to 0.5-0.7 V for using in real work. A PV module consists of 36 cells in series is called "12-V module" even that this module can generate voltage higher than 12 V [34].

PV Cell   PV Module   PV Array
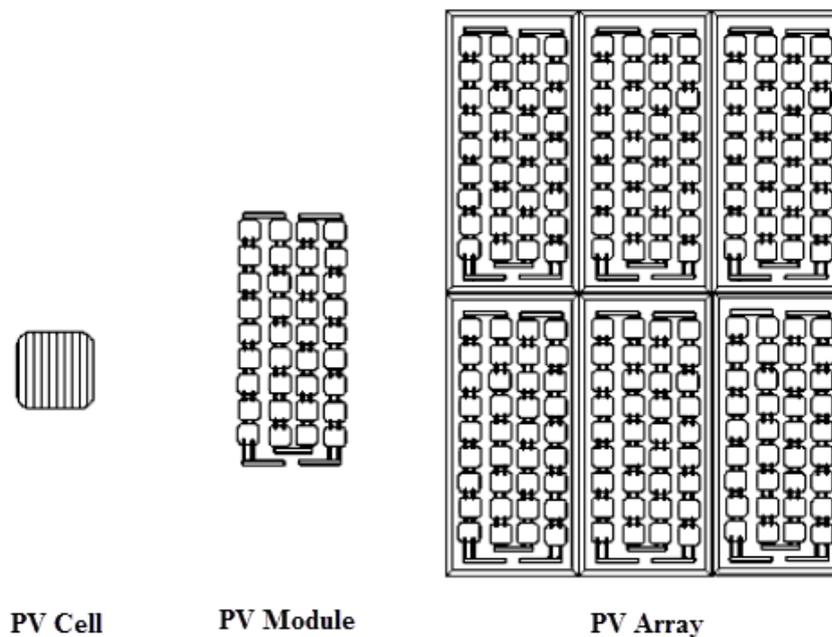
Figure 2.8. Configurations of PV cell, PV module, and PV array

(Ref: Book at page 39/ Green Energy and Technology/Ramchandra Pod and Boucar Diouf)

When some PV modules are connected in series, the generated voltage is higher. Whereas, a parallel connection of some PV modules can produce higher current. These

connections are illustrated in Figure 2.9 and Figure 2.10, respectively. In fact, a number of PV modules are connected both in series and parallel to form a PV array for generating power and interconnecting to power systems as shown in Figure 2.8.
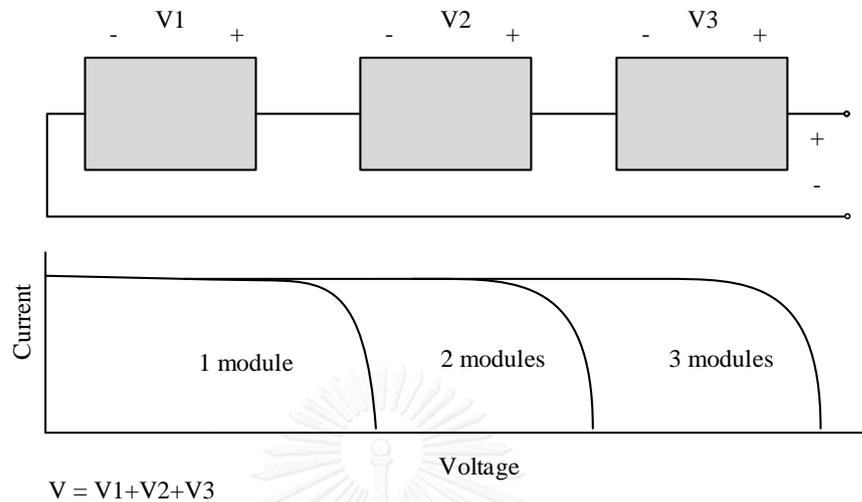
Figure 2.9. Illustration of voltage and current in series connection
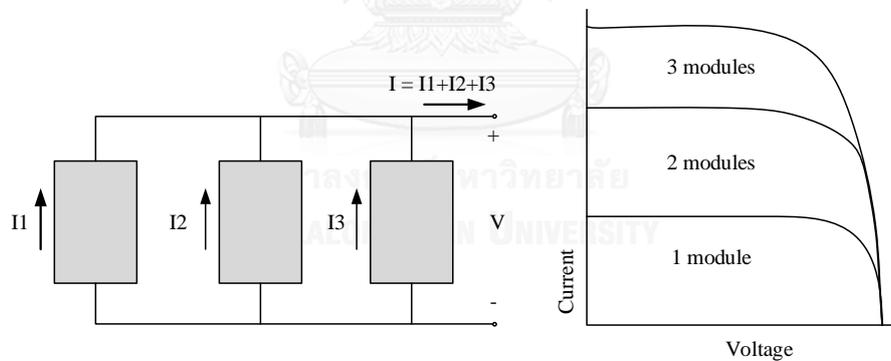
Figure 2.10. Illustration of voltage and current in parallel connection

2.5 Method for Parameter Estimation and Example of Calculation

This section presents basic calculation of some parameters for a PV module. It provides adequate parameters to develop a PV model of solar cells. An example of finding parameters will be illustrated. Then, the result will be compared with real experiment (data recorder at the Engineering Building 4 located inside Chulalongkorn University Campus) of a PV array with 10 modules in series connection. The type of PV module is SP120.

2.5.1 Parameter Estimation Method

Basically, a PV module is characterized by 8 parameters as shown in Table 2.1 and Table 2.2. These parameters are necessary to process of decreasing and increasing

power on the PV module. Besides, there are 4 parameters which are provided to use for preparing calculation. They are as follows.

1) Saturation current: I_o

The saturation current is given by (2.13).

$$I_o = \frac{I_{sc} + K_i(T - T_{stc})}{\exp\left(\dfrac{V_{oc} + K_v(T - T_{stc})}{aN_sV_{th}}\right) - 1} \tag{2.13}$$

2) Photoelectric current: I_{ph}

The photoelectric current is given by (2.14).

$$I_{ph} = \frac{R_{sh} + R_s}{R_{sh}} I_{sc} \tag{2.14}$$

3) Shunt resistance: R_{sh}

The shunt resistance is computed by (2.15).

$$R_{sh} = \frac{V_{MPP} + I_{MPP}R_s}{I_{ph} - I_o\left[\exp\left(\dfrac{V_{MPP} + I_{MPP}R_s}{aN_sV_{th}}\right) - 1\right] - I_{MPP}} \tag{2.15}$$

4) Series resistance: R_s

The series resistance is computed by (2.16).

$$R_s = \frac{V_{MPP}}{I_{MPP}} - \frac{aN_sV_{th}R_{sh}}{I_oR_{sh}\exp\left(\dfrac{V_{MPP} + I_{MPP}R_s}{aN_sV_{th}}\right) + aN_sV_{th}} \tag{2.16}$$

2.5.2 Example of Calculation

An array of 2 PV modules in series connection is depicted in Figure 2.11. Parameters of SP120 have been introduced in Table 2.1. The calculation here assumes irradiation of 929.25 W/m² and cell temperature of 47.5 ℃. This information was recorded at the rooftop of Engineering Building 4, in August of 2014 at 12:30 PM.
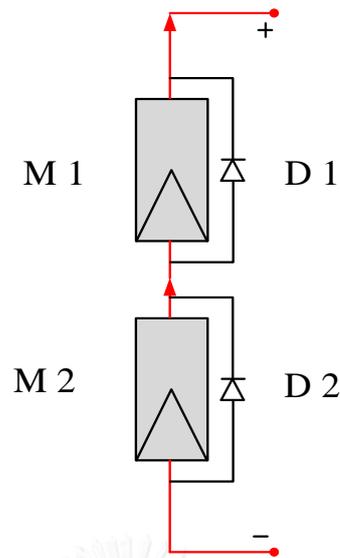
Figure 2.11. An array with 2 PV modules

Table 2.4. Estimated parameters of the array with 2 PV modules

I_{module} (A)	V_{module} (V)	P_{module} (W)	$I_{modules}$ (A)	$V_{modules}$ (V)	$P_{modules}$ (W)
7.14	0.00	0.00	7.14	0.00	0.00
7.14	0.05	0.36	7.14	0.10	0.71
7.14	0.10	0.71	7.14	0.20	1.43
7.14	0.20	1.43	7.14	0.40	2.86
7.14	0.30	2.14	7.14	0.60	4.28
7.14	0.40	2.86	7.14	0.80	5.71
7.14	0.50	3.57	7.14	1.00	7.14
7.14	0.60	4.28	7.14	1.20	8.57
7.14	0.70	5.00	7.14	1.40	9.99
7.14	0.80	5.71	7.14	1.60	11.42
7.14	0.90	6.42	7.14	1.80	12.85
7.14	1.00	7.14	7.14	2.00	14.27
7.13	2.00	14.26	7.13	4.00	28.53
7.13	3.00	21.38	7.13	6.00	42.76
7.12	4.00	28.49	7.12	8.00	56.98
7.12	5.00	35.59	7.12	10.00	71.18
7.11	6.00	42.68	7.11	12.00	85.35
7.11	7.00	49.75	7.11	14.00	99.50
7.10	8.00	56.80	7.10	16.00	113.61
7.09	9.00	63.83	7.09	18.00	127.66
7.08	10.00	70.80	7.08	20.00	141.59
7.06	11.00	77.65	7.06	22.00	155.29
7.02	12.00	84.23	7.02	24.00	168.47

I_{module} (A)	V_{module} (V)	P_{module} (W)	$I_{modules}$ (A)	$V_{modules}$ (V)	$P_{modules}$ (W)
6.94	13.00	90.25	6.94	26.00	180.50
6.79	14.00	94.99	6.79	28.00	189.98
6.76	14.10	95.35	6.76	28.20	190.69
6.74	14.20	95.67	6.74	28.40	191.34
6.71	14.30	95.97	6.71	28.60	191.93
6.68	14.40	96.23	6.68	28.80	192.45
6.65	14.50	96.45	6.65	29.00	192.90
6.62	14.60	96.63	6.62	29.20	193.26
6.58	14.70	96.77	6.58	29.40	193.54
6.54	14.80	96.86	6.54	29.60	193.72
6.50	14.90	96.90	6.50	29.80	193.80
6.46	14.99	96.89	6.46	29.98	193.78
6.46	15.00	96.89	6.46	30.00	193.77
5.78	16.00	92.45	5.78	32.00	184.91
4.35	17.00	73.95	4.35	34.00	147.91
1.35	18.00	24.29	1.35	36.00	48.57
0.91	18.10	16.43	0.91	36.20	32.86
0.43	18.20	7.86	0.43	36.40	15.73
0.00	18.29	0.00	0.00	36.58	0.00

In Table 2.4, when temperature and irradiance change, the array generates new values of current, voltage, and power (e.g., $I_{modules} = 6.50$ A, $V_{modules} = 29.80$ V and $P_{modules} = 193.80$ W). The relation among voltage, current and power is demonstrated in Figure 2.12 and Figure 2.13, respectively. For the real experiment on the rooftop the Engineering Building 4, in August of 2014 at 12:30 PM: $I_{modules} = 6.429$ A, $V_{modules} = 148.9$ V and $P_{modules} = 957.27$ W, respectively. It should be noted that these results were recorded for 10 modules in series. In addition, current, voltage and power for one module can be computed as $I_{module} = 6.429$ A, $V_{module} = 14.89$ V and $P_{module} = 95.727$ W, respectively. The comparison between simulation and real experiment is performed and illustrated in Table 2.5.
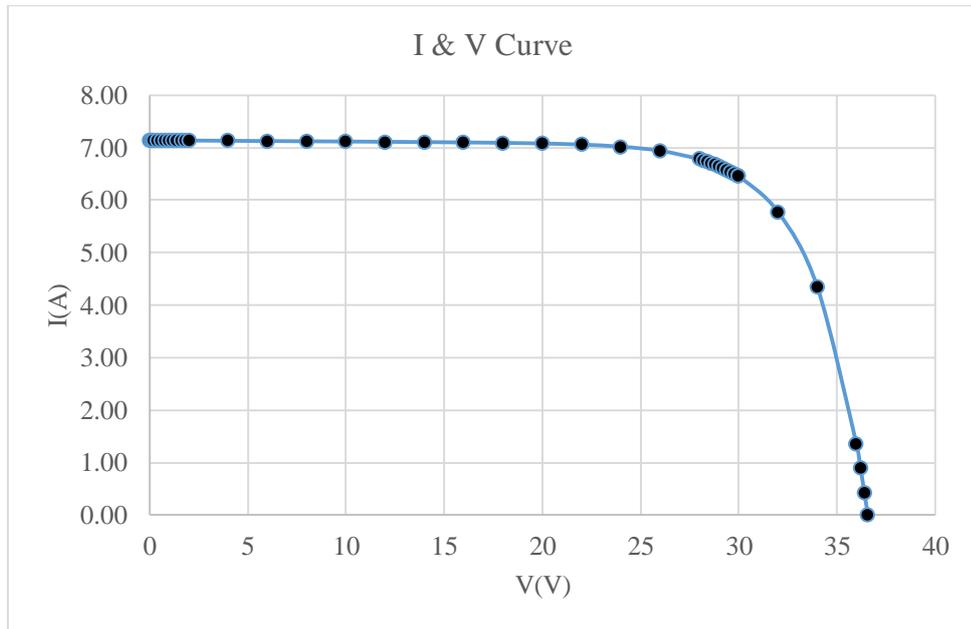
Figure 2.12. The relation between voltage and current for 2 PV modules in series connection
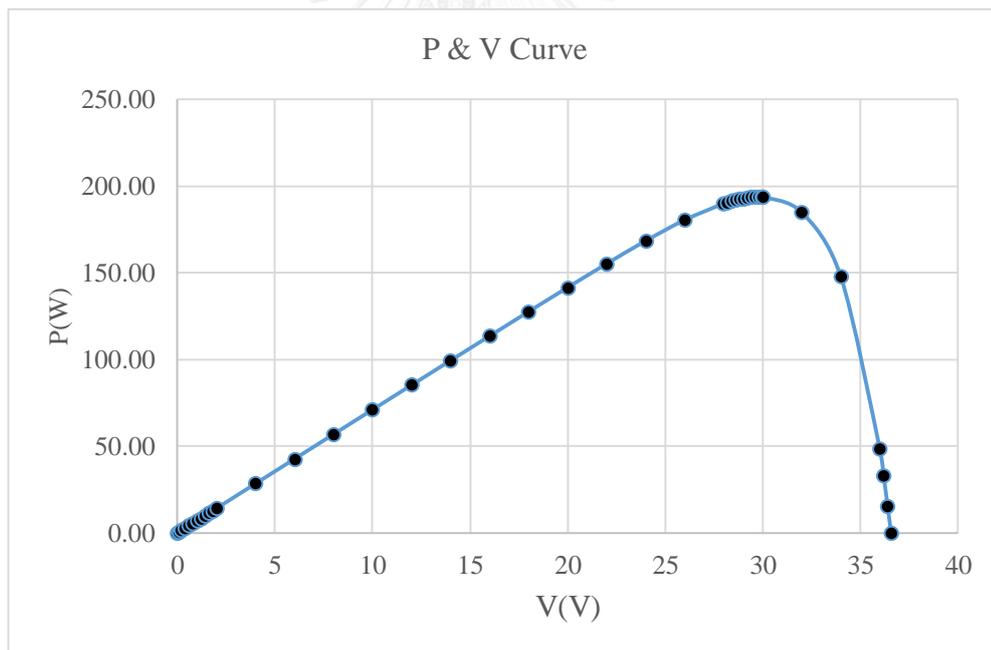
Figure 2.13. The relation between voltage and power for PV modules in series connection

2.6 The Basic of Solar Irradiance

Solar irradiance is a term used to describe visible irradiance which is emitted from sun as shown in Figure 2.14. The rise of sunlight is changed over months and irradiation varies in different locations as shown in Figure 2.15. An important factor is the distance between the sun and earth that it varies during the year. Therefore, solar

irradiance is incident to the earth's atmosphere or the horizontal extraterrestrial at any time throughout the year and it is approximated by (2.17) and (2.18) [35].
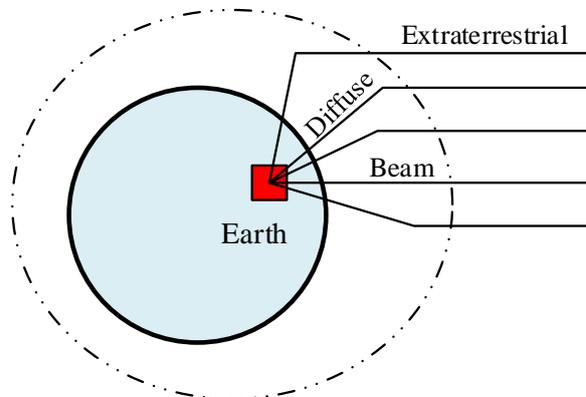
Figure 2.14. Solar irradiance components

In Figure 2.14, near noon time of a day without cloud, about 25% of the solar radiation is scattered and absorbed as it passes through the atmosphere. Therefore about 1000 w/m^2 of the incident solar radiation reaches the earth's surface without significantly scattering. This radiation, coming from the direction of the sun, is called *direct normal irradiance* or *beam irradiance*. Some of the scattered sunlight is scattered back into the space and some also reaches the surface of the earth. The scattered radiation reaching the earth's surface is called *diffuse radiation*. The total solar radiation on a horizontal surface is called *global irradiance* and is the sum of incident diffuse radiation plus the direct normal irradiance projected onto the horizontal surface.
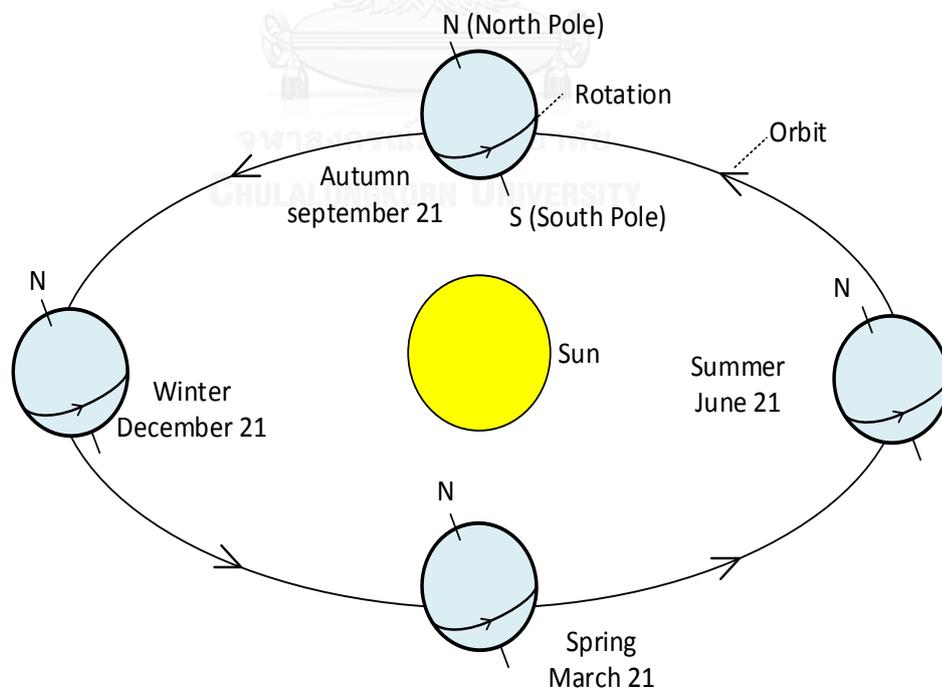
Figure 2.15. The earth revolving around the sun

In Figure 2.15, the earth's orbit is around the sun. As the earth moves around the sun, the axis is fixed if viewed from space. In June the orientation of the axis is such that the northern hemisphere is pointed towards the sun. In December the earth is on the other side of the sun and the earth's axis in the northern hemisphere is pointing away from the sun. During the spring and fall equinoxes the earth's axis is perpendicular to an imaginary line drawn between the earth and the sun.

$$I = I_0 \begin{pmatrix} 1.000110 + 0.034221\cos D + 0.001280\sin D + 0.000719\cos 2D \\ + 0.000077\sin 2D \end{pmatrix} \qquad (2.17)$$

$$D = \frac{360^\circ (n-1)}{365} \qquad (2.18)$$

Where:

I Horizontal extraterrestrial solar irradiance (W/m^2)

I_0 Solar constant (1367W/m^2)

D The day angle (degree)

N Day number, with January 1 as day 1 and December 31 being day number 365.

2.6.1 The Irradiance for Tiled Angle Surface

Electricity generated by the PV system is directly relevant to the solar energy received by the PV modules. Although the PV modules can be placed at any orientations and any tilted angles, most local observatories provide solar irradiation data on a horizontal surface only. Thus, an estimation of the solar irradiance on a tilted surface is calculated by adding the beam, diffuse, and reflected solar irradiance components on the tilted angle surface together [36], as shown in Figure 2.16.
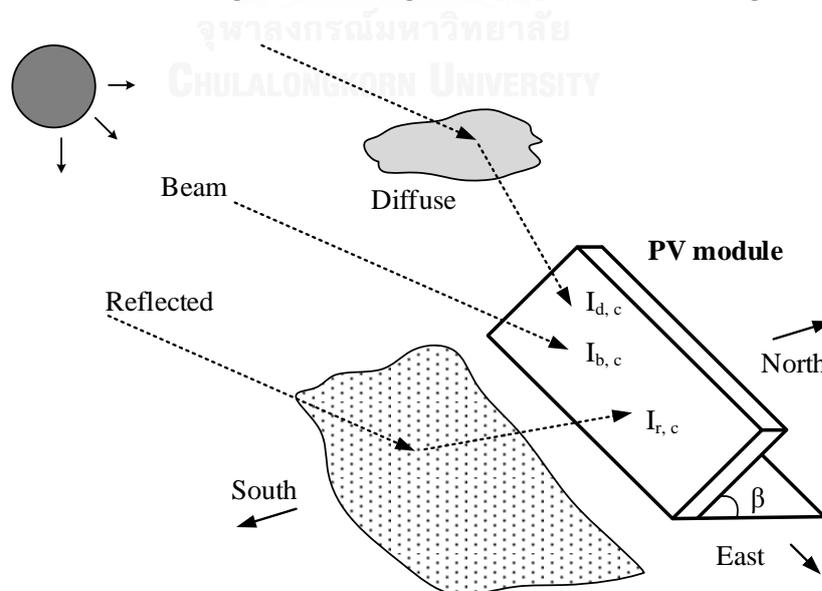
Figure 2.16. Solar irradiation on a horizontal surface

In Figure 2.16, the PV module is directed in south-facing, characterized by the zero value of the azimuth angle surface. Indeed, it is necessary to track the sunlight when sun moves along the time. An option is to change the tiled surface and azimuth angle as shown in Figure 2.17.
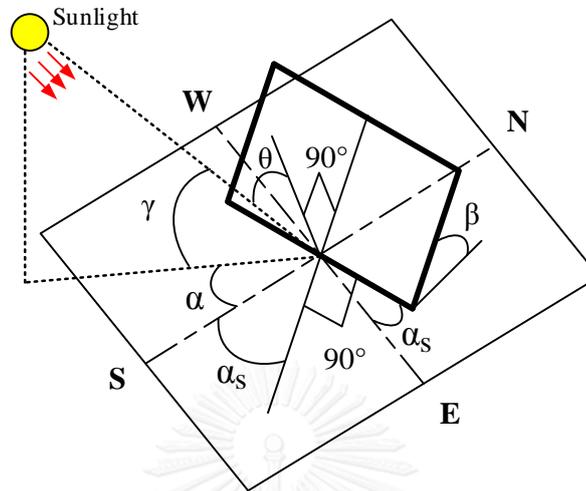
Figure 2.17. Solar PV with tracking both tilted angle surface and azimuth angle surface

In Figure 2.15, the total solar irradiance on tilted surface is defined by (2.19).

$$I_c = I_{b,c} + I_{d,c} + I_{r,c} \tag{2.19}$$

Where:

I_c The total solar irradiance on tilted surface (W/m²)

$I_{b,c}$ Direct or beam irradiance (W/m²)

$I_{d,c}$ Diffuse irradiance (W/m²)

$I_{r,c}$ Ground reflection (W/m²)

The beam, ground reflection and diffuse irradiance can be calculated by (2.20), (2.21) and (2.22), respectively.

$$I_{b,c} = I_{b,N} \cos\theta \tag{2.20}$$

$$I_{r,c} = \rho I_{b,N} (\sin\gamma + C_n) \left[\sin(\frac{\beta}{2}) \right]^2 \tag{2.21}$$

$$I_{d,c} = C_n I_{b,N} \left[\cos(\frac{\beta}{2}) \right]^2 \tag{2.22}$$

Then, those equations cloud be replaced by sub-equations in (2.23), (2.24), (2.25), (2.26), (2.27), (2.28), (2.29), (2.30), and (2.31), respectively.

$$\theta = \cos^{-1} \left[\cos\gamma \cos(\alpha - \alpha_S) \sin\beta + \sin\gamma \cos\beta \right] \tag{2.23}$$

$$\alpha = \sin^{-1} (\frac{\cos\delta \sin\omega}{\cos\gamma}) \tag{2.24}$$

$$I_{b,N} = C_n I e^{-(\frac{k'}{\sin\gamma})} \tag{2.25}$$

$$\gamma = \sin^{-1}\left(\sin\Phi\sin\delta + \cos\Phi\cos\delta\cos\omega\right) \tag{2.26}$$

$$\delta = \begin{pmatrix} 0.006918 - 0.399912\cos D + 0.070257\sin D - 0.006758\cos 2D \\ +0.000907\sin 2D - 0.002697\cos 3D + 0.00148\sin 3D)(\frac{180}{\pi}) \end{pmatrix} \tag{2.27}$$

$$\omega = \frac{ATS - 720\,\text{min}}{4\,\text{min/deg}} \tag{2.28}$$

$$ATS = LST + (4\,\text{min/deg})(L_{ST} - L_{Local}) + ET \tag{2.29}$$

$$L_{ST} = 15\left(\frac{L_{Local}}{15}\right)_{Interger} \tag{2.30}$$

$$ET = \begin{pmatrix} 0.000075 + 0.001868\cos D - 0.032077\sin D \\ -0.014615\cos 2D - 0.04089\sin 2D \end{pmatrix} 229.18 \tag{2.31}$$

Where:

θ Incident angle of direct irradiance on tilted surface (degree)

$I_{b,N}$ The direct or beam solar irradiance at earth surface (W/m^2)

k' Atmospheric optical depth

C_n Clearness number which varies between 0.85 and 1.15

Φ Latitude of the place with the angular location (degree), in north is positive and south is negative values.

ρ Ground reflection coefficient for forest and agricultural area are defined between 0.12 to 0.2 [37].

β Tiled surface in (degree)

γ Solar altitude angle (degree)

δ The declination angle between -23.45° and 23.45°

ω Hour angle (degree)

ATS The apparent solar time (minute)

LST Local standard time (hour)

L_{ST} Local longitude of standard time meridian (degree)

L_{Local} Local longitude (degree)

ET The equation of time (minute)

α Solar azimuth angle (degree), the angular displacement from south of the projection of direct irradiance on the horizontal plane, in addition, displace east of south is negative and west of south is positive.

2.6.2 The Irradiation for One and Two Axes Tracking Surface

The fixed and tracking PV system is a functional relationship between tilted, azimuth and incidence angle of direct irradiance.

For a fixed PV system, the azimuth of the surface is set to zero. Therefore, the incidence angle of direct irradiance can be written by (2.32).

$$\theta = \cos^{-1}(\cos\gamma\cos\alpha\sin\beta + \sin\gamma\cos\beta) \qquad (2.32)$$

For one axis tracking of PV system. The tiled angle (beta β) is fixed. The PV module is changed in the vertical axis. Also, solar azimuth is equally to surface azimuth ($\alpha=\alpha_s$) [35]. The incident angle can be defined by (2.33).

$$\theta = \cos^{-1}(\cos\theta_Z\cos\beta\sin\beta + \sin\theta_Z\sin\beta) \qquad (2.33)$$

where θ_z is zenith angle (*degree*) and given by (2.34)

$$\theta_Z = \cos^{-1}(\sin\gamma) \qquad (2.34)$$

For two axes tracking of PV system. The tilted surface of PV module is equally to the zenith angle ($\beta= \theta_z$). PV azimuth is equally to solar azimuth angle ($\alpha=\alpha_s$). Therefore, the incident angle can be calculated by (2.35) [35].

$$\cos\theta = 1 \qquad (2.35)$$

Chapter 3

Effect of Shading on Photovoltaic (PV) Generation System

3.1 Reasons of Shading

Shading is one of the most significant problems that cause active power reduction in PV generation systems. There are various reasons of shading in nature such as tree shadow, neighbor PV panels, high buildings, and moving clouds as shown in Figures 3.1 (a), (b), (c), and (d), respectively. A PV module arranged in series and parallel configurations should be installed in a shade-free location. However, a cloud is unavoidable and uncontrollable so that it can occur and move freely. Accordingly, a cloud might pass over the PV array, causing reduction of the power output considerably. Ideally, this reduction should be avoided. Regarding this mentioned shading problem, this research focuses on the effect of solar irradiation on PV generation system as demonstrated by Figure 3.2. In addition, some periodic decreasing irradiance has a critical effect on PV array output.

(a). The shading due to trees   (b). The shading due to other PV panels

(c). The shading due to building   (d). The shading from the moving clouds

Figure 3.1. Demonstration of various shading type

(Ref: www.solaredge.com)
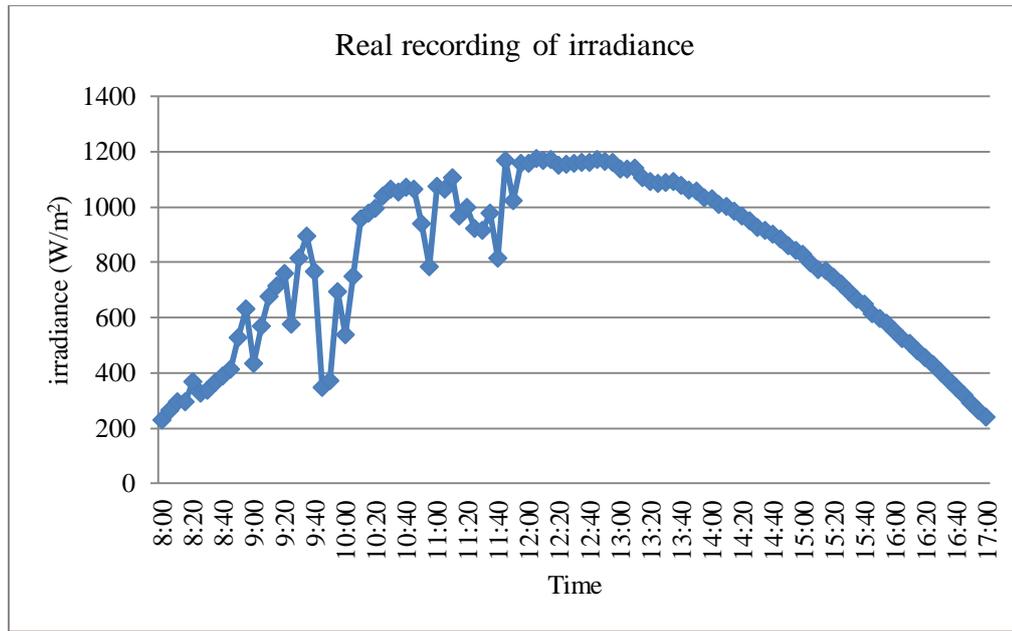
Figure 3.2. The relation between time and irradiance of a day

(This information is recorded at Engineering Building 4, 10 PV modules in series connection of SP120)

3.2 Effect of Shading on PV Cells

Shading is a problem for PV module if the module contains only one cell. That is, the power output may reduce to zero. The output power of the cell declines when it is shaded partly. The output power decreases proportionally to the shaded area. For completely opaque objects such as a leaf, the decline in current output of the cell is proportional to how large the area of the cell is covered.

For analyzing effects of shading, it is necessary to use the proposed approach in section (2.2.3.2) of Chapter 2. According to that approach, the light intensity is explained by using 2 factors: the photoelectric current (I_{ph}) and the shunt resistance (I_{sh}).

In addition, shading on PV cells causes the single maximum power output value to become multiple points (multiple MPP). These points affect the maximization of the power generation, if the process of finding the maximum power point tracking (MPPT) is not optimized, the maximum power point of the whole system (global maximum power point) is unreachable. As a result, the efficiency of electricity production is lower than it should be.

A simple model to explain the shading effect is shown in Figure 3.3

Istring

+

+

Vunshaded

-

No shaded

+

Vunshaded

-

Vstring

+

Vshaded

-

Shaded

+

Vshaded

-

-
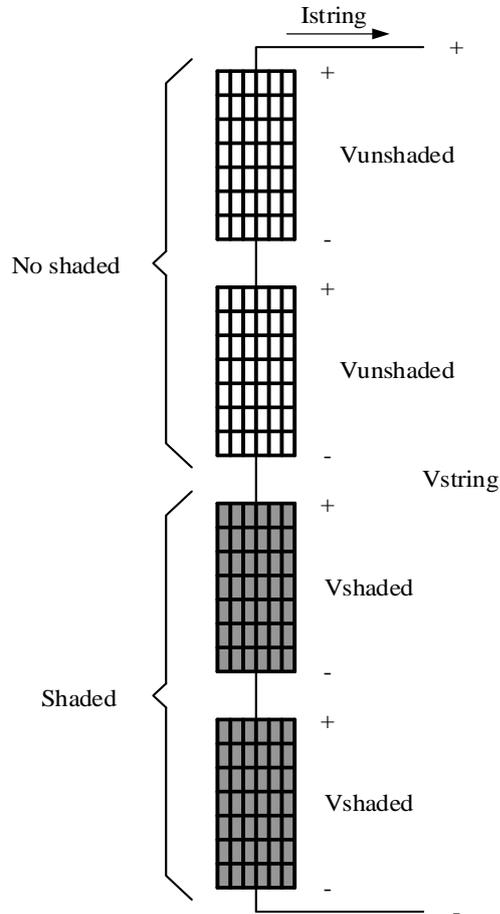
Figure 3.3. The simple model of modules shading in series connection

In Figure 3.3, a part of the string is assumed to be shaded. The voltage in system can be estimated by (3.1).

$$V_{string} = (N_{unshaded})V_{unshaded} + (N_{shaded})V_{shaded} \qquad (3.1)$$

Where:

V_{string}	String voltage (V)
$N_{unshaded}$	Number of unshaded modules
$V_{unshaded}$	Unshaded module voltage (V)
N_{shaded}	Number of shaded modules
V_{shaded}	Shaded module voltage (V)

In fact, the shading has many patterns depending on cloud shapes. In this research, PV modules are separated in different groups with consideration of the number of modules and same irradiation as the illustration in Figure 3.4.
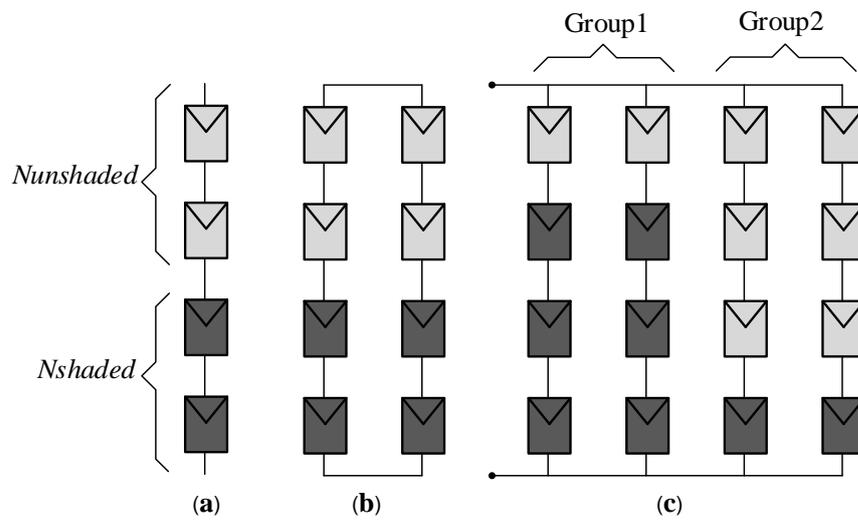
Figure 3.4. Illustration of grouping PV modules (a) Shading in a string
(b) One group of shading in PV array (c) Two groups of shading in PV array

Figure 3.4 (a) consists of a number of shaded modules (N_{shaded}) and a number of unshaded modules ($N_{unshaded}$) in a string. The total number of modules is thus computed by (3.2). In addition, Figure 3.4 (b) has 2 strings which has the same number of shaded modules. These two strings are considered as "a group". An array may contain more than one group as shown in Figure 3.4 (c).

$$N_{total} = N_{unshaded} + N_{shaded} \qquad (3.2)$$

This section is discussing about the shading on modules, which are generating power output when the shading occurs. The model can be explained by using a single diode as shown in Figure 3.5. The current of the shaded module (I_{shaded}) is given by (3.3).
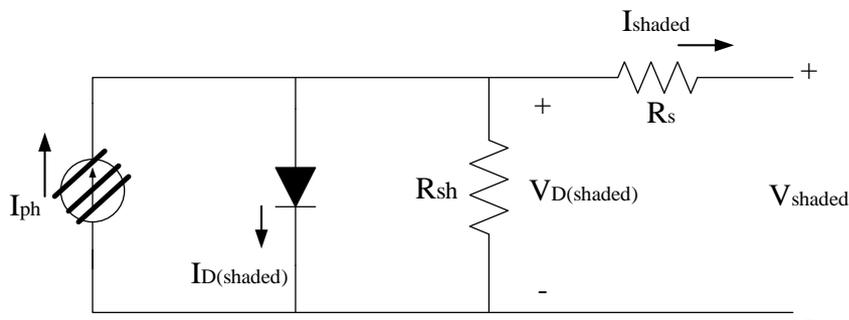
Figure 3.5. A single diode with shaded model

$$I_{shaded} = I_{ph,shaded} - I_{D,shaded} - I_{Rsh} \qquad (3.3)$$

Where:

I_{shaded} Shaded module current (A)

$I_{ph,shaded}$ Photoelectric current of the shaded module (A)

$I_{D,shaded}$ Current flowing through the diode in the shaded module (A)

I_{Rsh} Current flowing through the shunt resistance (R_{sh}) in the shaded module (A)

The currents $I_{D,shaded}$ and I_{Rsh} can be calculated by the voltage in (3.1), the instantaneous current when the module is shaded can be written by (3.4).

$$I_{shade} = I_{ph(shade)} - I_{o(shade)} \left[\exp(\frac{V_{shade} + I_{shade}R_s}{aN_sV_{th}}) - 1 \right] - \frac{V_{shade} + I_{shade}R_s}{R_{sh(shade)}} \qquad (3.4)$$

Where:

V_{th} Threshold voltage for cell in single diode (V) defined by (2.4)

$I_{o\,(shaded)}$ Saturation current of the shaded module (A)

R_S Series resistance of a module (Ω)

R_{sh} Shunt resistance of the shaded module (Ω)

N_s Number of cells in series connection of a module

a Factor of diode which depend on material production $a = 1.025$

3.3 Effect of Shading on MPP

Effects of shading on the MPPT finding process are illustrated through the following example. There are 10 modules in series connection and each module has the open-circuit voltage $V_{oc} = 21.7$ V, the short-circuit current $I_{sc} = 7.45$ A, and the other parameters in Table 2.1. The examination is considered in two cases: a normal case of irradiation of 1000 W/m^2 and temperature of 25°C; and a case of irradiation of 500 W/m^2. In order to present the relationship among voltage, current, and power with a comparison between the two cases, graphs are used as shown in Figures 3.6, 3.7, 3.8 and 3.9.
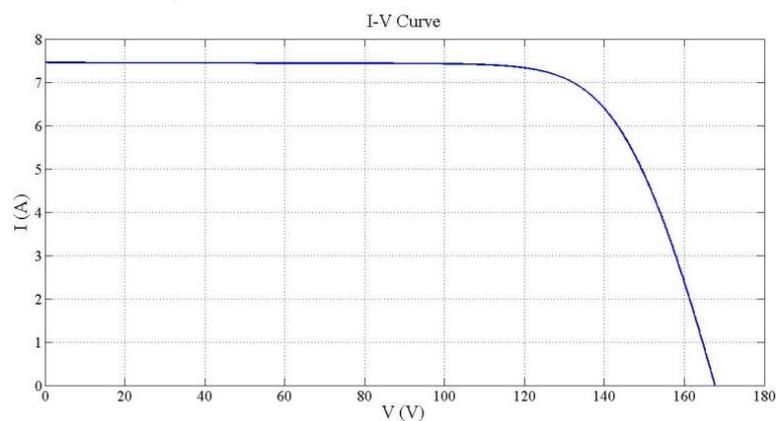
Figure 3.6. The relation between voltage and current of 10 modules in series the normal case
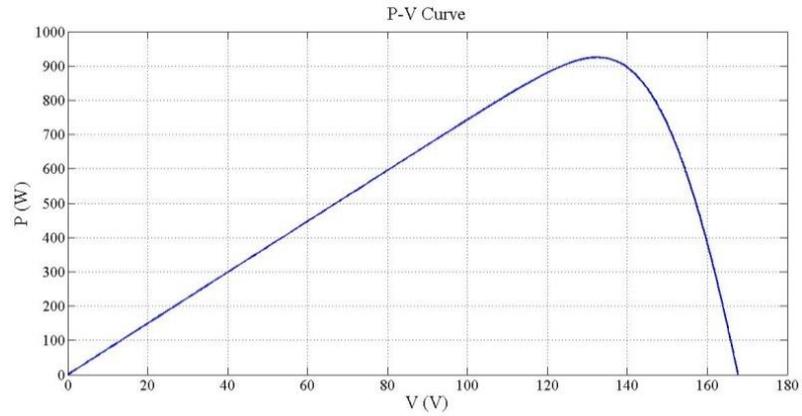
Figure 3.7.The relation between voltage and power of 10 modules in series in the normal case
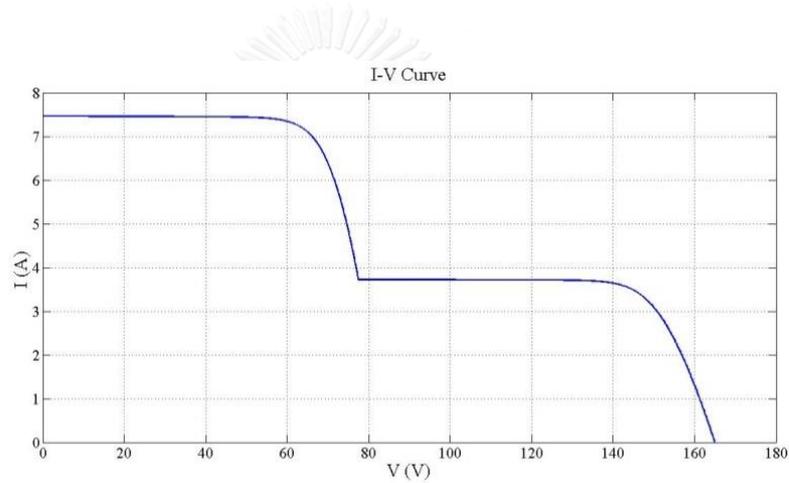
Figure 3.8.The relation between voltage and current of 10 modules in series in the shading case
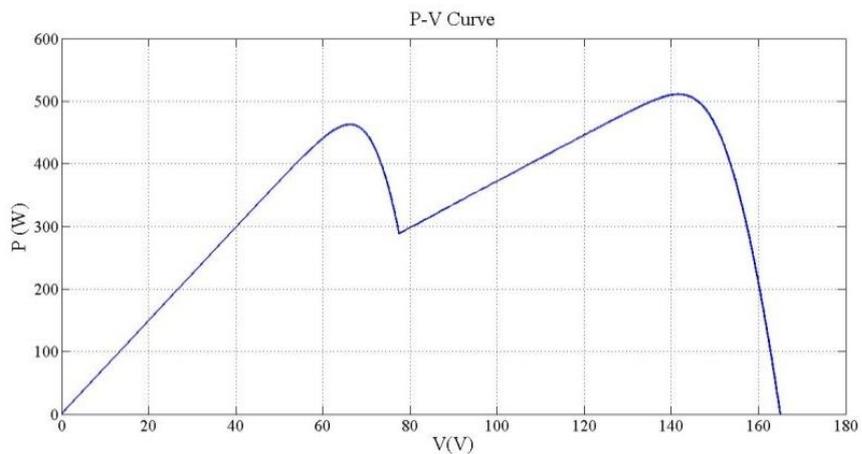
Figure 3.9. The relation between voltage and power of 10 modules in series in the shading case

Figure 3.9 illustrates a curve with multiple MPPs generated on the PV system in the shading case. They may cause the process of finding the MPP to be unable to efficiently generate the real MPP.

3.4 PV Cells Connection without Bypass Diode

The literature of shading effect on PV cells in the connection without using bypass diode can be considered in two cases of unshaded and shaded cells.

3.4.1 Unshaded Cells without Bypass Diode

Generally, cells in a module are unnecessary to be connected with a bypass diode if it is unshaded by anything that reduces sunlight intensity. The relationship between current and voltage can be written as (3.5).

$$I_{unshaded} = I_{ph,unshaded} - I_{o,unshaded}\left[\exp(\frac{V_{unshaded} + I_{unshaded}R_s}{aN_sV_{th}}) - 1\right] - \frac{V_{unshaded} + I_{unshaded}R_s}{R_{sh}} \qquad (3.5)$$

Where:

$I_{ph,unshaded}$	Photoelectric current of the unshaded module (A)
$V_{unshaded}$	Module voltage of the unshaded (V)
$I_{o,unshaded}$	Saturation current of the unshaded (A)

3.4.2 Shaded cells without Bypass Diode

When cells connected without bypass diode are shaded, the photoelectric current ($I_{ph,shaded}$) decreases and becomes lower than the value in the case of being unshaded: $I_{ph,shaded} < I_{unshaded}$. Therefore, a model of a PV module shown in Figure 3.10 can be used to create a string (PV module in series connection). If one module in the string is shaded, the module can be considered as a load or a source depending on the string current as the following cases.

- The module becomes a load if the string current is limited by $I_{ph,shaded} \leq I_{string} \leq I_{ph,unshaded}$,

- The module becomes a source if the string current is limited by $0 < I_{string} < I_{ph,unshaded}$

1) The string current is limited by $I_{ph,shaded} \leq I_{string} \leq I_{ph,unshaded}$

In a shaded module, the diode allows the reverse current to flow through it, hence, the reverse of power flows in the PV system. The current in the string can be defined in (3.6).
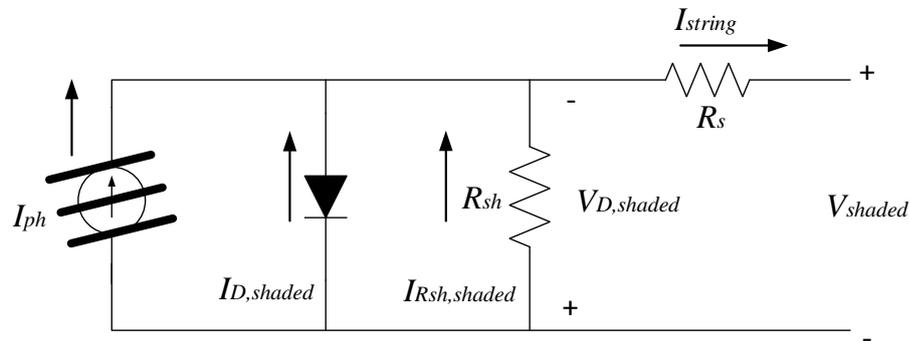
Figure 3.10. Equivalent circuit of a shaded module without bypass diode

In Figure 3.10, the string current can be defined by (3.6).

$$I_{string} = I_{ph,shaded} + I_{o,shaded}\left[\exp(\frac{-V_{shaded} - I_{string}R_s}{aN_sV_{th}}) - 1\right] + \frac{-V_{shaded} - I_{string}R_s}{R_{sh}} \quad (3.6)$$

where I_{string} is the module current flows through string with shading.

In a shaded PV module, the saturation current (I_0) reaches the lowest value. The string current and the shaded voltage can be presented by (3.7), (3.8), respectively.

$$I_{string} \cong I_{ph(shade)} + \frac{-V_{shade} - I_{string}R_s}{R_{sh(shade)}} \quad (3.7)$$

$$I_{string} \cong I_{ph(shade)} + \frac{-V_{shade} - I_{string}R_s}{R_{sh(shade)}} \quad (3.8)$$

2) The string current is limited by $0 < I_{string} < I_{ph,unshaded}$

A module becomes a source to supply current to load. The shaded module current can be defined by (3.9).

$$I_{shade} = I_{ph,shaded} - I_{o,shaded}\left[\exp(\frac{V_{shaded} + I_{string}R_s}{aN_sV_{th}}) - 1\right] - \frac{V_{shaded} + I_{string}R_s}{R_{p,shaded}} \quad (3.9)$$

3.5 PV Cells Connection with Bypass Diode

In an integrated PV generation system, it is difficult to avoid partial shading on modules or array due to neighboring obstructions in nature, e.g. buildings, trees, other PV panels, and the moving clouds. The study of partial shading on modules is a key to understand the performance of a PV array. The shaded PV module may experience reverse biased current and acts as a load.

Also, in order to protect the PV array system from such premature, modules and arrays are necessarily connected with bypass diodes in parallel. When the module current cannot flow through cells, it can flow through the bypass diode instead. Each module is connected in parallel with one bypass diode as the illustration in Figure 3.11.
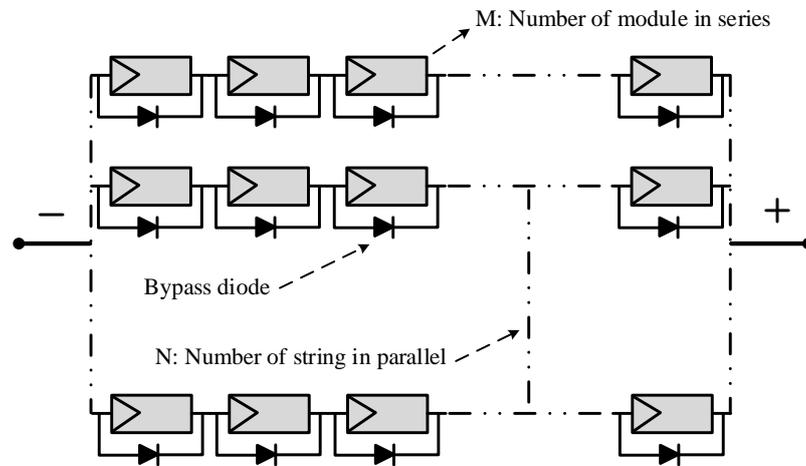
Figure 3.11. Connection of bypass diodes

Shading effects on solar cells with bypass diode can be categorized into two cases as:

1) Unshaded cells with bypass diode
2) Shaded cells with bypass diode

3.5.1 Unshaded cells with Bypass Diode

In this case the bypass diode does not affect the current of the module. Thus, it is similar to the case of unshaded cells without bypass diode in Section 3.4.1. The relationship between current and voltage has been defined by (3.5).

3.5.2 Shaded Cells with Bypass Diode

When cells connected with bypass diode are shaded, the photoelectric current ($I_{ph,shaded}$) decreases and becomes lower than the value in the case of being unshaded: $I_{ph,shaded} < I_{unshaded}$. If a module in the string is shaded, the string current flows through the bypass diode. Like in the previous section, there are 2 cases to be considered as: 1) string current is limited in $I_{ph,shaded} \leq I_{string} \leq I_{ph,unshaded}$ and 2) string current is limited in $0 < I_{string} < I_{ph,unshaded}$.

1) The string current is limited in $I_{ph,shaded} \leq I_{string} \leq I_{ph,unshaded}$

A PV module generates reverse voltage (forward bias) as shown in Figure 3.12. The string current only passes through the bypass diode. Moreover, the voltage of the shaded module reaches the lowest value that could be close to zero as the representation in (3.10).
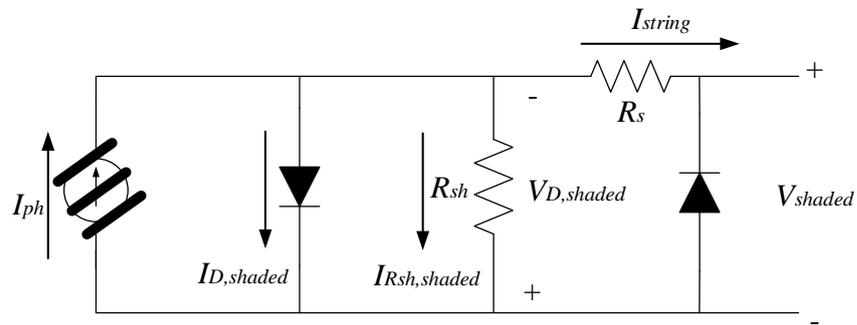
Figure 3.12. A model of PV module connects bypass diode under shading

$$V_{shaded} \cong 0 \tag{3.10}$$

2) The string current is limited in $0 < I_{string} < I_{ph,unshaded}$

The PV current passing through the bypass diode to supply to load. The string current can be given by (3.9) in Section 3.4.2.

3.6 Algorithm for Determining Relationship among Voltage, Current and Power of a Shaded String

In fact, a string consists of both shaded and unshaded modules. In a string connected by a series of modules, the string current is equal to the module current and the string voltage is the sum of all module voltages. An algorithm depicted in Figure 3.13 is proposed to determine the relationship among voltage, current and power of a shaded string.
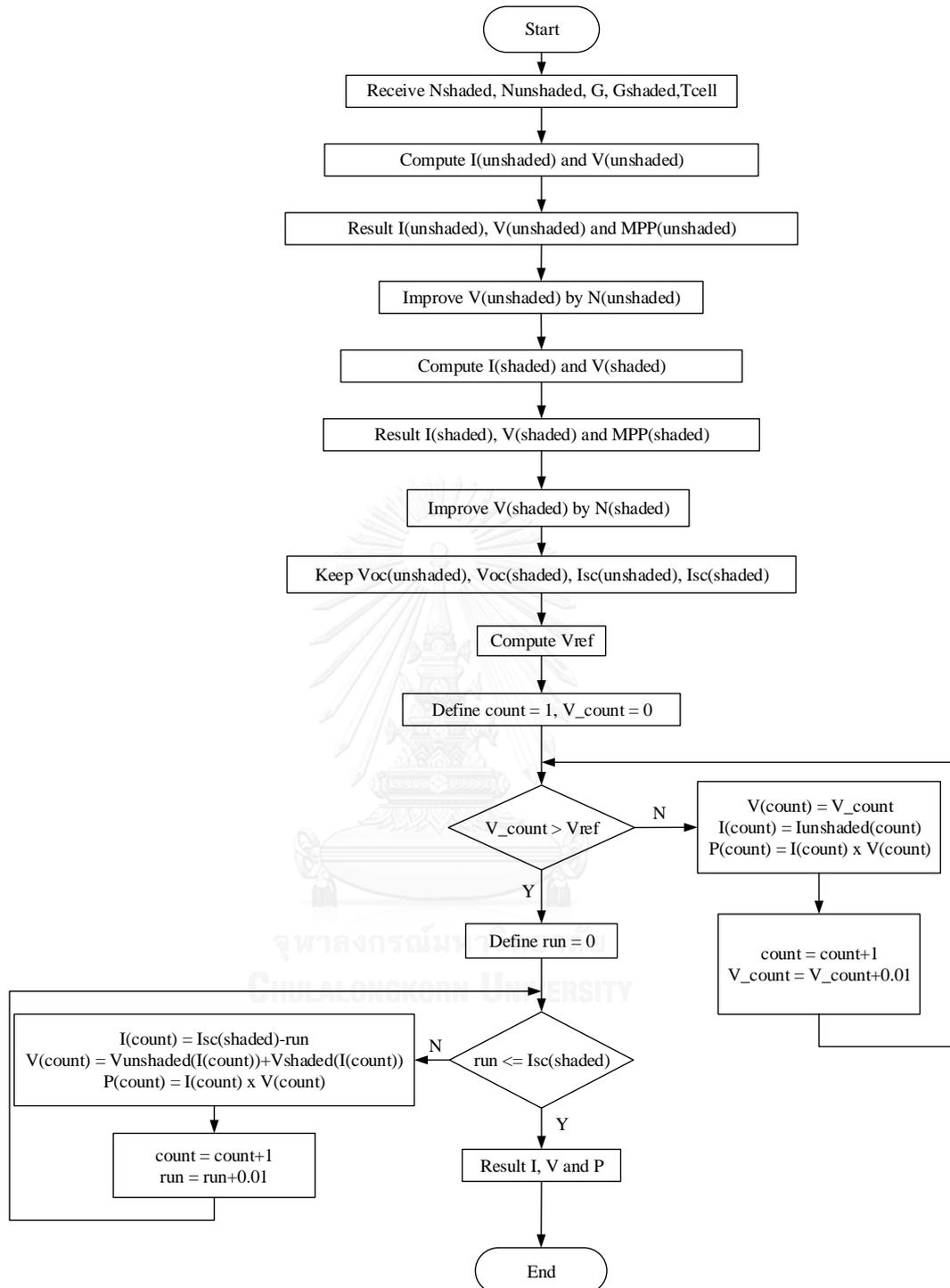
Figure 3.13. Algorithm for determining relationships among voltage, current and power of a shaded string

In Figure 3.13, the algorithm starts from receiving data which consist the number of shaded modules (Nshaded), unshaded modules (Nunshaded), unshaded solar irradiance (G), shaded solar irradiance (Gshaded) and cell temperature (Tcell). After calculating the unshaded current I(unshaded) and voltage V(unshaded), unshaded maximum power point MPP(unshaded) is multiplied by both unshaded current and

voltage [I(unshaded), V (unshaded)]. After that, unshaded voltage is improved by using unshaded modules. And shaded maximum power point MPP(shaded) is multiplied by both shade current and voltage [I(shaded), V (shaded)], which voltage is improved by using shaded modules.

In addition, the processing keeps the value of the open-circuit voltage (V_{oc}) and short-circuit current (I_{sc}) as both terms of shaded and unshaded modules and computing the reference voltage (V_{ref}). Whereas, the voltage counter (V_count) is limited by zero and the counting (count) is limited by one. If V_count is less than V_{ref}, V_count will be added an additional 0.01 until V_count > V_{ref}. Finally, the current (A), voltage (V) and power (W) are processed.

3.7 Algorithm for Determining Relationship among Voltage, Current and Power of a

Shaded Array

An algorithm depicted in Figure 3.14 is proposed to determine the relationship among voltage, current and power of a shaded array.
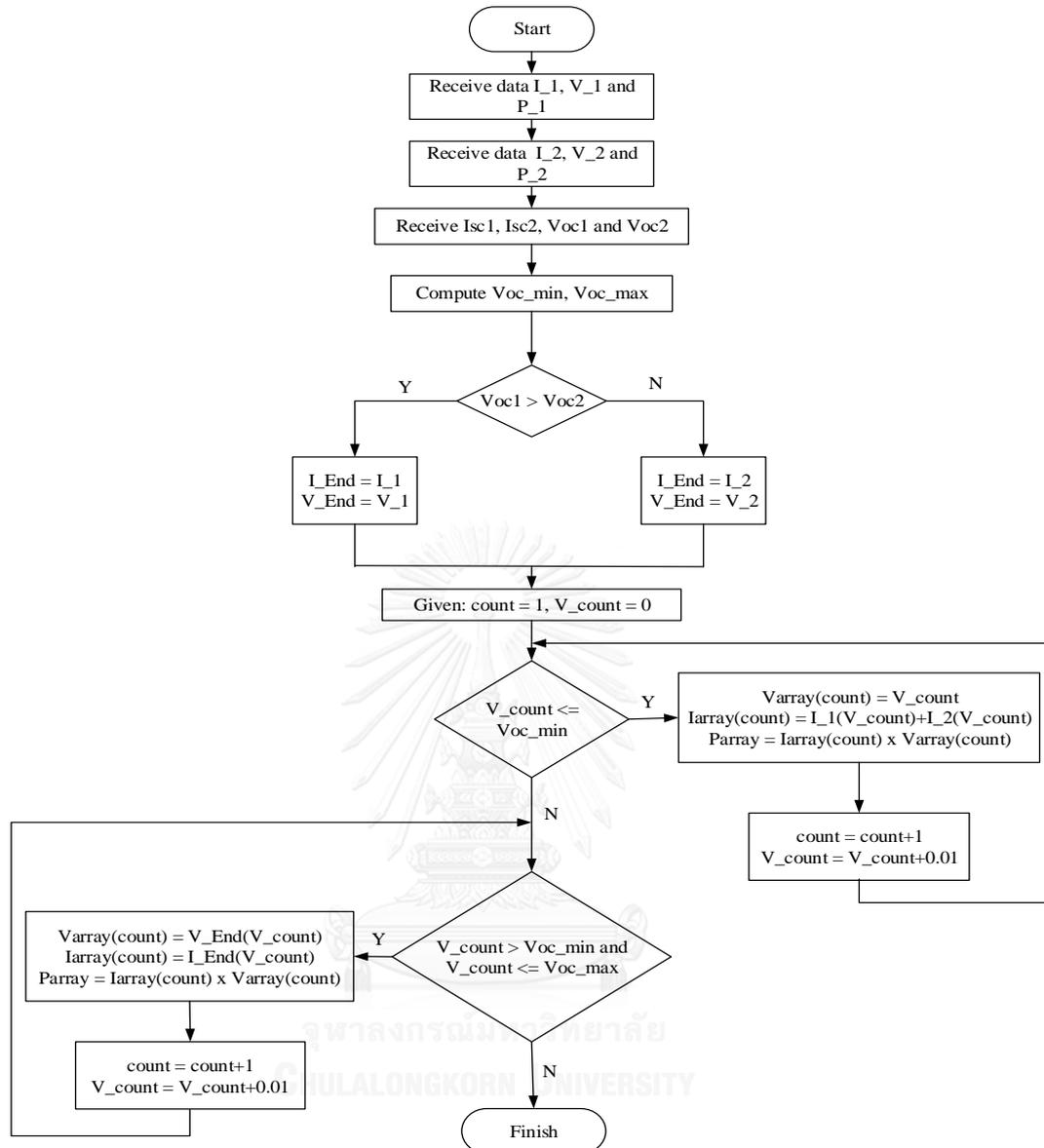
Figure 3.14.Algorithm for determining relationships among voltage, current and power of a shaded array

In Figure 3.14, the algorithm starts from receiving data of two groups including current (A), voltage (V) and power (W). These I_1, V_1 and P_1 are given by strings of group one. These I_2, V_2 and P_2 are given by strings of group two. Then, the open-circuit voltage including of V_{oc_min} and V_{oc_max} are calculated. Afterwards, the V_{oc1} and V_{oc2} are defined. If $V_{oc1} > V_{oc2}$, I_1 and V_1 are computed. Otherwise, I_2 and V_2 are computed instead. Next, the counter (count) is given by one and $V_{\_count}$ is given by zero. After that, $V_{\_count}$ and $V_{\_count\_min}$ are limited. If $V_{\_count} <= V_{\_count\_min}$, $V_{\_count}$ will be added an additional 0.01 until it is larger than $V_{\_count\_min}$. Finally, the current (A), voltage (V) and power (W) are processed.

Chapter 4

Arrangement of PV Module Connection in an Array

4.1 PV Module Connection in an Array

A PV array system is usually connected from modules in both series and parallel. A set of modules in a series connection is called a string and a set of strings in parallel connection is known as an array.

There are two most common array configurations as series-parallel connection and Total Cross-Tied connection.

4.1.1 Series-parallel Connection

A solar PV module produces direct current (DC) electricity. Thus multiple solar PV modules can be wired together to form a solar PV array. They can be connected in both series and parallel as shown in Figure 4.1 to generate a required voltage and current combination.
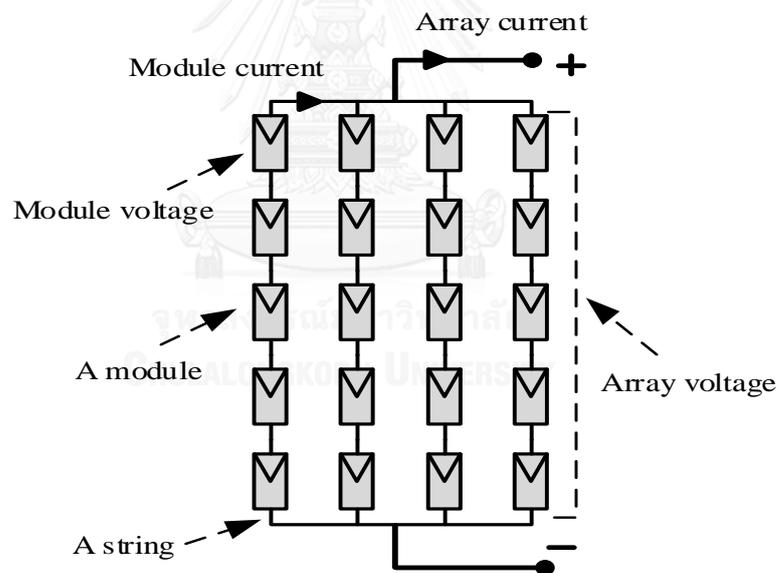
Figure 4.1. Solar PV modules in series-parallel connection

In Figure 4.1, the total array voltage and current can be written by (4.1) and (4.2).

$$V_{array} = \sum_{i=1}^{m} V_i \qquad (4.1)$$

$$I_{array} = \sum_{j=1}^{n} I_j \qquad (4.2)$$

where:

V_{array}	Total array voltage	(V)	I_j	String current	(A)
V_i	Module voltage	(V)	m	Number of module in a string	
I_{array}	Total array current	(A)	n	Number of string in an array	
I_i	Module current	(A)			

4.1.2 Total Cross-Tied Connection

This type of solar PV module connection is obtained by re-wiring modules in Figure 4.1. Modules in the same row are connected in series, namely, a horizontal string. Then rows are connected together in parallel for generating the same voltage. Whereas, the total current is the summation of horizontal string currents. More details are illustrated in Figure 4.2.

In addition, the Cross-Tied connection (CTC) of solar PV modules can be called rearrangement (new connection). It can operate in both uniform and mismatching conditions.
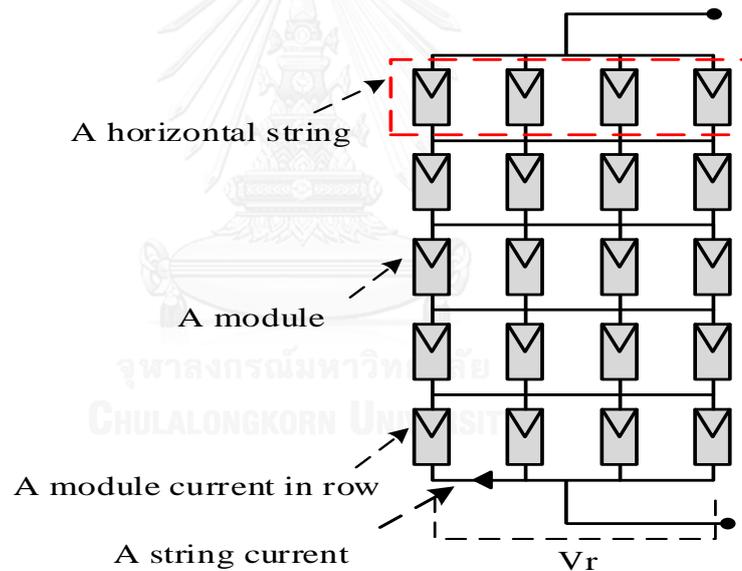
Figure 4.2. Solar PV modules in Cross-Tied connection

In Figure 4.2, the total array voltage and current can be given by (4.3) and (4.4).

$$V_{array} = \sum_{r=1}^{m} V_r \tag{4.3}$$

$$I_r = \sum_{i=1}^{n} I_i \tag{4.4}$$

Where:

V_r String voltage in row (V)

I_r String current in row (A)

I_m Module current in a row (A)

4.2 Grid-connected PV System

A grid-connected PV system generally consists of PV arrays, a battery to store the electricity, a charge controller to regulate the charging of the batteries, and an inverter to convert the solar-generated direct current (dc) power into alternating current (ac) power at compatible voltage and frequency with the grid to which the PV system is connected. At present, PV systems are already connected to the grid by using a grid-tied power electronic unit to generate electricity to the existing utility grid. There are three structures of connection as shown in Fig. 4.3.
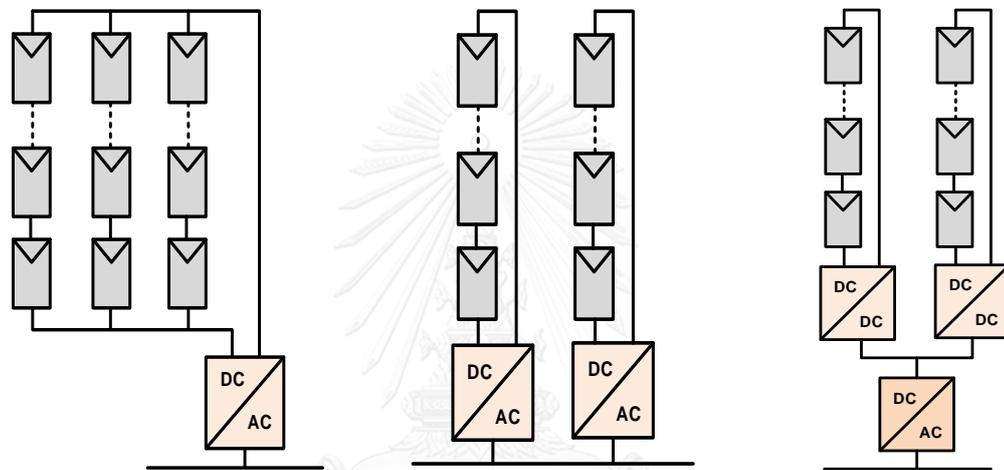
Figure 4.3. Structures of PV array with inverters: (a) Centralized inverter, (b) Multiple centralized string inverter, (c) Multiple string inverters with a centralized inverter

In Figure 4.3 (a), the PV array is controlled by a centralized inverter which is connected to the medium-voltage (MV) grid through a transformer. In addition, the centralized inverter performs a unique maximum power point tracking (MPPT) and operates an algorithm for all strings and interfaces to the MV grid. Advantages include low cost and easy maintenance. One of disadvantages is the low conversion efficiency.

In Figure 4.3 (b), each string is connected to a DC/AC inverter which performs MPPT and converts the PV string output voltage into the voltage at a controlled bus. The DC bus then feeds the central inverter. Generally, the inverters allow the PV panels to operate over a wide voltage range. One feature is the ability to reduce power loss due to panel mismatch and partial shading, hence, increasing high conversion efficiency. However, this structure contributes to increasing the investment cost.

In Figure 4.3 (c), multiple strings are separated to control. Therefore, the MPP can be found more flexibly and efficiently. A downside of multiple string inverters with a centralized inverter is the high investment cost and the low reliability because so many electronic devices are involved.

4.3 Structure of PV Modules

There is usually a fixed number of modules in series and parallel in a solar PV array as the description in Figure 4.2. When a shading due to moving cloud occurs, the overall generated power is reduced because of the fixed module connection. So that, this thesis proposes a rearrangeable module structure as shown in Figure 4.4. The structure is used to reduce the impact of changing sunlight intensity and to increase generated power.
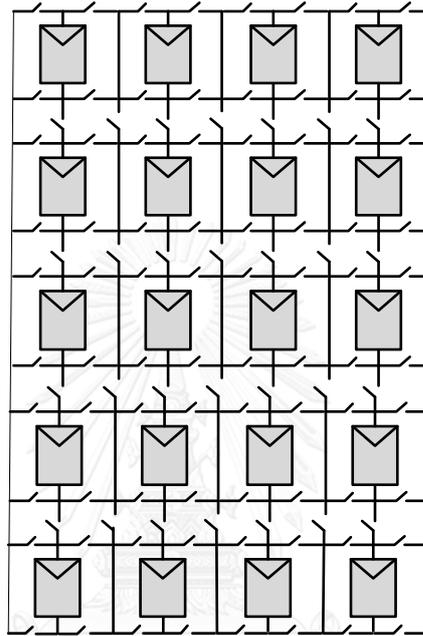
Figure 4.4. Proposed structure of a PV array

The PV array can be arranged by using switches. The number of switches depends on how many PV modules are connected in series and parallel as provided by (4.5) where N_{switch} is the number of switches in the PV array.

$$N_{switch} = 4mn + (2n-1)(m-1)$$

(4.5)

4.4 The Operation of Switches

A switch is an electrical component which can break an electrical circuit, then interrupting the current flow or diverting it from one conductor to another. In real work, it may be operated directly by human operator to control a circuit, or some sensing elements for pressure or temperature. It generally works on 2 states: ON and OFF. Figure 4.5 shows a PV module connected to 6 switches. It is comfortably for selecting the path of connected PV modules together to form a PV array.
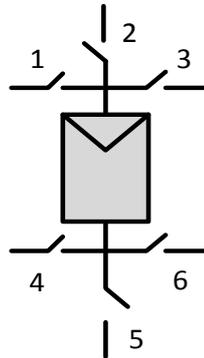
Figure 4.5. Operation of switch in PV module

Generally, only 2 switches are closed (ON) and 4 switches are opened (OFF). In PV modules which consists of series and parallel shown in Figure 4.1, these switches are operated by closing switch number 2 and 5 but the other switches are opened, i.e. switches 1, 3, 4 and 6.

4.5 Proposed Arrangement of PV Modules in an Array

The proposed arrangement of PV modules in an array is presented by the following 2 instructions.

1) A part of shaded modules in column

2) The same size of arrangement in series and parallel connection

4.5.1 A Part of Shaded Modules in Column

As explained before, power in a solar PV array decreases because of the shaded modules. Therefore, the pattern of shaded modules is necessary for estimating power efficiency of a PV system. In Figure 4.6, the shaded modules in rows result in a worse impact than shaded modules in column. This is because all string currents of shaded modules in rows fall down as the illustration in (4.6), (4.7), (4.8), (4.9) and (4.10), respectively.

Figure 4.7 (a) demonstrates the relationship between voltage (V) and current (I) when a row is shaded. Whereas, Figure 4.7 (b) illustrates the relationship between voltage (V) and current (I) when a column is shaded. Then, multiple MPP in Figure 4.8 (a) are decreased to become a MPP with higher power as shown in Figure 4.8 (b).

$$
I_j = \begin{cases} I_{ph} - I_D - I_{Rsh} & ; V \in [0, (N_{unshaded} \times V_{oc,unshaded})] \\ I_{ph,shaded} - I_{D,shaded} - I_{Rsh,shaded} & ; V \in [(N_{unshaded} \times V_{oc,unshaded}), \\ & ((N_{unshaded} \times V_{oc,unshaded}) + (N_{shaded} \times V_{oc,shaded}))] \end{cases} \tag{4.6}
$$

$$
I_D = I_{o,unshaded}[\exp(\frac{V_{unshaded} + I_{unshaded}R_s}{an_sV_{th}}) - 1] \tag{4.7}
$$

$$I_{Rsh} = \frac{V_{unshaded} + I_{unshaded}R_s}{R_{sh,unshaded}} \qquad (4.8)$$

$$I_{D,shaded} = I_{o,shaded}[\exp(\frac{V_{shaded} + I_{shaded}R_s}{an_sV_{th}}) - 1] \qquad (4.9)$$

$$I_{Rsh,shaded} = \frac{V_{shaded} + I_{shaded}R_s}{R_{sh,shaded}} \qquad (4.10)$$

(a) Shaded modules in row (b) Shaded modules in column
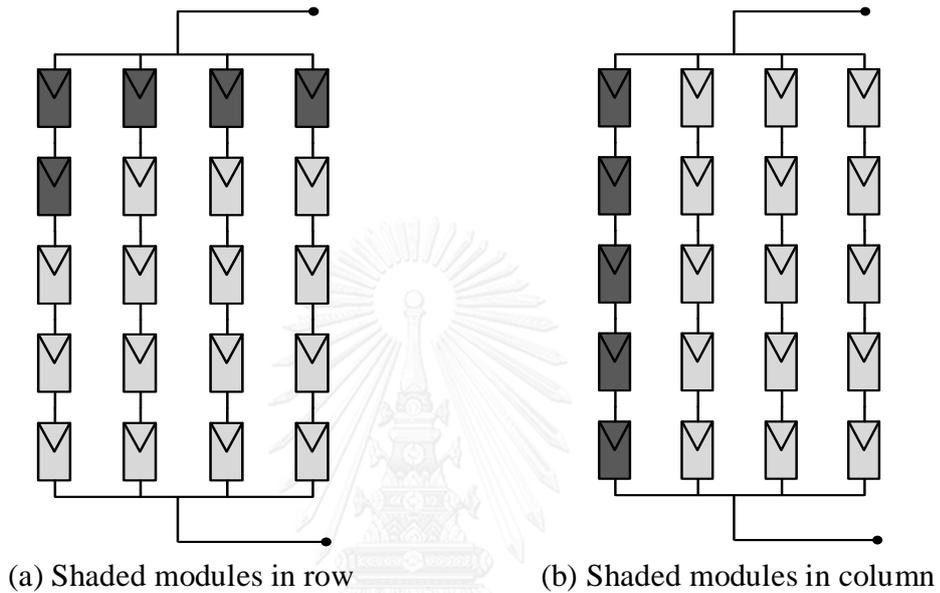
Figure 4.6. Shaded modules in PV array
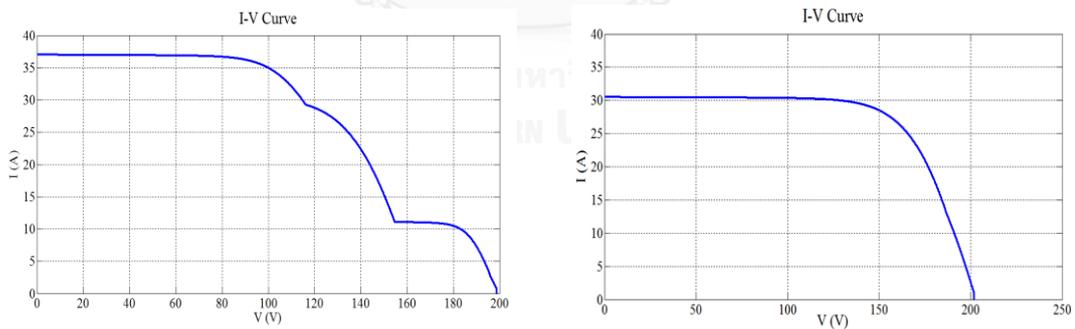
(a) The relation between voltage (V) and current (I) of shaded modules in row (b) The relation between voltage (V) and current (I) of shaded modules in column

Figure 4.7. The relationship between voltage (V) and current (I) of shaded modules in row and column

(a) The relation between voltage (V) and power (P) of shaded modules in row

(b) The relation between shaded voltage (V) and power (P) of shaded modules in column
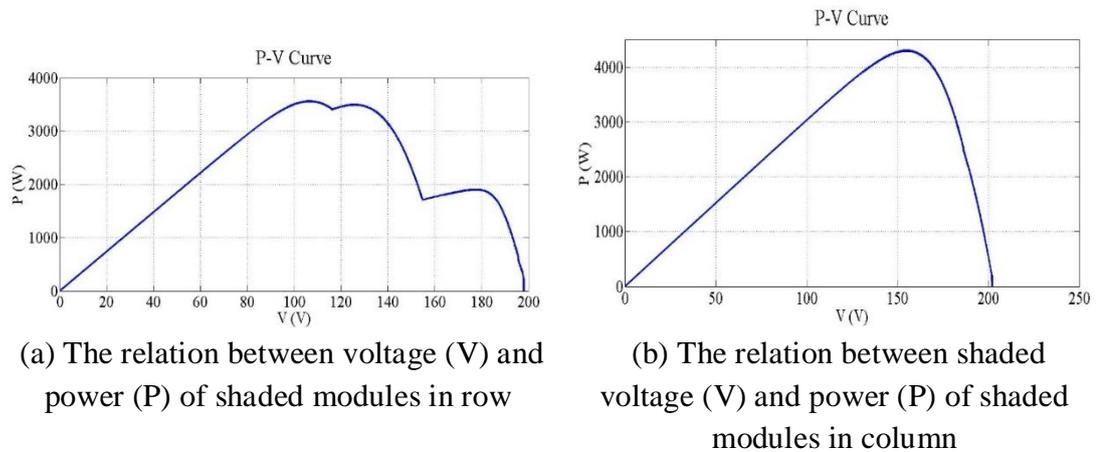
Figure 4.8. The relationship between voltage (V) and power (P) of shaded modules in row and column

4.5.2 Retaining Arrangement Size

The rearrangement should be considered with the number of PV modules in series and parallel connection. It is noted that impacts of this structural module connection on voltage and current of inverter are limited. In addition, the array size with the rearrangement is equal to its old size.

4.6 Aims of an Rearrangement in an Array

A major purpose is to alleviate the decreasing power generation in solar PV array caused by moving clouds. Accordingly, a solar PV array is rearranged in a form of series and parallel connections to generate power more than the case of being shaded. The algorithm for rearrangement is diagrammatized in Figure 4.9.
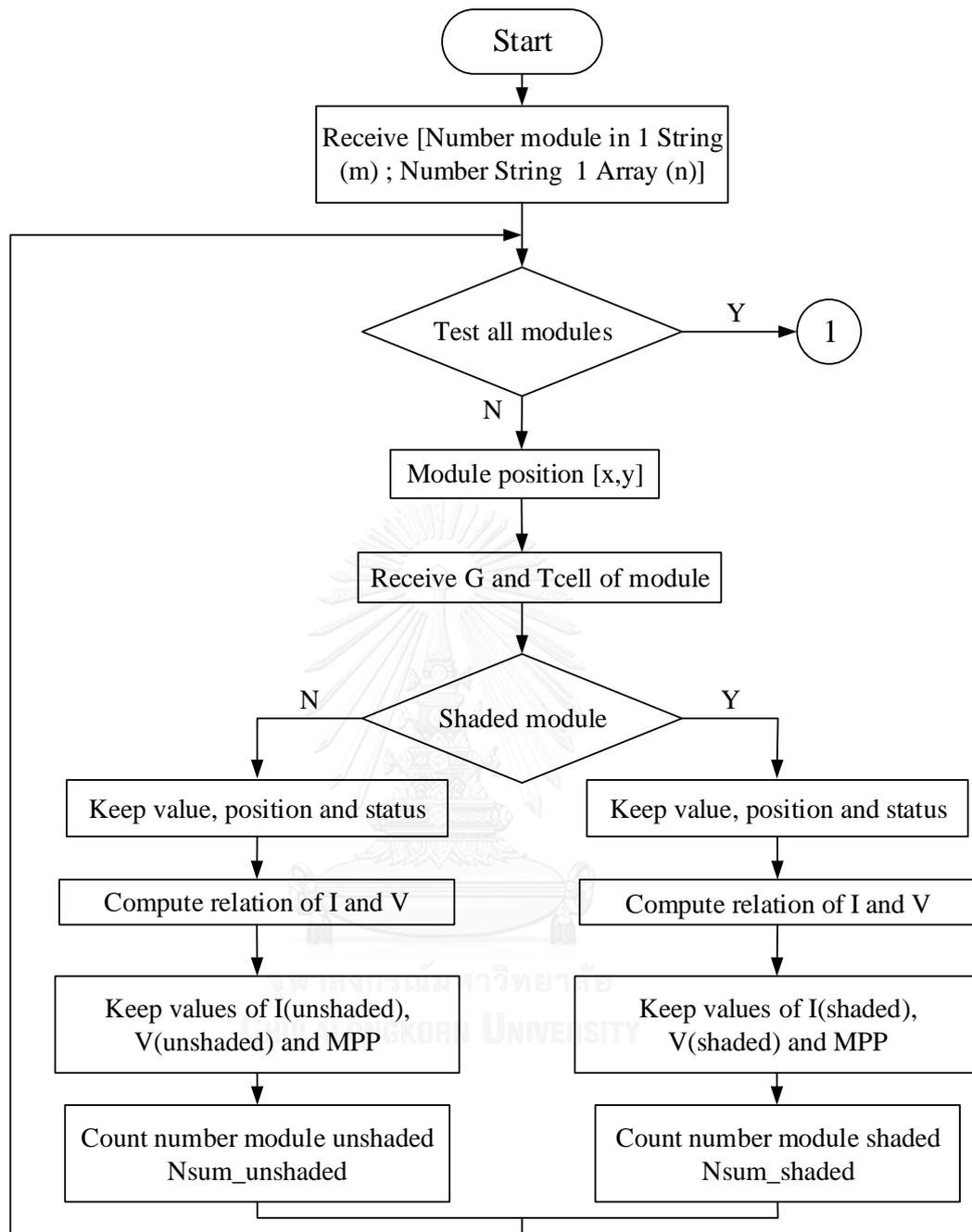
Figure 4.9. The algorithm for rearrangement in PV array

In Figure 4.9, the algorithm starts from receiving consisting of the number of modules in string (m) and the number of string (n) in an array. All modules in the system are tested, resulting in two states: Yes or No. For the state of Yes, an arrangement process (1) will be done later. Otherwise, the module is checked in position and status. Then, the module is checked if it is shaded (Yes) or not (No). Finally, it returns to test all module again until the process (1) is reached. The arrangement process (1) is as follows.
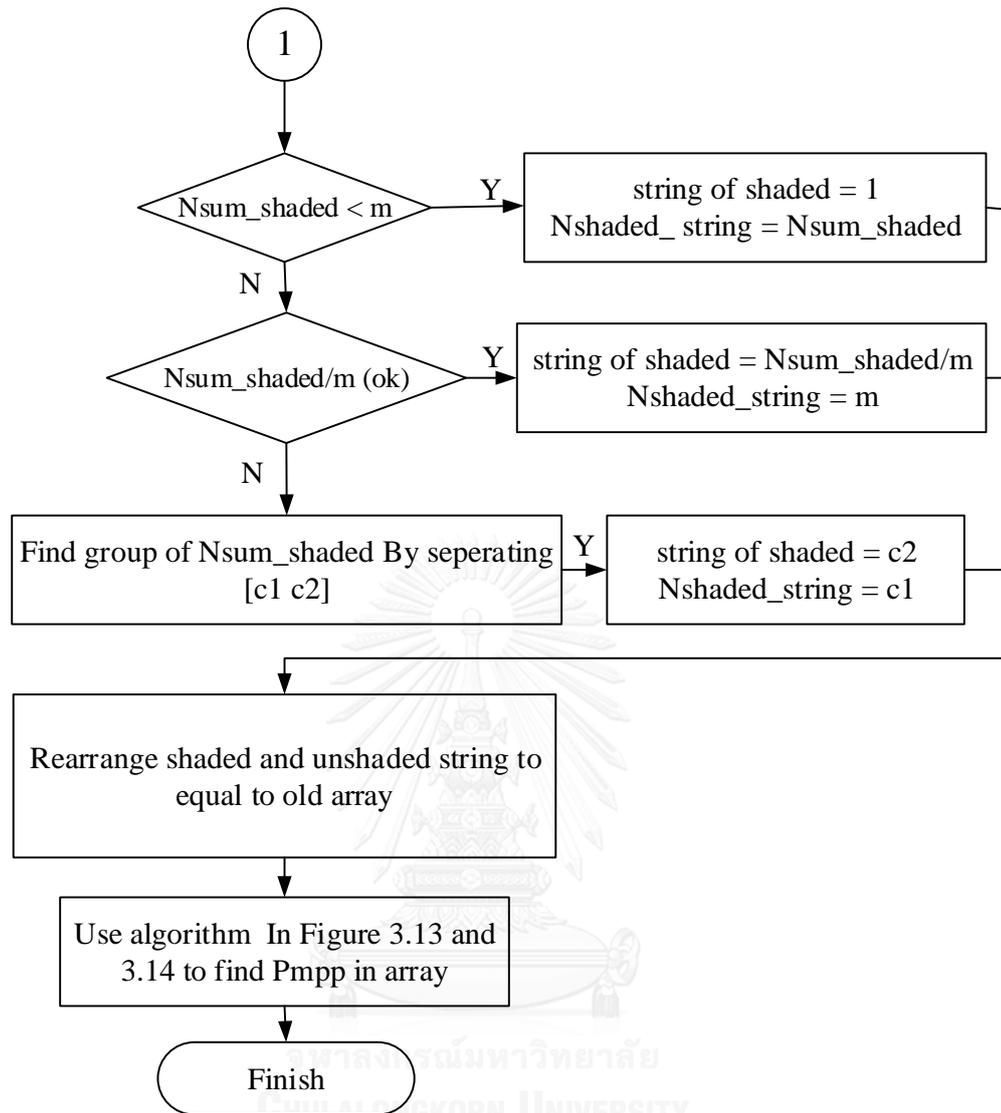
Figure 4.9 (Continued). The algorithm for rearrangement in PV array

The total number of the shaded modules is considered until it is less than the number of modules in string (m). Then, shaded and unshaded strings are rearranged. Finally, the algorithm of Figures 3.13 and 3.14 are used to find the maximum power point MPP in the array.

Chapter 5

Test Systems and Results

This chapter introduces 2 solar PV systems. The first system is a small one and located inside the Campus of Chulalongkorn University. The second system is larger and owned by a private company in Thailand (anonymous). Then the power generated from these systems are simulated to evaluate the effect of shading as well as the effectiveness of the proposed method.

5.1 A Solar PV System at Chulalongkorn University

This system with the installed capacity of 1.2 kW is located on the rooftop of Engineering Building 4, Faculty of Engineering. It contains 10 SP120 modules connected in series. The tilted surface is installed at 15° to the ground floor and 40° for the azimuth surface. That is, the PV modules are directed in southwest-facing [38]. The material of the solar cell is poly-crystalline. Solartron public company limited installed the system in 2011 as shown in Figure 5.1.

Figure 5.1. The PV system on the rooftop of Building 4

The dc/ac inverter is Sunny Boy 2100TL, pictured in Figure 5.2, of SMA solar company limited. Technical data are provided in Table 5.1 [39].

Figure 5.2. Sunny Boy 2100TL

Table 5.1.Technical data of Sunny Boy 2100TL

Input (DC)	Max. DC power (@ $\cos\varphi = 1$)	2,200 kW
	Max. input voltage	600 V
	MPP voltage range	200 V - 480 V
	Max. input voltage/ initial voltage	125 V / 150 V
	Max. input current	12 A
Output (AC)	Max. apparent AC power	2,100 VA
	Max. output current	11 A
	Normal AC voltage range	180 V – 260 V
	Max. efficiency	96 %

There are 2 sensors for measuring solar irradiance and temperature as shown in Figure 5.3 [40]. The irradiance sensor measures the sunlight intensity in W/m^2 while the temperature sensor is for measuring module and ambient temperature. Tiled angle and azimuth surface of irradiance sensor are similar to the PV modules installation in Section 5.1.
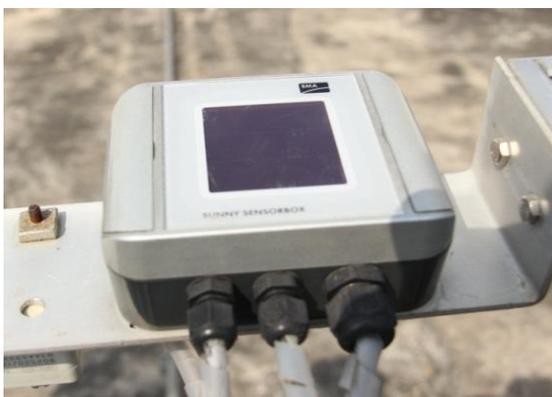
(a) Irradiance sensor   (b) Temperature sensor

Figure 5.3.Irradiance and temperature sensors

There are some suggestions for installing PV devices including PV module, sensors, and inverter as follows.

5.1.1 PV module installation

The most important parameter that affects PV modules performance is solar radiation. Obviously, PV modules must be installed outside for achieving the sunlight. The position and angle of a PV module are 2 major factors in PV system design. The PV tilted angle should be limited from 15 to 32° [41] and the module should be directed in south-facing for generating the highest power [42].

5.1.2 Irradiance sensor

This device must be installed along with the PV module and with the same angle and direction. Whereas, its place should be close to the PV module to measure the sunlight intensity more accurately.

5.1.3 Temperature sensor

The sensor should be installed near the PV module for recording module temperature and the ambient temperature. Both temperatures are useful for analyzing PV generation. The environmental temperature in the work of photometric is in the range [-25°C, +70°C].

5.1.4 Inverter

An inverter is an important part for converting DC to AC electricity in a solar PV system. Most components inside are electronic devices. The inverter must be installed inside a room or covered by a container to prevent strong sunlight and humidity.

In addition, there is a data recorder inside the Sunny Webbox as shown in Figure 5.4 [43]. This device records temperature, sunlight intensity and voltage, current and power of the inverter. These data can be linked to a Global System for Mobile communications modem (GSM modem).

Figure 5.4. Sunny Webbox data recorder

A single line diagram of the solar PV system is depicted in Figure 5.5
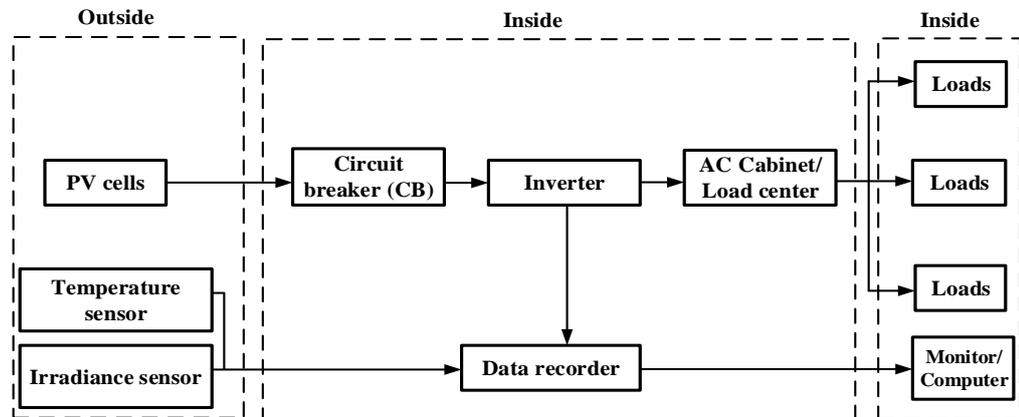
Figure 5.5. Single line diagram of the solar PV system on the rooftop of Building 4

In Figure 5.5, the data recorder receives information from the inverter and sensors. These information is delivered to a monitor or a computer. The resolution of the data transmission is 5 minutes. Table 5.2 lists some parameters with recorded values at 12:15 pm on 20/March/2014.

Table 5.2. Parameters of the data recorder

Time	IntSolIrr	TmpAmb	TmpMdul	Wind Vel	dI	E-Total	Fac	h-On
hh:mm	W/m^2	°C	°C	m/s	mA	kWh	Hz	hr
12:15	778.98	33.61	47.48	0	4	4,181.33	49.99	13,015.3

Parameters (continued)

h-Total	Iac-Ist	Ipv	Pac	Status	Uac	Upv-Soll	Zac
hr	mA	mA	W		V	V	Ohm
9,973.2	2,862.64	4,705.62	651.53	7: Mpp	227.78	149.5	0.45

where:

Time	Time recorder every 5 minutes (Hr:min)
IntSolIrr	Average irradiation every 5 minutes (W/m^2)
TmpAmb	Ambient temperature (°C)
TmpMdul	Module temperature (°C)
dI	Leakage current (mA)
E-Total	Energy in system (kWh)
Fac	Frequency system (Hz)
h-On	Total hour of PV operation (Hr)
h-Total	Total hour PV system supply power to load (Hr)
Iac-Ist	PV current system (mA)
Ipv	PV direct current (mA)
Pac	Real power system (W)

Status	Mode operation
Uac	Voltage system (V)
Upv-Soll	PV voltage in DC (V)
Zac	Grid impedance (Ω)

5.2 Ayutthaya PV System

This PV system shown in Figure 5.6 is located in an area of 800,000 square meters (500 rais in Thai measurement system) in Ayutthaya province of Thailand. The installed capacity is 44 MW.

Figure 5.6. Ayutthaya PV system

The connection of electrical equipment in this PV system consists of many transformers, PV arrays, and inverters. PV arrays are installed by Suntech Power Company limited with 150,000 modules of Suntech STP295-24/Vd [33]. The technical data are shown in Table 5.3. The inverters are installed by SMA Solar Limited who co-operates with Suntech Power Company limited. There are 61 inverters of Sunny Central (630HE) [44] with technical data shown in Table 5.4. In addition, 10 transformers are installed in this PV system which is connected to the utility systems of both the Provincial Electricity Authority (PEA) and the Electricity Generating Authority of Thailand (EGAT). These transformers are connected by different number of inverters. There are more or less than 7 inverters which are connected to a transformer. As an example as in Figure 5.7, a transformer is connected to 7 inverters and an inverter is connected to 9 PV arrays with different sizes.
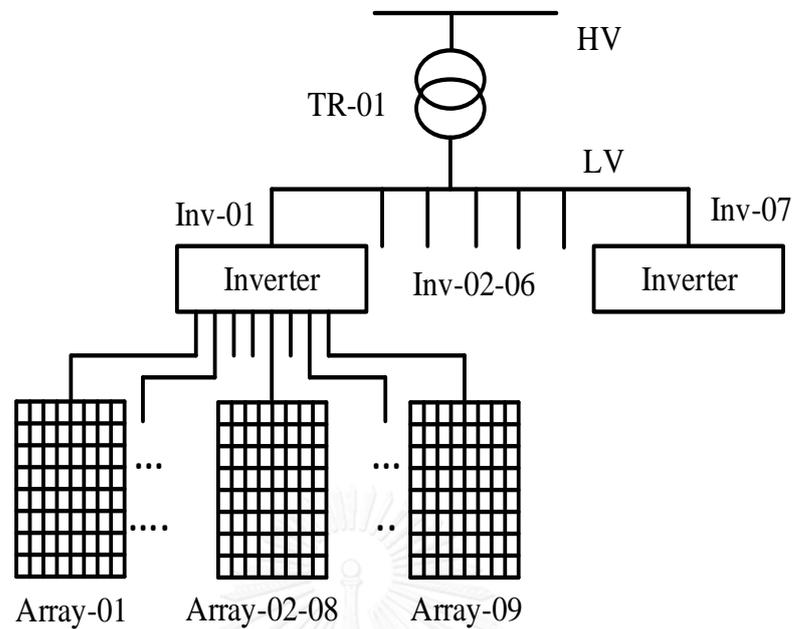
Figure 5.7. A transformer with inverters and PV arrays connection

Table 5.3. STP295-24/Vd solar module from Suntech Power Company limited

Parameters	Units
Maximum power (P_{MPP})	295 W
Maximum power voltage (V_{MPP})	35.7 V
Maximum power current (I_{MPP})	8.27 A
Open circuit voltage (V_{OC})	45.1 V
Shot circuit current (I_{SC})	8.57 A
Temperature coefficient of short circuit current (K_i)	0.055 A/°C
Temperature coefficient of open circuit voltage (K_v)	-0.33 V/°C
Number cell per module (N_s)	72 Cells

Table 5.4. Technical data of inverter for SMA Sunny Central 630HE

Max. DC power (@ cosφ=1)	642 kW
Max. input voltage	1,000 V
Max. input current	1,350 A
MPP voltage range	500 V - 820 V
Max. apparent AC power	630 kVA
Max. output current	1,155 A
Normal AC voltage range	315 V
Max. efficiency	98.6 %

This system only considers one array size 8x20 modules, 20 modules in series connection is named a string, 8 strings in parallel are called an array as shown in Figure

5.8. The reason to consider this array dimension is examination of reducing power due to moving clouds.
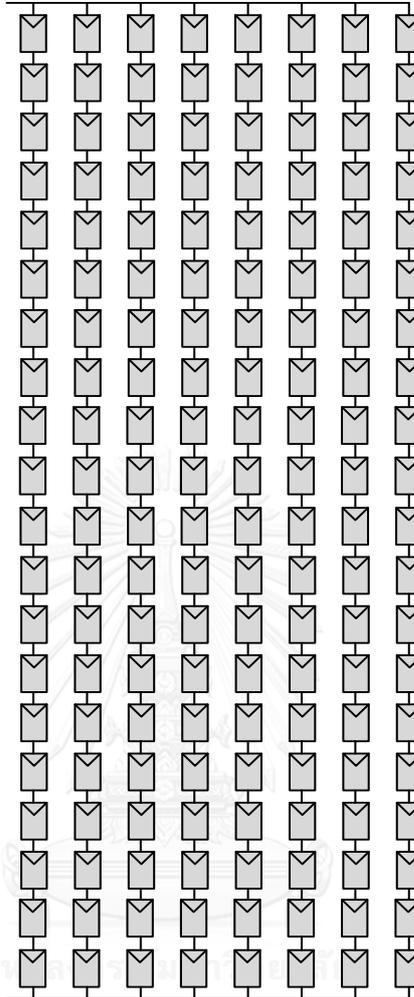
Figure 5.8. An array of 8x20 modules in series and parallel connections

5.3 The Simulated Results of PV Module

Table 5.5 shows technical data of SP120. These data are used in the simulated model for single diode. Also, 4 parameters was computed as shown in Table 5.6.

Table 5.5. SP120-24/Vd PV module from Solartron Public Company limited

Parameters	Units
Maximum power (P_{MPP})	120 W
Maximum power voltage (V_{MPP})	17.28 V
Maximum power current (I_{MPP})	7 A
Open circuit voltage (V_{OC})	21.7 V
Shot circuit current (I_{SC})	7.45 A
Temperature coefficient of short circuit current (K_i)	0.033 A/K
Temperature coefficient of open circuit voltage (K_v)	-0.0074 V/K
Number cell per module (N_s)	36 Cells

Table 5.6. Four parameters in simulated model

Shunt resistance	198.09 (Ω)
Series resistance	0.158 (Ω)
Saturation current	212 (nA)
Photoelectric current	7.61 (A)

5.3.1 The Effect of Temperature

In the simulation, temperature is assumed at 75°C, 50°C and 25°C. Irradiation is set constantly at 1000 W/m². Both the irradiation and temperature were used in simulated model as introduced in Section 2.2.3.1 of Chapter 2. Therefore, the relationships among voltage (V), current (I) and power (P) can be demonstrated in Figures 5.9 and 5.10.
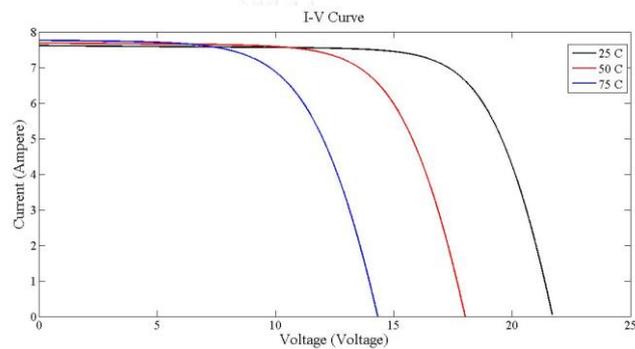
Figure 5.9. Relationships between voltage and current at different temperatures
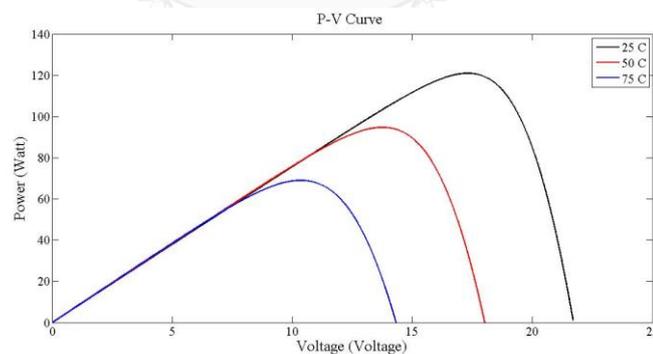
Figure 5.10. Relationships between voltage and power at different temperatures

5.3.2 The Effect of Sunlight Intensity

In simulation, irradiation is tested at 1000, 800, 600, 400, and 200 W/m². Temperature is set constantly at 25°C. Both the irradiation and temperature were used in the simulated model introduced in Section 2.2.3.2 of Chapter 2. Relationships among voltage (V), current (I) and power (P) are illustrated in Figures 5.11 and 5.12.
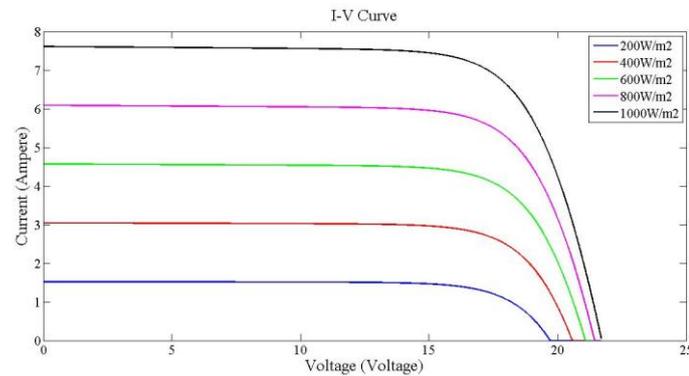
Figure 5.11. Relationships between voltage and current at different irradiation
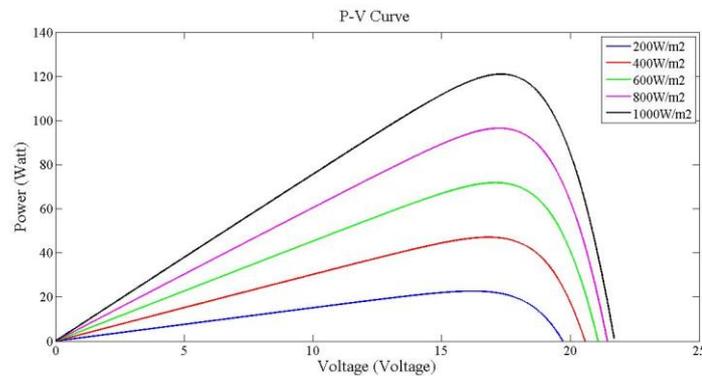
Figure 5.12. Relationships between voltage and power at different irradiation

5.4 Simulation

The simulation is carried out with a string of SP120. Then, operation of a PV array in size of 5x10 modules is simulated.

5.4.1 The simulation on a string of 1x10 modules

The simulation is performed on a string of 10 PV modules for evaluating the impact of partial shading. The simulation is divided into 6 cases. Experimental results are summarized in Table 5.7. For example, two modules are arranged to be shaded in Case 1 as shown in Figure 5.13. The radiation is set at 45% of 1000 W/m^2. Relationship between voltage (V) and current (I) is illustrated in Figure 5.14 (a). Changing of power (P) is demonstrated by Figure 5.14 (b) where multiple maximum power points (MPPs) are located at 925.60 W and 723.20 W.

Table 5.7. Summary of simulated setting and results

Cases	Irradiation (Out of 1000 W/m²)	Number of shaded modules	Multiple Maximum Power Points (W)	
			Point 1	Point 2
1	45%	2	925.60	723.20
2	45%	5	578.47	685.56
3	45%	8	231.40	648.40
4	25%	5	578.50	918.00
5	50%	5	578.50	624.60
6	70%	5	578.50	233.00

Figure 5.13. Case 1: A string with 2 shaded modules
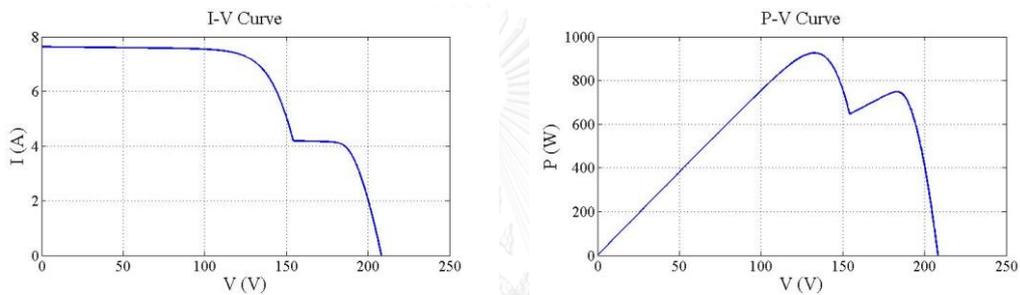
(a) voltage and current   (b) voltage and power

Figure 5.14. Relationships among voltage, current and power with 2 shaded modules in Case 1
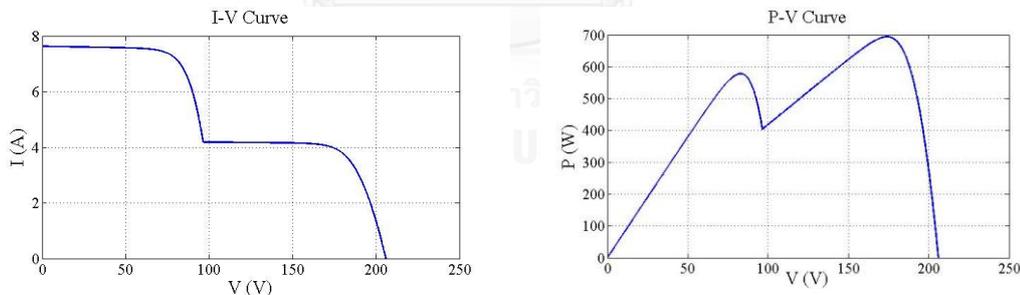
(a) voltage and current   (b) voltage and power

Figure 5.15. Relationships among voltage, current and power in Case 2
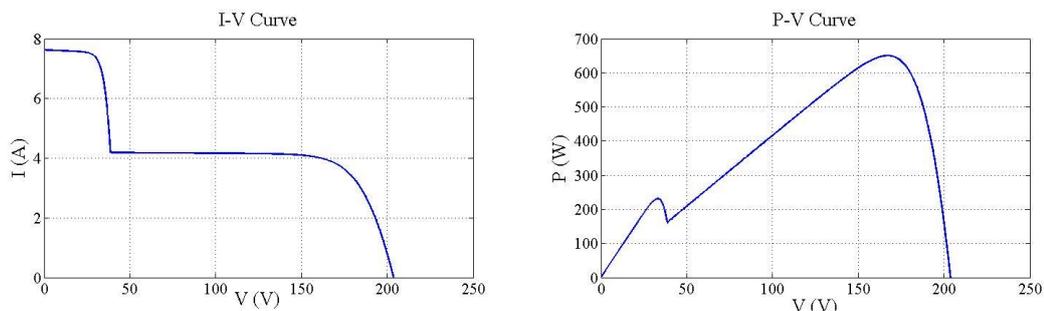
(a) voltage and current   (b) voltage and power

Figure 5.16. The relationships in Case 3
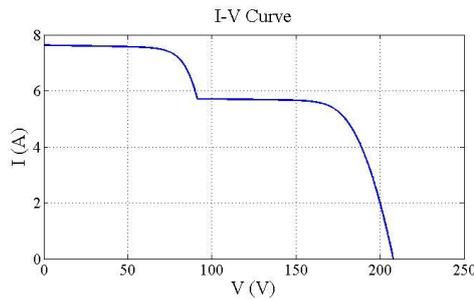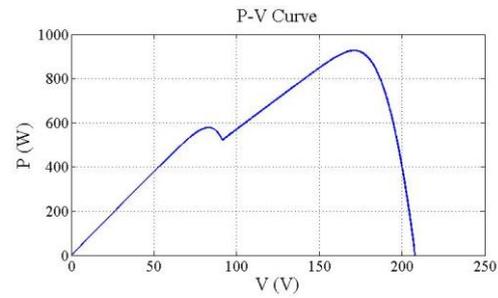
(a) voltage and current   (b) voltage and power

Figure 5.17.The relationships in Case 4
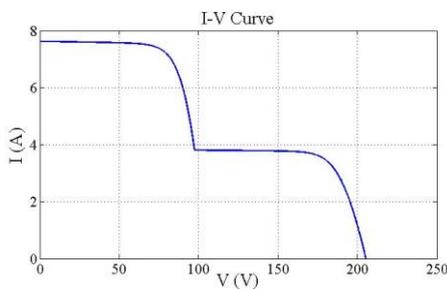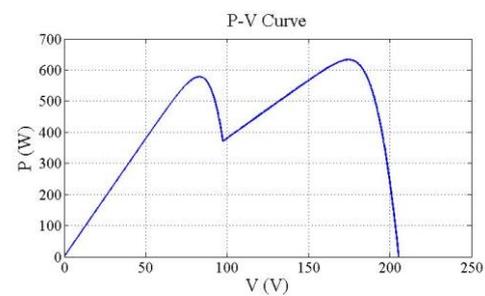
(a) voltage and current   (b) voltage and power

Figure 5.18.Relationships in Case 5
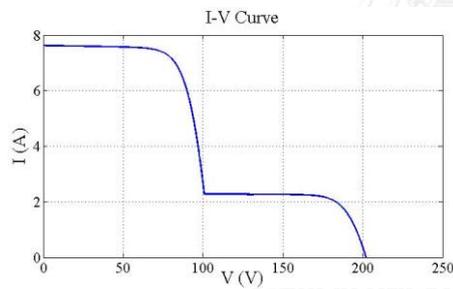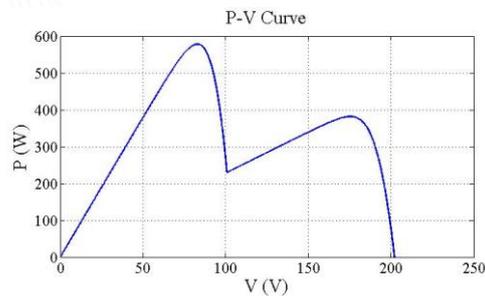
(a) voltage and current   (b) voltage and power

Figure 5.19. Relationships in Case 6

5.4.2 Simulation on an Array of 5x10 Modules

Instead of using one string as in the simulation in Section 5.4.2, in this Section, 5 strings are used. Some of the PV modules are shaded at 50% of the full irradiance. In the simulation, the shading patterns are divided into three cases which will be simulated by Mathlab. The shaded modules in an array can use the algorithm of Section 3.7 in chapter 3. The rearrangement can use the algorithm of Section 4.6 in chapter 4. The test system is example which uses the characteristics of SP120 in section 5.4.1 in this chapter.

Case 1. Two rows are shaded as shown in Figure 5.20. Relationship between voltage (V) and current (I) is illustrated in Figure 5.21 (a). Changing of power (P) is demonstrated by Figures 5.21 (b) where multiple maximum power points (MPPs) are located at 4,627 W and 3,425 W.
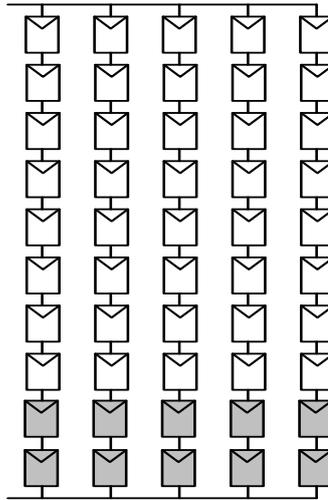
Figure 5.20. An array with 2 shaded rows
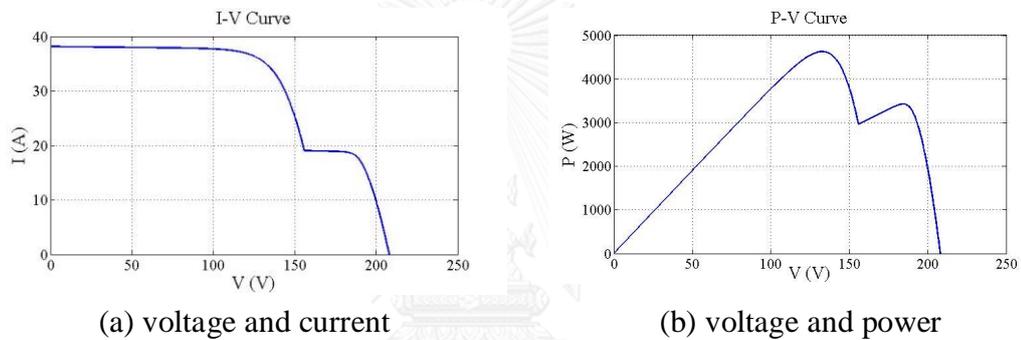
(a) voltage and current   (b) voltage and power

Figure 5.21. Relationships in the Simulation Case 1

Case 2: A half of 2 strings are shaded as shown in Figure 5.22. Relationship between voltage (V) and current (I) is illustrated in Figure 5.23 (a). Changing of power (P) is demonstrated by Figure 5.23 (b) where multiple maximum power points (MPPs) are located at 4,741 W and 3,158 W.
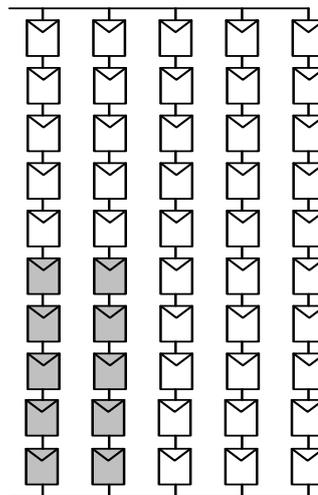
Figure 5.22.An array with a half of 2 strings shaded
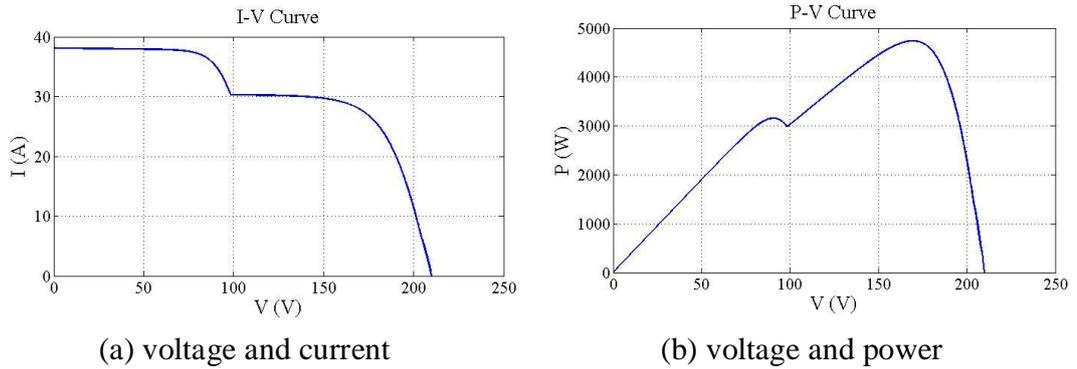
(a) voltage and current   (b) voltage and power

Figure 5.23. Relationships in Simulation Case 2

Case 3: One string is shaded as shown in Figure 5.24. Relationship between voltage (V) and current (I) is illustrated in Figure 5.25 (a). Changing of power (P) is demonstrated by Figure 5.25 (b) where only one maximum power point (MPP) is located at 5,219 W.
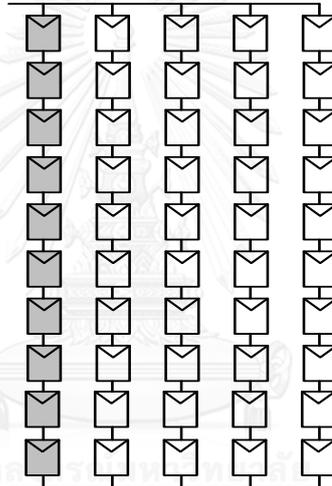
Figure 5.24. An array with 1 shaded string
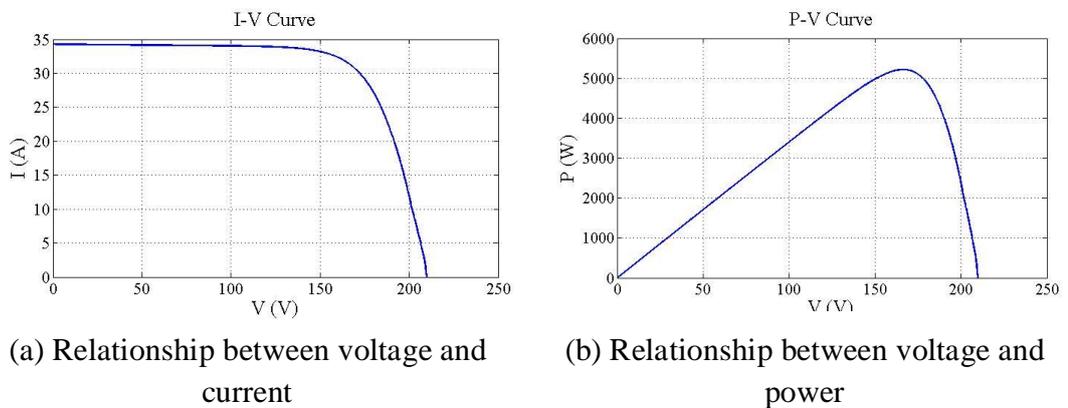
(a) Relationship between voltage and current   (b) Relationship between voltage and power

Figure 5.25. Relationships in Simulation Case 3

Simulation results of three cases are listed in Table 5.8.

Table 5.8. Simulation results

Cases	Irradiation (Out of 1000 W/m^2)	Maximum Power Points (W)		Increase of MPP compared to the base case (Case 1) (%)
		Point 1	Point 2	
1	50%	4,627	3,425	0.00
2	50%	4,741	3,158	2.46
3	50%	5,219		12.79

5.5 Rearrangement

In this simulation, the PV array of 5x10 modules in Section 5.4.2 continues to be utilized. The shaded patterns in a PV array are shown in Figure 5.26 (a), (b), (c), and (d), respectively.

(a) Two shaded rows on the bottom   (b) Two shaded rows on the top

(c) Half of 2 strings on the bottom-left   (d) Half of 2 strings on the top-right with
                  with shading   shading
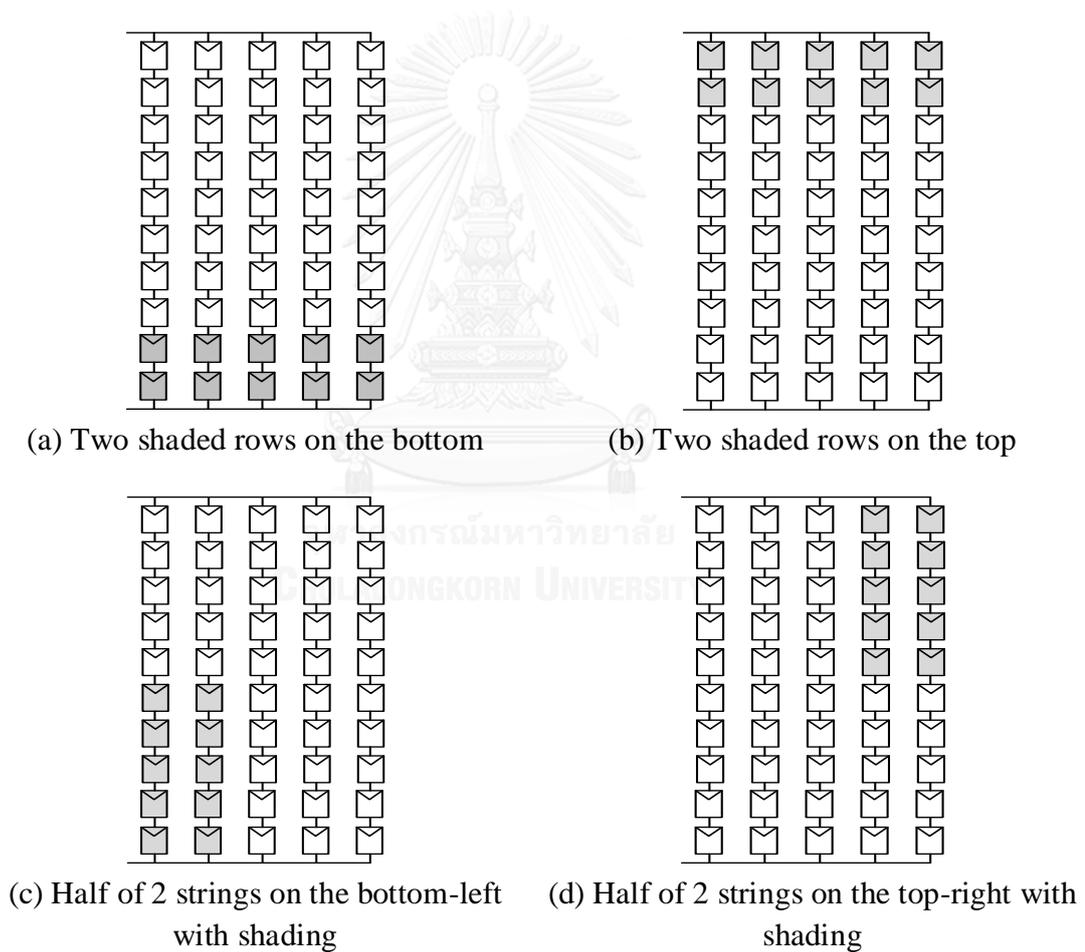
Figure 5.26. Different shaded patterns

The different shaded patterns in Figure 5.26 (a) and (b) result in the same I-V and P-V curves as shown in Figure 5.27. Whereas, the two shaded patterns in Figure 5.26 (c) and (d) result in the same I-V and P-V curves as shown in Figure 5.28.
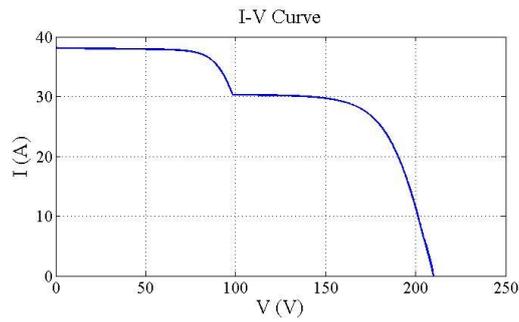
(a) Relationship between voltage and current
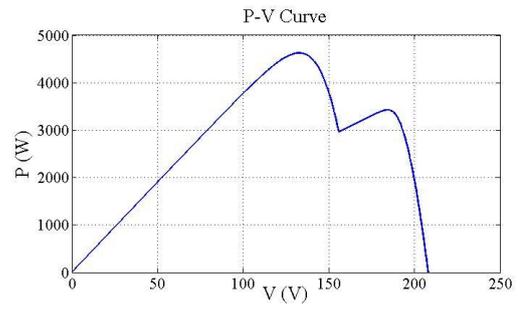
(b) Relationship between voltage and power

Figure 5.27. Relationships among voltage, current and power with two shaded rows
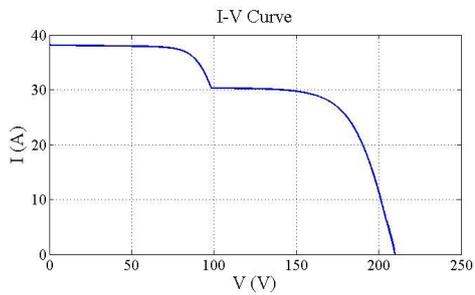
(a) Relationship between voltage and current
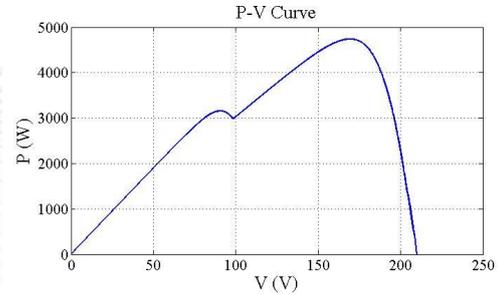
(b) Relationship between voltage and power

Figure 5.28.Relationships among voltage, current and power when a half of 2 strings are shaded

Effects of these shaded patterns can be mitigated by rearranging electrical connection of PV modules as show in Figures 5.29 (a), (b), (c) and (d), respectively.

(a)

(b)
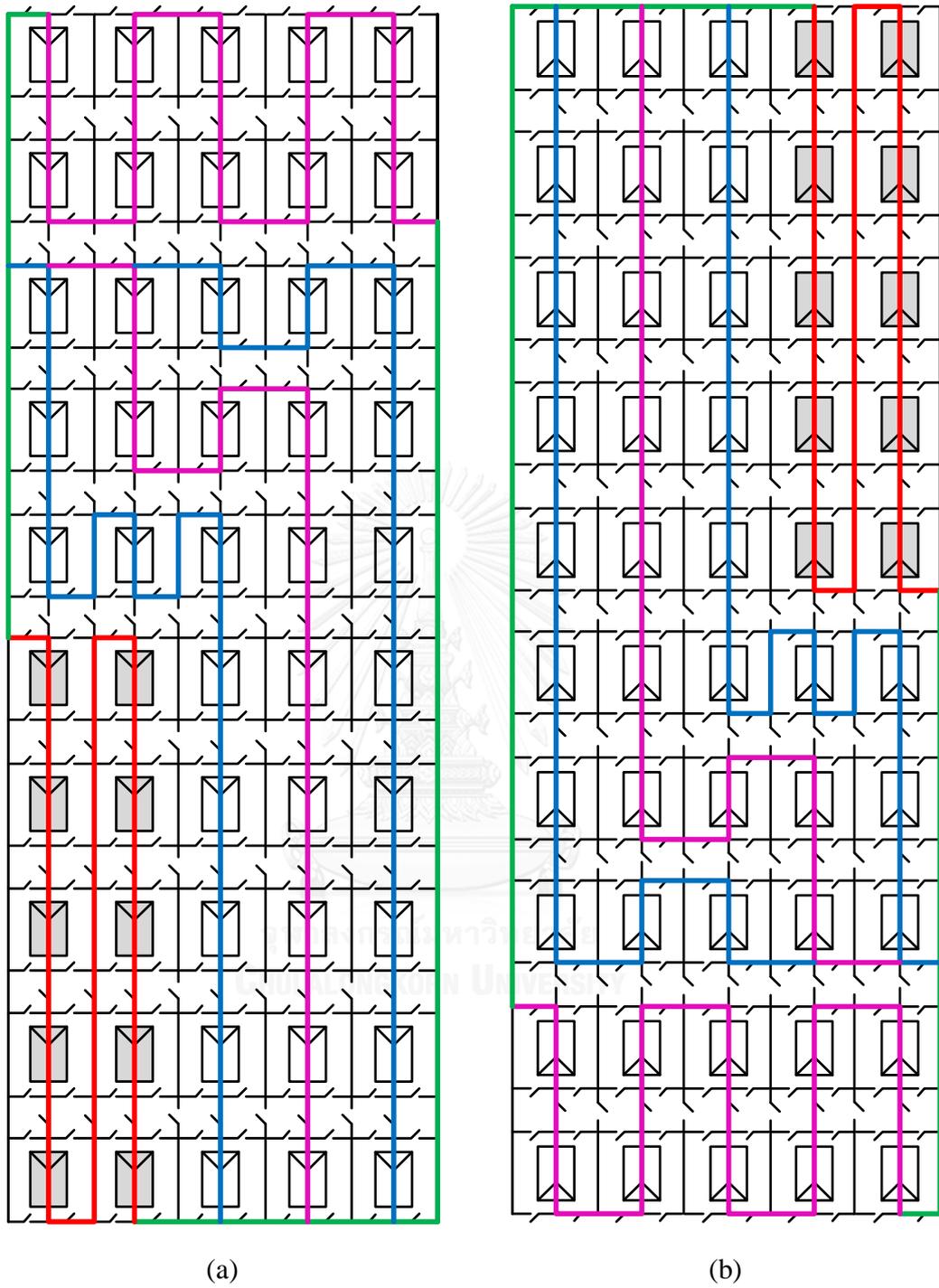
Figure 5.29. Rearrangement in PV array
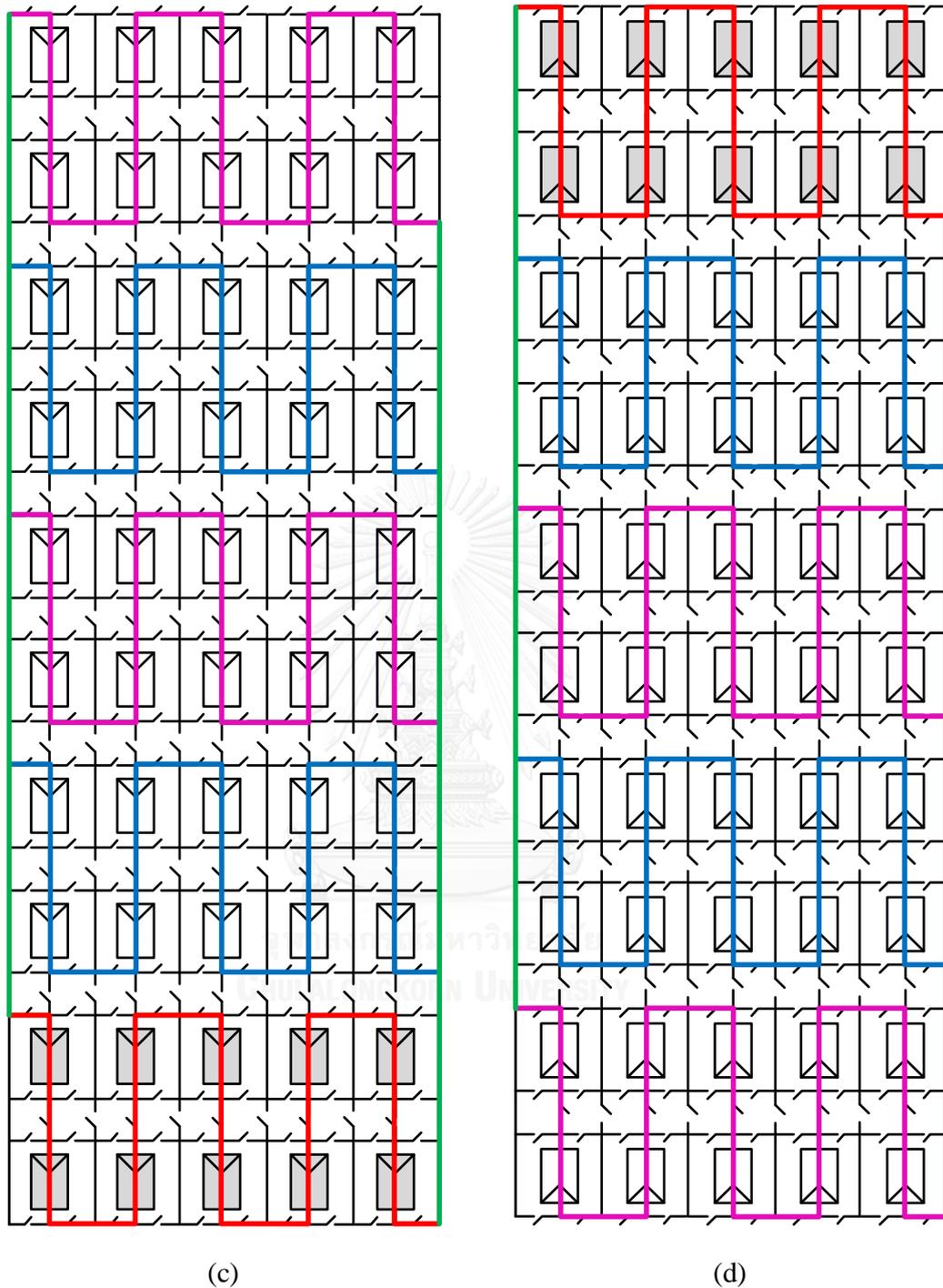
(c)   (d)

Figure 5.29 (Continued). Rearrangement in PV array

Finally, with the rearrangement shown in Figures 5.29, the number of MPPs are reduced from 2 to only one MPP as shown in Figure 5.30 in which the highest MPP is located at 5,219 W.
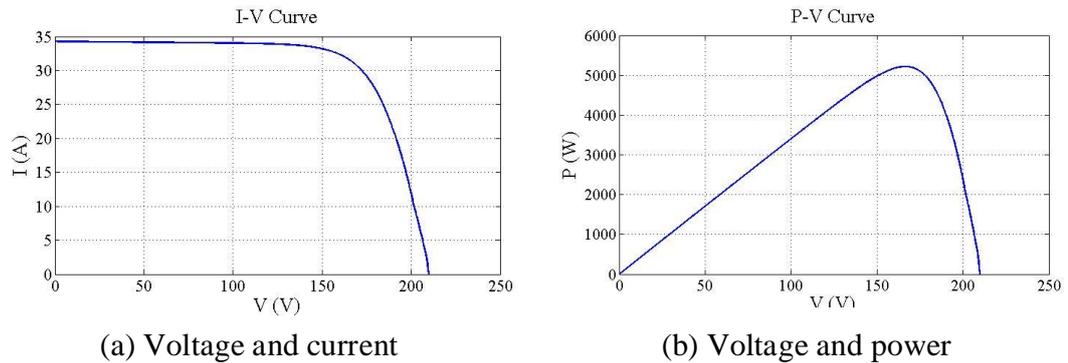
(a) Voltage and current   (b) Voltage and power

Figure 5.30. Relationships among voltage, current and power with one MPP

5.6 Simulation on an Array of 8x20 Modules with Consideration of Tilted Angle

In this section, a PV array of 8x20 modules is simulated with the tilted angle of 15° and the azimuth surface of 40° Southwest-facing. These PV modules are STP295-24/Vd, Suntech Power Company limited. There are six shaded patterns as shown in Figure 5.31 associated with three levels of 20%, 50% and 80% of full irradiation. The real information about temperature and irradiation recorded on the rooftop of Engineering Building 4, 21/March/2014 is shown in Table 5.9.

Table 5.9. Real information

Duration of time	10:00	11:00	12:00	13:00	14:00
Irradiation (W/m^2)	990.13	1,065.60	1,083.55	989.28	991.32
Ambient temperature (℃)	32.69	33.63	34.76	33.81	34.65
Module temperature (℃)	44.31	50.79	51.35	47.65	49.49
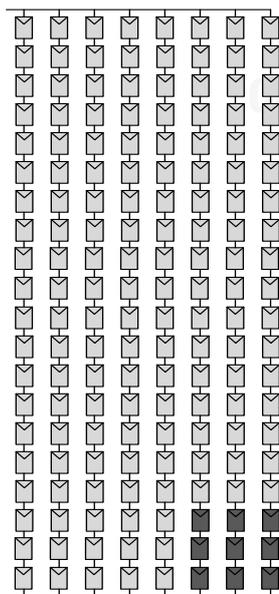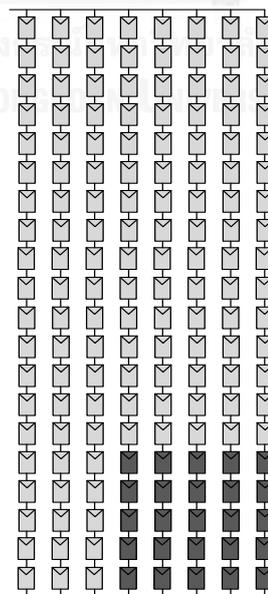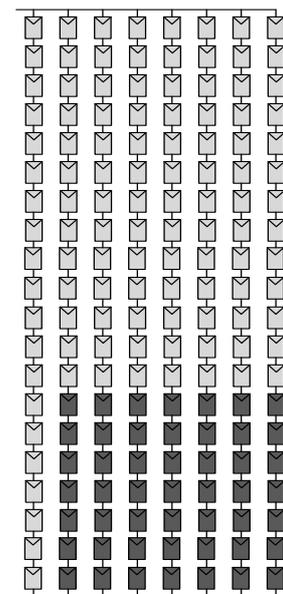
Shaded pattern 1   Shaded pattern 2   Shaded pattern 3
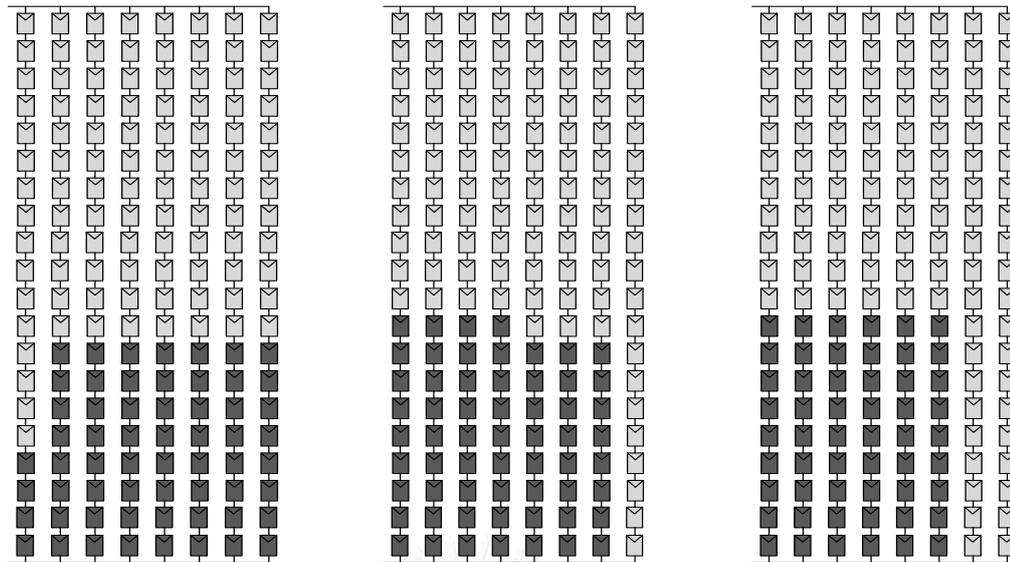
Shaded pattern 4   Shaded pattern 5   Shaded pattern 6
Figure 5.31. Shaded patterns on an array of 8x20 modules

For the ease of demonstration, the rearrangement of PV modules can be represented by tables where rows and columns are considered as PV modules. Six shaded patterns are demonstrated by six tables as Tables 5.10, 5.11, 5.12, 5.13, 5.14, and 5.15.

In pattern 1, nine modules are shaded so that the PV array can be categorized into 2 groups. The first group consists of five unshaded strings. The second group, which is structured from the rest 3 strings, is with 3 shaded modules per string as shown in Table 5.10. Similar categorizations are performed for the other patterns.

Table 5.10. Shaded pattern 1 before rearrangement

A PV array of 8x20 modules							
String1	String2	String3	String4	String5	String6	String7	String8
1.1	2.1	3.1	4.1	5.1	6.1	7.1	8.1
1.2	2.2	3.2	4.2	5.2	6.2	7.2	8.2
1.3	2.3	3.3	4.3	5.3	6.3	7.3	8.3
1.4	2.4	3.4	4.4	5.4	6.4	7.4	8.4
1.5	2.5	3.5	4.5	5.5	6.5	7.5	8.5
1.6	2.6	3.6	4.6	5.6	6.6	7.6	8.6
1.7	2.7	3.7	4.7	5.7	6.7	7.7	8.7
1.8	2.8	3.8	4.8	5.8	6.8	7.8	8.8
1.9	2.9	3.9	4.9	5.9	6.9	7.9	8.9
1.10	2.10	3.10	4.10	5.10	6.10	7.10	8.10
1.11	2.11	3.11	4.11	5.11	6.11	7.11	8.11
1.12	2.12	3.12	4.12	5.12	6.12	7.12	8.12
1.13	2.13	3.13	4.13	5.13	6.13	7.13	8.13
1.14	2.14	3.14	4.14	5.14	6.14	7.14	8.14
1.15	2.15	3.15	4.15	5.15	6.15	7.15	8.15
1.16	2.16	3.16	4.16	5.16	6.16	7.16	8.16
1.17	2.17	3.17	4.17	5.17	6.17	7.17	8.17
1.18	2.18	3.18	4.18	5.18	6.18	7.18	8.18
1.19	2.19	3.19	4.19	5.19	6.19	7.19	8.19
1.20	2.20	3.20	4.20	5.20	6.20	7.20	8.20

Table 5.11. Shaded pattern 2 before rearrangement

A PV array of 8x20 modules							
String1	String2	String3	String4	String5	String6	String7	String8
1.1	2.1	3.1	4.1	5.1	6.1	7.1	8.1
1.2	2.2	3.2	4.2	5.2	6.2	7.2	8.2
1.3	2.3	3.3	4.3	5.3	6.3	7.3	8.3
1.4	2.4	3.4	4.4	5.4	6.4	7.4	8.4
1.5	2.5	3.5	4.5	5.5	6.5	7.5	8.5
1.6	2.6	3.6	4.6	5.6	6.6	7.6	8.6
1.7	2.7	3.7	4.7	5.7	6.7	7.7	8.7
1.8	2.8	3.8	4.8	5.8	6.8	7.8	8.8
1.9	2.9	3.9	4.9	5.9	6.9	7.9	8.9
1.10	2.10	3.10	4.10	5.10	6.10	7.10	8.10
1.11	2.11	3.11	4.11	5.11	6.11	7.11	8.11
1.12	2.12	3.12	4.12	5.12	6.12	7.12	8.12
1.13	2.13	3.13	4.13	5.13	6.13	7.13	8.13
1.14	2.14	3.14	4.14	5.14	6.14	7.14	8.14
1.15	2.15	3.15	4.15	5.15	6.15	7.15	8.15
1.16	2.16	3.16	4.16	5.16	6.16	7.16	8.16
1.17	2.17	3.17	4.17	5.17	6.17	7.17	8.17
1.18	2.18	3.18	4.18	5.18	6.18	7.18	8.18
1.19	2.19	3.19	4.19	5.19	6.19	7.19	8.19
1.20	2.20	3.20	4.20	5.20	6.20	7.20	8.20

Table 5.12. Shaded pattern 3 before rearrangement

A PV array of 8x20 modules							
String1	String2	String3	String4	String5	String6	String7	String8
1.1	2.1	3.1	4.1	5.1	6.1	7.1	8.1
1.2	2.2	3.2	4.2	5.2	6.2	7.2	8.2
1.3	2.3	3.3	4.3	5.3	6.3	7.3	8.3
1.4	2.4	3.4	4.4	5.4	6.4	7.4	8.4
1.5	2.5	3.5	4.5	5.5	6.5	7.5	8.5
1.6	2.6	3.6	4.6	5.6	6.6	7.6	8.6
1.7	2.7	3.7	4.7	5.7	6.7	7.7	8.7
1.8	2.8	3.8	4.8	5.8	6.8	7.8	8.8
1.9	2.9	3.9	4.9	5.9	6.9	7.9	8.9
1.10	2.10	3.10	4.10	5.10	6.10	7.10	8.10
1.11	2.11	3.11	4.11	5.11	6.11	7.11	8.11
1.12	2.12	3.12	4.12	5.12	6.12	7.12	8.12
1.13	2.13	3.13	4.13	5.13	6.13	7.13	8.13
1.14	2.14	3.14	4.14	5.14	6.14	7.14	8.14
1.15	2.15	3.15	4.15	5.15	6.15	7.15	8.15
1.16	2.16	3.16	4.16	5.16	6.16	7.16	8.16
1.17	2.17	3.17	4.17	5.17	6.17	7.17	8.17
1.18	2.18	3.18	4.18	5.18	6.18	7.18	8.18
1.19	2.19	3.19	4.19	5.19	6.19	7.19	8.19
1.20	2.20	3.20	4.20	5.20	6.20	7.20	8.20

Table 5.13. Shaded pattern 4 before rearrangement

A PV array of 8x20 modules							
String1	String2	String3	String4	String5	String6	String7	String8
1.1	2.1	3.1	4.1	5.1	6.1	7.1	8.1
1.2	2.2	3.2	4.2	5.2	6.2	7.2	8.2
1.3	2.3	3.3	4.3	5.3	6.3	7.3	8.3
1.4	2.4	3.4	4.4	5.4	6.4	7.4	8.4
1.5	2.5	3.5	4.5	5.5	6.5	7.5	8.5
1.6	2.6	3.6	4.6	5.6	6.6	7.6	8.6
1.7	2.7	3.7	4.7	5.7	6.7	7.7	8.7
1.8	2.8	3.8	4.8	5.8	6.8	7.8	8.8
1.9	2.9	3.9	4.9	5.9	6.9	7.9	8.9
1.10	2.10	3.10	4.10	5.10	6.10	7.10	8.10
1.11	2.11	3.11	4.11	5.11	6.11	7.11	8.11
1.12	2.12	3.12	4.12	5.12	6.12	7.12	8.12
1.13	2.13	3.13	4.13	5.13	6.13	7.13	8.13
1.14	2.14	3.14	4.14	5.14	6.14	7.14	8.14
1.15	2.15	3.15	4.15	5.15	6.15	7.15	8.15
1.16	2.16	3.16	4.16	5.16	6.16	7.16	8.16
1.17	2.17	3.17	4.17	5.17	6.17	7.17	8.17
1.18	2.18	3.18	4.18	5.18	6.18	7.18	8.18
1.19	2.19	3.19	4.19	5.19	6.19	7.19	8.19
1.20	2.20	3.20	4.20	5.20	6.20	7.20	8.20

.

Table 5.14. Shaded pattern 5 before rearrangement

A PV array of 8x20 modules							
String1	String2	String3	String4	String5	String6	String7	String8
1.1	2.1	3.1	4.1	5.1	6.1	7.1	8.1
1.2	2.2	3.2	4.2	5.2	6.2	7.2	8.2
1.3	2.3	3.3	4.3	5.3	6.3	7.3	8.3
1.4	2.4	3.4	4.4	5.4	6.4	7.4	8.4
1.5	2.5	3.5	4.5	5.5	6.5	7.5	8.5
1.6	2.6	3.6	4.6	5.6	6.6	7.6	8.6
1.7	2.7	3.7	4.7	5.7	6.7	7.7	8.7
1.8	2.8	3.8	4.8	5.8	6.8	7.8	8.8
1.9	2.9	3.9	4.9	5.9	6.9	7.9	8.9
1.10	2.10	3.10	4.10	5.10	6.10	7.10	8.10
1.11	2.11	3.11	4.11	5.11	6.11	7.11	8.11
1.12	2.12	3.12	4.12	5.12	6.12	7.12	8.12
1.13	2.13	3.13	4.13	5.13	6.13	7.13	8.13
1.14	2.14	3.14	4.14	5.14	6.14	7.14	8.14
1.15	2.15	3.15	4.15	5.15	6.15	7.15	8.15
1.16	2.16	3.16	4.16	5.16	6.16	7.16	8.16
1.17	2.17	3.17	4.17	5.17	6.17	7.17	8.17
1.18	2.18	3.18	4.18	5.18	6.18	7.18	8.18
1.19	2.19	3.19	4.19	5.19	6.19	7.19	8.19
1.20	2.20	3.20	4.20	5.20	6.20	7.20	8.20

Table 5.15. Shaded pattern 6 before rearrangement

A PV array of 8x20 modules							
String1	String2	String3	String4	String5	String6	String7	String8
1.1	2.1	3.1	4.1	5.1	6.1	7.1	8.1
1.2	2.2	3.2	4.2	5.2	6.2	7.2	8.2
1.3	2.3	3.3	4.3	5.3	6.3	7.3	8.3
1.4	2.4	3.4	4.4	5.4	6.4	7.4	8.4
1.5	2.5	3.5	4.5	5.5	6.5	7.5	8.5
1.6	2.6	3.6	4.6	5.6	6.6	7.6	8.6
1.7	2.7	3.7	4.7	5.7	6.7	7.7	8.7
1.8	2.8	3.8	4.8	5.8	6.8	7.8	8.8
1.9	2.9	3.9	4.9	5.9	6.9	7.9	8.9
1.10	2.10	3.10	4.10	5.10	6.10	7.10	8.10
1.11	2.11	3.11	4.11	5.11	6.11	7.11	8.11
1.12	2.12	3.12	4.12	5.12	6.12	7.12	8.12
1.13	2.13	3.13	4.13	5.13	6.13	7.13	8.13
1.14	2.14	3.14	4.14	5.14	6.14	7.14	8.14
1.15	2.15	3.15	4.15	5.15	6.15	7.15	8.15
1.16	2.16	3.16	4.16	5.16	6.16	7.16	8.16
1.17	2.17	3.17	4.17	5.17	6.17	7.17	8.17
1.18	2.18	3.18	4.18	5.18	6.18	7.18	8.18
1.19	2.19	3.19	4.19	5.19	6.19	7.19	8.19
1.20	2.20	3.20	4.20	5.20	6.20	7.20	8.20

The rearrangements performed by re-wiring PV modules are illustrated by Tables 5.16, 5.17, 5.18, 5.19, 5.20, and 5.21, respectively.

In pattern 1, there are nine shaded modules. The reconnection is performed so that all shaded modules are move to one string only, let say String 1, as shown in Table 5.16.

Table 5.16. Shaded pattern 1 after rearrangement

A PV array of 8x20 modules							
String1	String2	String3	String4	String5	String6	String7	String8
8.18	8.16	8.13	8.11	8.8	8.6	8.3	8.1
8.19	8.17	8.14	8.12	8.9	8.7	8.4	8.2
8.20	7.16	8.15	7.11	8.10	7.6	8.5	7.1
7.18	7.17	7.13	7.12	7.8	7.7	7.3	7.2
7.19	6.16	7.14	6.11	7.9	6.6	7.4	6.1
7.20	6.17	7.15	6.12	7.10	6.7	7.5	6.2
6.18	5.16	6.13	5.11	6.8	5.6	6.3	5.1
6.19	5.17	6.14	5.12	6.9	5.7	6.4	5.2
6.20	4.16	6.15	4.11	6.10	4.6	6.5	4.1
5.18	4.17	5.13	4.12	5.8	4.7	5.3	4.2
5.19	4.18	5.14	4.13	5.9	4.8	5.4	4.3
5.20	3.16	5.15	3.11	5.10	3.6	5.5	3.1
4.19	3.17	4.14	3.12	4.9	3.7	4.4	3.2
4.20	3.18	4.15	3.13	4.10	3.8	4.5	3.3
3.19	2.16	3.14	2.11	3.9	2.6	3.4	2.1
3.20	2.17	3.15	2.12	3.10	2.7	3.5	2.2
2.19	2.18	2.14	2.13	2.9	2.8	2.4	2.3
2.20	1.16	2.15	1.11	2.10	1.6	2.5	1.1
1.19	1.17	1.14	1.12	1.9	1.7	1.4	1.2
1.20	1.18	1.15	1.13	1.10	1.8	1.5	1.3

Similarly, twenty-five shaded modules in pattern 2 are rearranged so that String 1 is fully shaded, the rest shaded modules are distributed to String 2 as shown in Table 5.17. Other cases are also carry out in the same idea of arrangement and illustrated by Tables 5.18, 5.19, 5.20 and 5.21.

Table 5.17. Shaded pattern 2 after rearrangement

A PV array of 8x20 modules							
String1	String2	String3	String4	String5	String6	String7	String8
8.17	8.14	8.12	8.11	8.8	8.6	8.3	8.1
8.18	8.15	8.13	7.11	8.9	8.7	8.4	8.2
8.19	8.16	7.12	6.11	8.10	7.6	8.5	7.1
8.20	7.14	7.13	5.11	7.8	7.7	7.3	7.2
7.17	7.15	6.12	4.11	7.9	6.6	7.4	6.1
7.18	7.16	6.13	4.12	7.10	6.7	7.5	6.2
7.19	6.14	5.12	3.11	6.8	5.6	6.3	5.1
7.20	6.15	5.13	3.12	6.9	5.7	6.4	5.2
6.17	6.16	4.13	2.11	6.10	4.6	6.5	4.1
6.18	5.14	4.14	2.12	5.8	4.7	5.3	4.2
6.19	5.15	3.13	1.11	5.9	4.8	5.4	4.3
6.20	5.16	3.14	1.12	5.10	3.6	5.5	3.1
5.17	4.15	2.13	1.13	4.9	3.7	4.4	3.2
5.18	4.16	2.14	1.14	4.10	3.8	4.5	3.3
5.19	3.15	2.15	1.15	3.9	2.6	3.4	2.1
5.20	3.16	2.16	1.16	3.10	2.7	3.5	2.2
4.17	3.17	2.17	1.17	2.9	2.8	2.4	2.3
4.18	3.18	2.18	1.18	2.10	1.6	2.5	1.1
4.19	3.19	2.19	1.19	1.9	1.7	1.4	1.2
4.20	3.20	2.20	1.20	1.10	1.8	1.5	1.3

Table 5.18. Shaded pattern 3 after rearrangement

A PV array of 8x20 modules							
String1	String2	String3	String4	String5	String6	String7	String8
8.17	8.15	8.13	8.11	8.8	8.6	8.3	8.1
8.18	8.16	8.14	8.12	8.9	8.7	8.4	8.2
8.19	7.15	7.13	7.11	8.10	7.6	8.5	7.1
8.20	7.16	7.14	7.12	7.8	7.7	7.3	7.2
7.17	6.15	6.13	6.11	7.9	6.6	7.4	6.1
7.18	6.16	6.14	6.12	7.10	6.7	7.5	6.2
7.19	6.17	5.13	5.11	6.8	5.6	6.3	5.1
7.20	5.15	5.14	5.12	6.9	5.7	6.4	5.2
6.18	5.16	4.14	4.11	6.10	4.6	6.5	4.1
6.19	5.17	3.14	4.12	5.8	4.7	5.3	4.2
6.20	4.15	3.15	4.13	5.9	4.8	5.4	4.3
5.18	4.16	2.14	3.11	5.10	3.6	5.5	3.1
5.19	4.17	2.15	3.12	4.9	3.7	4.4	3.2
5.20	3.16	1.14	3.13	4.10	3.8	4.5	3.3
4.18	3.17	1.15	2.11	3.9	2.6	3.4	2.1
4.19	2.16	1.16	2.12	3.10	2.7	3.5	2.2
4.20	2.17	1.17	2.13	2.9	2.8	2.4	2.3
3.18	2.18	1.18	1.11	2.10	1.6	2.5	1.1
3.19	2.19	1.19	1.12	1.9	1.7	1.4	1.2
3.20	2.20	1.20	1.13	1.10	1.8	1.5	1.3

Table 5.19. Shaded pattern 4 after rearrangement

A PV array of 8x20 modules							
String1	String2	String3	String4	String5	String6	String7	String8
8.17	8.15	8.13	8.11	8.8	8.6	8.3	8.1
8.18	8.16	8.14	8.12	8.9	8.7	8.4	8.2
8.19	7.15	7.13	7.11	8.10	7.6	8.5	7.1
8.20	7.16	7.14	7.12	7.8	7.7	7.3	7.2
7.18	7.17	6.13	6.11	7.9	6.6	7.4	6.1
7.19	6.15	6.14	6.12	7.10	6.7	7.5	6.2
7.20	6.16	5.13	5.11	6.8	5.6	6.3	5.1
6.18	6.17	5.14	5.12	6.9	5.7	6.4	5.2
6.19	5.15	4.13	4.11	6.10	4.6	6.5	4.1
6.20	5.16	4.14	4.12	5.8	4.7	5.3	4.2
5.18	5.17	4.15	3.11	5.9	4.8	5.4	4.3
5.19	4.16	3.13	3.12	5.10	3.6	5.5	3.1
5.20	4.17	3.14	2.11	4.9	3.7	4.4	3.2
4.19	4.18	3.15	2.12	4.10	3.8	4.5	3.3
4.20	3.16	2.13	1.11	3.9	2.6	3.4	2.1
3.19	3.17	2.14	1.12	3.10	2.7	3.5	2.2
3.20	3.18	2.15	1.13	2.9	2.8	2.4	2.3
2.19	2.18	2.16	1.14	2.10	1.6	2.5	1.1
2.20	1.18	2.17	1.15	1.9	1.7	1.4	1.2
1.20	1.19	1.17	1.16	1.10	1.8	1.5	1.3

Table 5.20. Shaded pattern 5 after rearrangement

A PV array of 8x20 modules							
String1	String2	String3	String4	String5	String6	String7	String8
1.17	1.14	1.12	1.11	1.8	1.6	1.3	1.1
1.18	1.15	1.13	2.11	1.9	1.7	1.4	1.2
1.19	1.16	2.12	3.11	1.10	2.6	1.5	2.1
1.20	2.14	2.13	4.11	2.8	2.7	2.3	2.2
2.17	2.15	3.12	5.11	2.9	3.6	2.4	3.1
2.18	2.16	3.13	5.12	2.10	3.7	2.5	3.2
2.19	3.14	4.12	6.11	3.8	4.6	3.3	4.1
2.20	3.15	4.13	6.12	3.9	4.7	3.4	4.2
3.17	3.16	5.13	7.11	3.10	5.6	3.5	5.1
3.18	4.14	5.14	7.12	4.8	5.7	4.3	5.2
3.19	4.15	6.13	8.11	4.9	5.8	4.4	5.3
3.20	4.16	6.14	8.12	4.10	6.6	4.5	6.1
4.17	5.15	7.13	8.13	5.9	6.7	5.4	6.2
4.18	5.16	7.14	8.14	5.10	6.8	5.5	6.3
4.19	6.15	7.15	8.15	6.9	7.6	6.4	7.1
4.20	6.16	7.16	8.16	6.10	7.7	6.5	7.2
5.17	6.17	7.17	8.17	7.9	7.8	7.4	7.3
5.18	6.18	7.18	8.18	7.10	8.6	7.5	8.1
5.19	6.19	7.19	8.19	8.9	8.7	8.4	8.2
5.20	6.20	7.20	8.20	8.10	8.8	8.5	8.3

Table 5.21. Shaded pattern 6 after rearrangement

A PV array of 8x20 modules							
String1	String2	String3	String4	String5	String6	String7	String8
1.16	1.13	1.11	1.9	1.8	1.6	1.3	1.1
1.17	1.14	1.12	1.10	2.8	1.7	1.4	1.2
1.18	1.15	2.11	2.9	3.8	2.6	1.5	2.1
1.19	2.13	2.12	2.10	4.8	2.7	2.3	2.2
1.20	2.14	3.11	3.9	4.9	3.6	2.4	3.1
2.16	2.15	3.12	3.10	5.9	3.7	2.5	3.2
2.17	3.13	4.11	4.10	6.9	4.6	3.3	4.1
2.18	3.14	4.12	5.10	7.9	4.7	3.4	4.2
2.19	3.15	5.11	6.10	8.9	5.6	3.5	5.1
2.20	4.13	5.12	7.10	8.10	5.7	4.3	5.2
3.16	4.14	6.11	7.11	8.11	5.8	4.4	5.3
3.17	4.15	6.12	7.12	8.12	6.6	4.5	6.1
3.18	5.13	6.13	7.13	8.13	6.7	5.4	6.2
3.19	5.14	6.14	7.14	8.14	6.8	5.5	6.3
3.20	5.15	6.15	7.15	8.15	7.6	6.4	7.1
4.16	5.16	6.16	7.16	8.16	7.7	6.5	7.2
4.17	5.17	6.17	7.17	8.17	7.8	7.4	7.3
4.18	5.18	6.18	7.18	8.18	8.6	7.5	8.1
4.19	5.19	6.19	7.19	8.19	8.7	8.4	8.2
4.20	5.20	6.20	7.20	8.20	8.8	8.5	8.3

5.6.1 Simulation of Power Generation in Shading Rearrangement

These simulations of the PV array size of 8x20 modules are carried out with real information about irradiation, temperature, tilted angle, and azimuth angle. Both irradiation and temperature are recorded at Building 4, Chulalongkorn University. The PV modules were installed by 15° of tilted angle and 40° of azimuth angle which directed in southwest-facing. Power generation for each shaded pattern can be simulated and demonstrated in Figures 5.32, 5.33, 5.34, 5.35, 5.36 and 5.37.

❖ Shaded pattern 1 before rearrangement
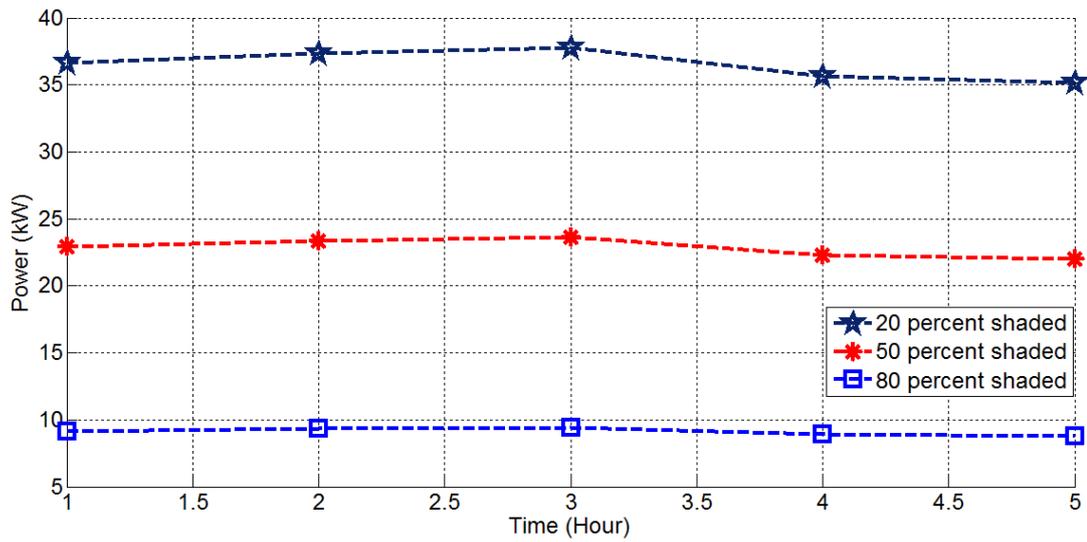
Figure 5.32. Power before rearrangement of shaded pattern 1

❖ Shaded pattern 2 before rearrangement
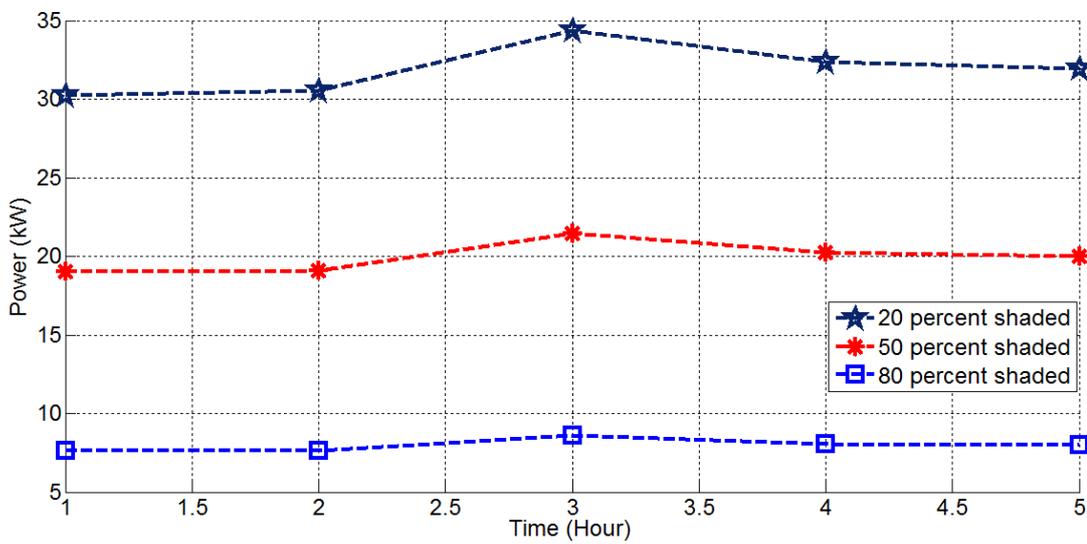
Figure 5.33. Power before rearrangement of shaded pattern 2

❖ Shaded pattern 3 before rearrangement
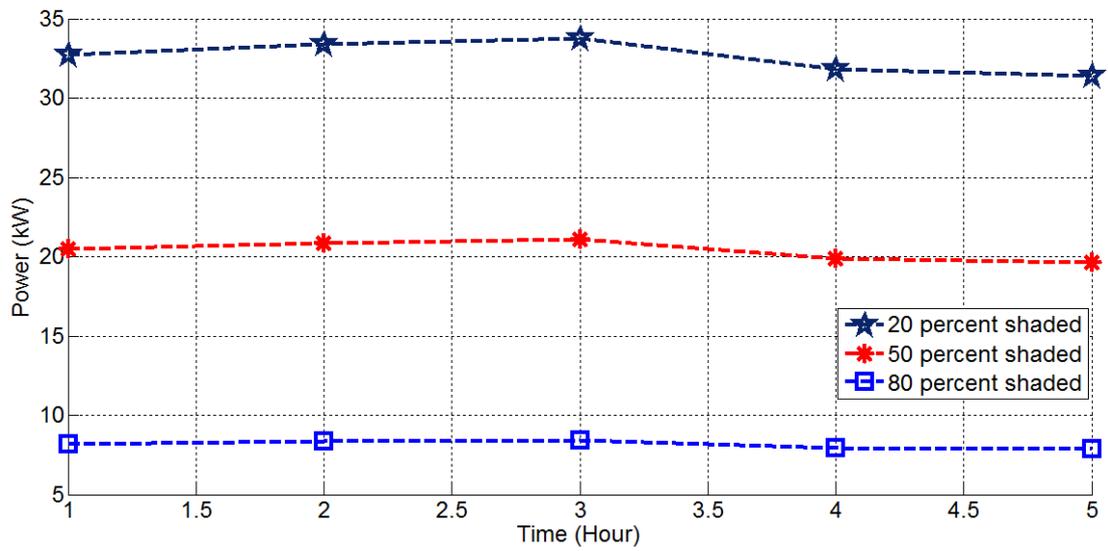
Figure 5.34. Power before rearrangement of shaded pattern 3

❖ Shaded pattern 4 before rearrangement
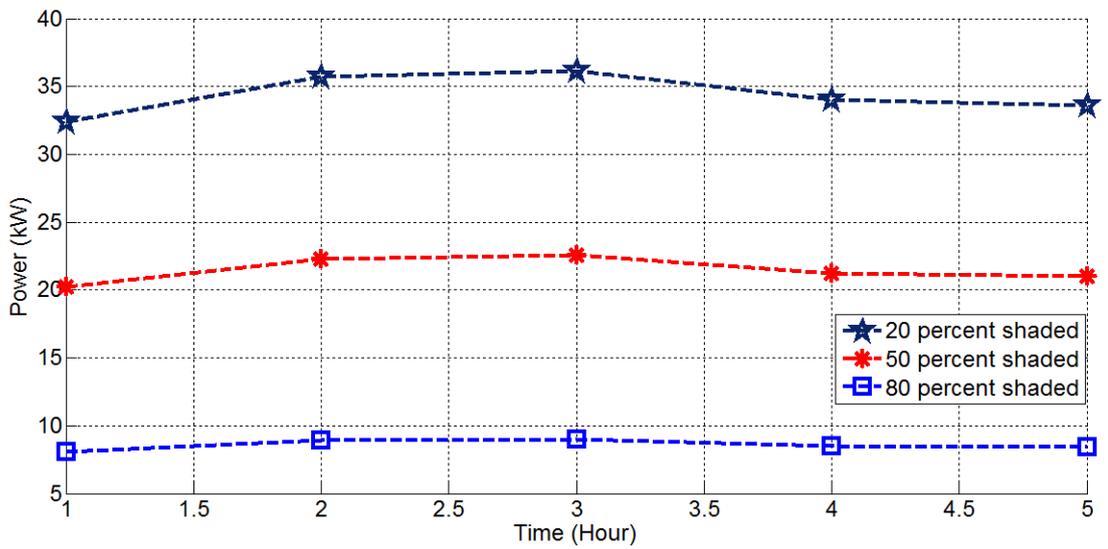
Figure 5.35. Power before rearrangement of shaded pattern 4

❖ Shaded pattern 5 before rearrangement
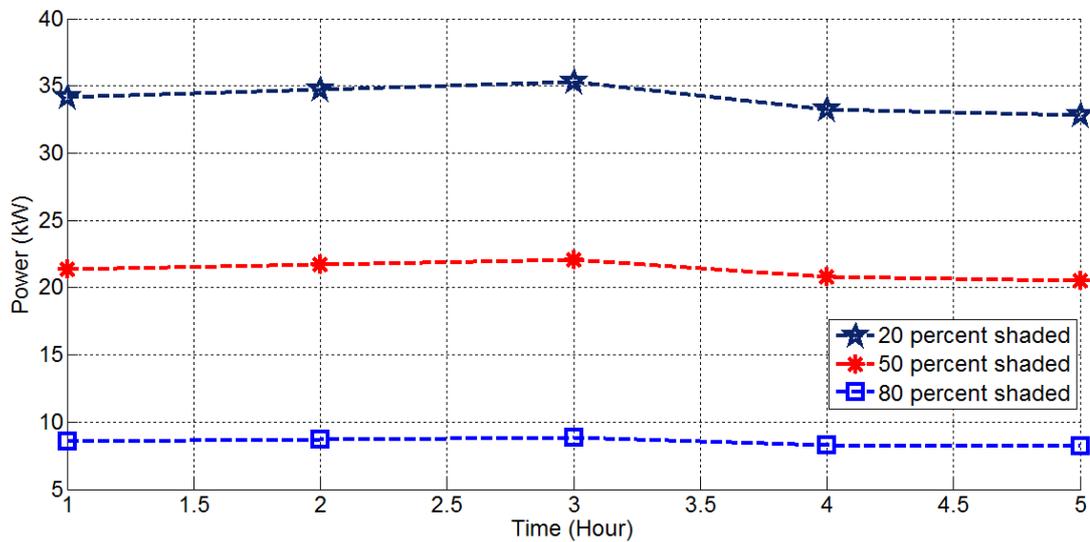
Figure 5.36. Power before rearrangement of shaded pattern 5

❖ Shaded pattern 6 before rearrangement
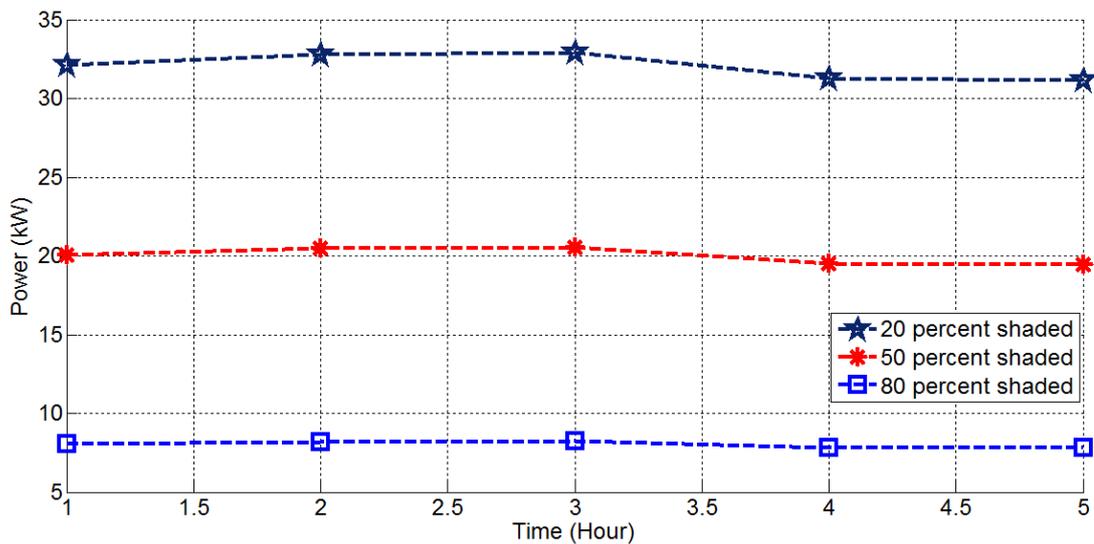
Figure 5.37. Power before rearrangement of shaded pattern 6

Obviously, the PV array produced the highest power the lowest shaded level (20%). Conversely, the lowest power are produced at the highest shaded level (80%). The highest and lowest power generation are also affected by the shaded patterns. Moreover, the number of shaded modules are an important factor.

5.6.2 Simulation of Power Generation in Shading after Rearrangement

After rearranging the shaded modules, generated power is obtained from simulations under the same condition as before rearranging. Results show that power generation after the rearrangement is increased.

❖ Shaded pattern 1 after rearrangement

Figure 5.38. Power after rearrangement of shaded pattern 1

Table 5.22. The results of shaded pattern 1 before and after rearrangement

Description / Irradiation (W/m²)		990.13	1,065.60	1,083.55	989.28	991.32
Time (Hour)		10:00	11:00	12:00	13:00	14:00
Power without shading (kW)		39.39	40.01	40.46	38.27	37.73
Power before rearrangement (kW)	shading 20%	36.66	37.34	37.76	35.66	35.18
	shading 50%	22.92	23.34	23.60	22.29	21.98
	shading 80%	9.17	9.33	9.44	8.92	8.79
Power after rearrangement (kW)	shading 20%	37.46	38.23	38.67	36.47	36.00
	shading 50%	23.41	23.89	24.17	22.80	22.50
	shading 80%	9.36	9.56	9.67	9.12	9.00
Percentage of increased power (%)	shading 20%	2.11	2.33	2.35	2.22	2.28
	shading 50%					
	shading 80%					

❖ Shaded pattern 2 after rearrangement

Figure 5.39. Power after rearrangement of shaded pattern 2

Table 5.23. The results of shaded pattern 2 before and after rearrangement

Description \ Irradiation(W/m^2)		990.13	1,065.60	1,083.55	989.28	991.32
Time (Hour)		10:00	11:00	12:00	13:00	14:00
Power without shading (kW)		39.39	40.01	40.46	38.27	37.73
Power before rearrangement (kW)	shading 20%	31.50	30.53	34.36	32.37	31.94
	shading 50%	19.06	19.08	21.47	20.23	19.97
	shading 80%	7.63	7.63	8.59	8.09	7.99
Power after rearrangement (kW)	shading 20%	37.18	37.91	38.34	36.19	35.71
	shading 50%	23.24	23.69	23.96	22.62	22.32
	shading 80%	9.30	9.48	9.59	9.05	8.93
Percentage of increased power (%)	shading 20%					
	shading 50%	15.28	19.47	10.39	10.54	10.53
	shading 80%					

❖ Shaded pattern 3 after rearrangement

Figure 5.40. Power after rearrangement of shaded pattern 3

Table 5.24. The results of shaded pattern 3 before and after rearrangement

Description / Irradiation(W/m²)		990.13	1,065.60	1,083.55	989.28	991.32
Time (Hour)		10:00	11:00	12:00	13:00	14:00
Power without shading (kW)		39.39	40.01	40.46	38.27	37.73
Power before rearrangement (kW)	shading 20%	32.73	33.38	33.77	31.84	31.41
	shading 50%	20.46	20.86	21.11	19.90	19.63
	shading 80%	8.18	8.34	8.44	7.96	7.85
Power after rearrangement (kW)	shading 20%	36.92	37.61	38.04	35.92	35.43
	shading 50%	23.07	23.51	23.78	22.45	22.14
	shading 80%	9.23	9.40	9.51	8.98	8.86
Percentage of increased power (%)	shading 20%	11.35	11.26	11.23	11.36	11.35
	shading 50%					
	shading 80%					

❖ Shaded pattern 4 after rearrangement

Figure 5.41. Power after rearrangement of shaded pattern 4

Table 5.25. The results of shaded pattern 4 before and after rearrangement

Irradiation(W/m²) Description		990.13	1,065.60	1,083.55	989.28	991.32
Time (Hour)		10:00	11:00	12:00	13:00	14:00
Power without shading (kW)		39.39	40.01	40.46	38.27	37.73
Power before rearrangement (kW)	shading 20%	32.40	35.70	36.13	34.02	33.59
	shading 50%	20.25	22.31	22.58	21.26	20.99
	shading 80%	8.10	8.93	9.03	8.51	8.40
Power after rearrangement (kW)	shading 20%	35.48	36.07	36.48	34.48	33.99
	shading 50%	22.17	22.55	22.80	21.55	21.24
	shading 80%	8.87	9.02	9.12	8.62	8.50
Percentage of increased power (%)	shading 20%	8.68	1.03	0.97	1.32	1.18
	shading 50%					
	shading 80%					

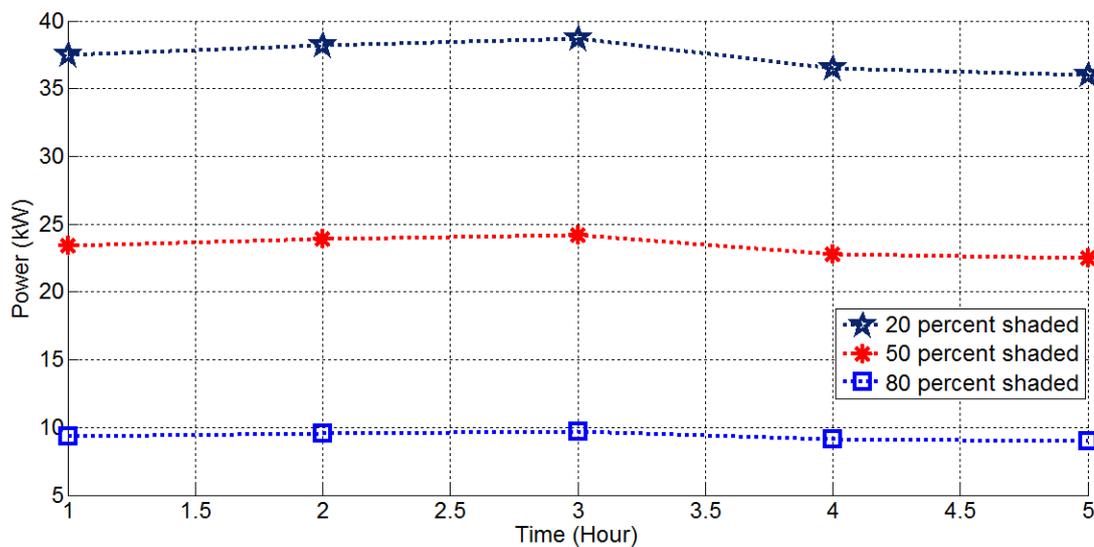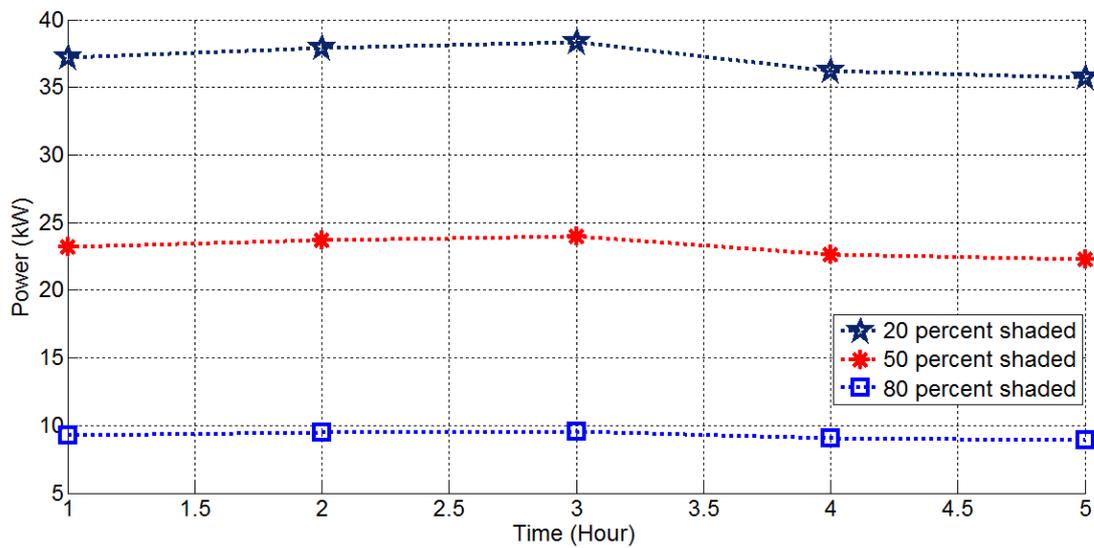❖ Shaded pattern 5 after rearrangement
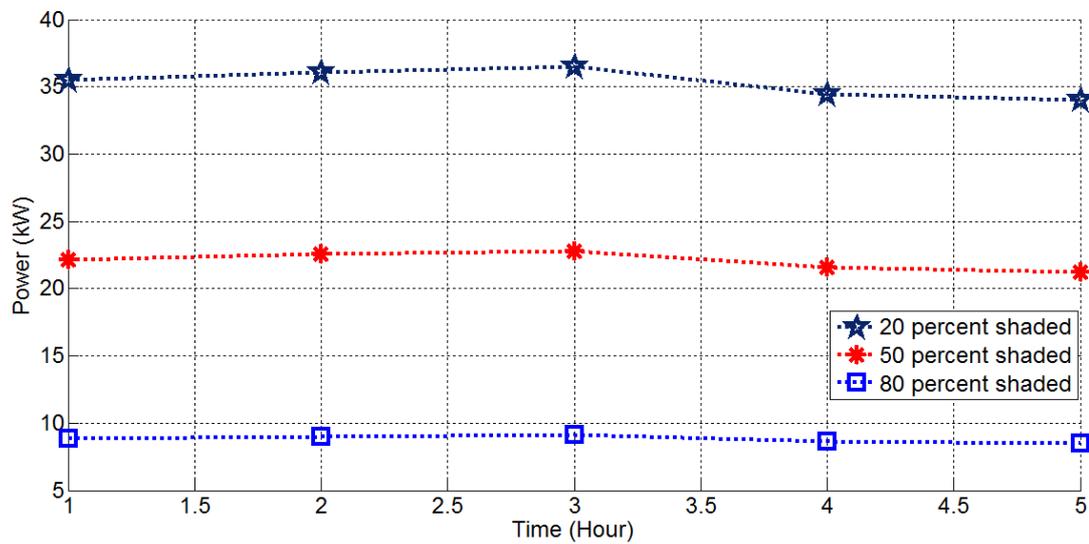
Figure 5.42. Power after rearrangement of shaded pattern 5

Table 5.26. The results of shaded pattern 5 before and after rearrangement

Description　　　Irradiation(W/m²)		990.13	1,065.60	1,083.55	989.28	991.32
Time (Hour)		10:00	11:00	12:00	13:00	14:00
Power without shading (kW)		39.39	40.01	40.46	38.27	37.73
Power before rearrangement (kW)	shading 20%	34.16	34.75	35.29	33.26	32.82
	shading 50%	21.35	21.72	22.06	20.79	20.51
	shading 80%	8.54	8.69	8.82	8.31	8.21
Power after rearrangement (kW)	shading 20%	35.48	36.07	36.48	36.48	33.99
	shading 50%	22.17	22.55	22.80	21.55	21.24
	shading 80%	8.87	9.02	9.12	8.62	8.50
Percentage of increased power (%)	shading 20%	3.72	3.67	3.25	8.84	3.44
	shading 50%					
	shading 80%					

❖ Shaded pattern 6 after rearrangement

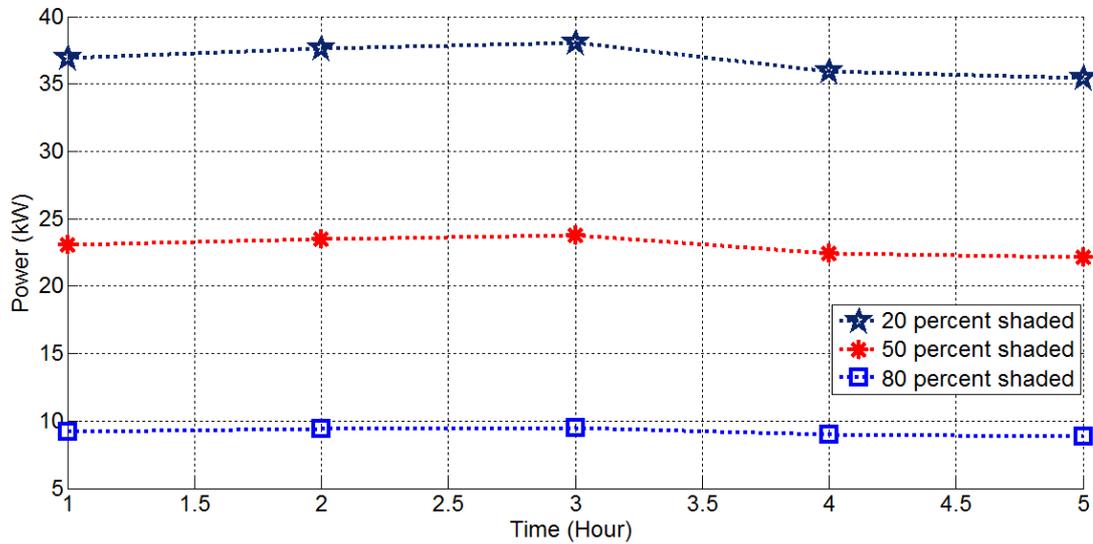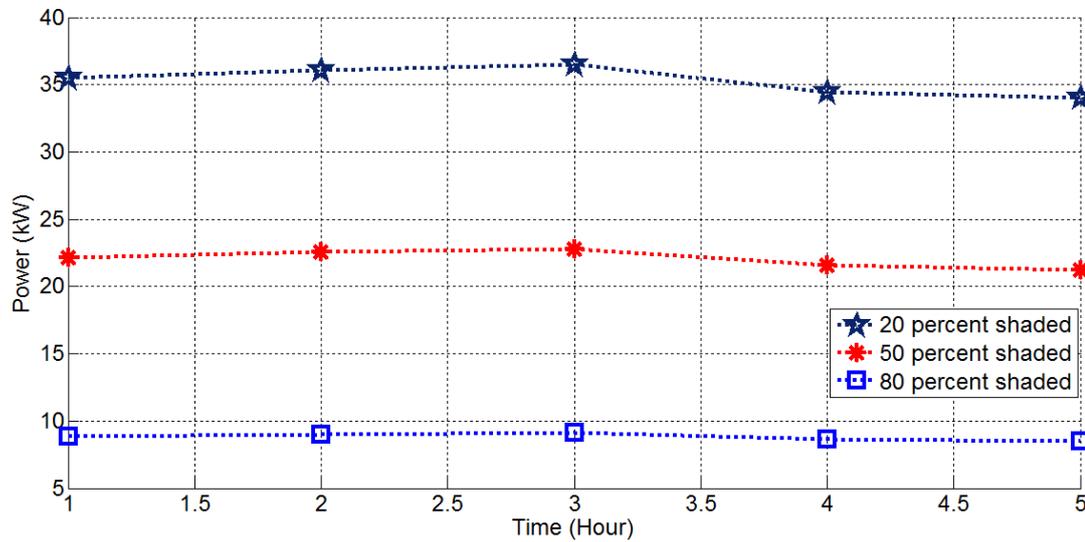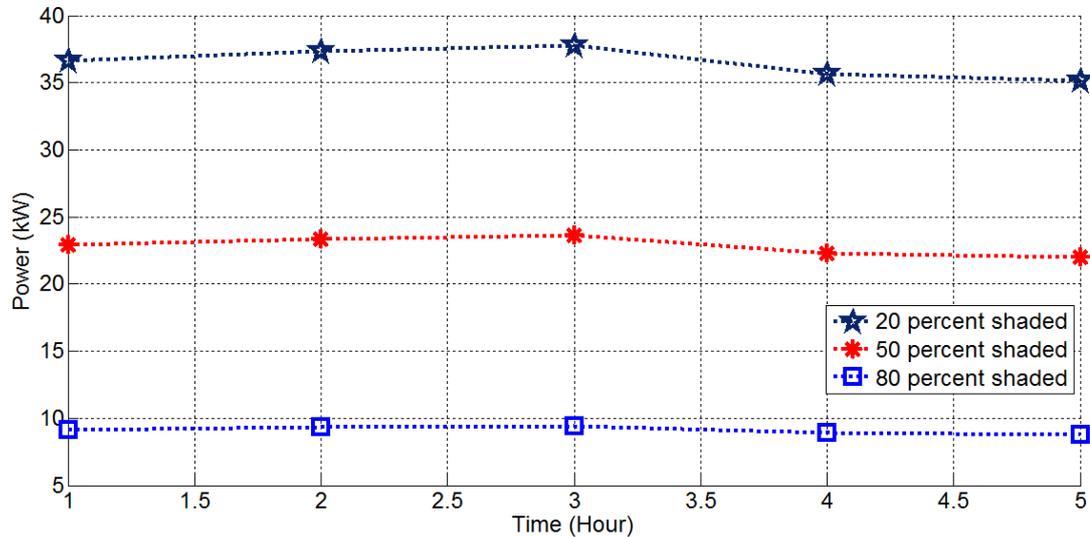

Figure 5.43. Power after rearrangement of shaded pattern 6

Table 5.27. The results of shaded pattern 5 before and after rearrangement

Description \ Irradiation (W/m²)		990.13	1,065.60	1,083.55	989.28	991.32
Time (Hour)		10:00	11:00	12:00	13:00	14:00
Power without shading (kW)		39.39	40.01	40.46	38.27	37.73
Power before rearrangement (kW)	shading 20%	32.15	32.76	32.90	31.26	31.15
	shading 50%	20.09	20.47	20.56	19.54	19.47
	shading 80%	8.04	8.19	8.23	7.82	7.79
Power after rearrangement (kW)	shading 20%	36.66	37.34	37.76	35.66	35.18
	shading 50%	22.92	23.34	23.60	22.29	21.98
	shading 80%	9.17	9.33	9.44	8.92	8.79
Percentage of increased power (%)	shading 20%	14.04	13.98	14.78	14.08	12.92
	shading 50%					
	shading 80%					

5.7 Solar Irradiation

This section forecasts solar irradiance for the different tilted angle and azimuth angle surface in Bangkok (Thailand), latitude of 13.75°N and longitude of 100.58°E [45] by using a method proposed by D Yogi Goswami [36]. The simulating irradiance is compared with the measurement from devices associated with the PV array on the rooftop of Building 4. After that, power generation before and after rearrangement is compared.

Figure 5.44 illustrates the comparison between the forecasted irradiance and the measurement during the whole year. The error between simulation and measurement solar irradiance is smallest at 10:00, 11:00, 12:00, 13:00 and 14:00. The corresponding errors are 5.70%, 0.50%, -1.60%, -0.42% and 1.72%, respectively. The negative error values indicate the real measurement is higher than simulation.

❖ Solar irradiance on January
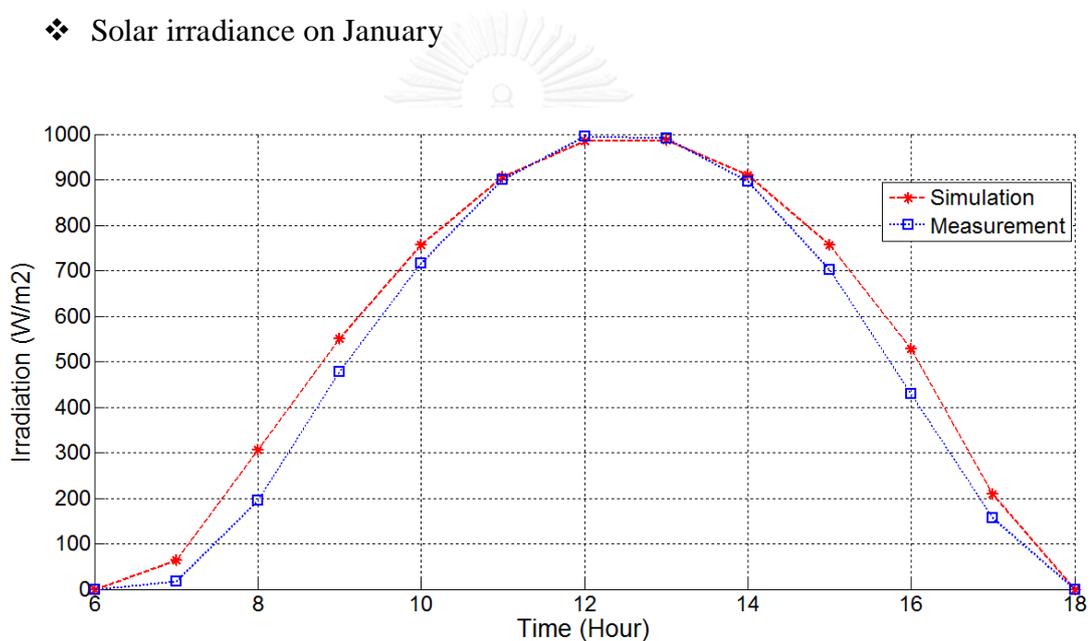
Figure 5.44. Comparison solar irradiance between simulation and measurement

❖ Solar irradiance on February

Figure 5.45. Comparison solar irradiance between simulation and measurement

The error between simulation and measurement solar irradiance is smallest at 10:00, 11:00, 12:00, 13:00 and 14:00 and errors are 6.08%, 4.68%, 2.08%, 1.22% and 1.71%, respectively.

❖ Solar irradiance on March

Figure 5.46. Comparison solar irradiance between simulation and measurement

The error between simulation and measurement solar irradiance is smallest at 10:00, 11:00, 12:00, 13:00 and 14:00 and errors are 6.72%, 0.86%, -0.36%, 0.26%, and 2.77%, respectively.

❖ Solar irradiance on April

Figure 5.47. Comparison solar irradiance between simulation and measurement

The error between simulation and measurement solar irradiance is smallest at 10:00, 11:00, 12:00, 13:00 and 14:00 and errors are 4.28%, 2.26%, 0.72%, 1.86% and 3.56%, respectively.

❖ Solar irradiance on May

Figure 5.48. Comparison solar irradiance between simulation and measurement

The error between simulation and measurement solar irradiance is smallest at 10:00, 11:00, 12:00, 13:00 and 14:00 and errors are 3.67%, 0.50%, 2.02%, 3.29% and 1.57%, respectively.

❖ Solar irradiance on June
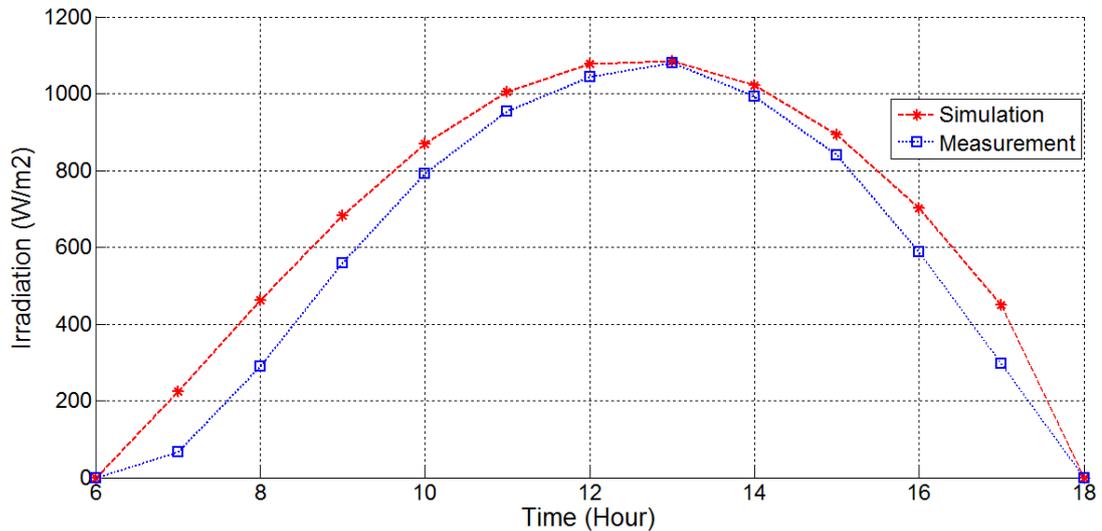
Figure 5.49. Comparison solar irradiance between simulation and measurement

The error between simulation and measurement solar irradiance is smallest at 10:00, 11:00, 12:00, 13:00 and 14:00 and errors are 9.68%, 5.23%, 3.37%, 0.46% and 3.01%, respectively.

❖ Solar irradiance on July
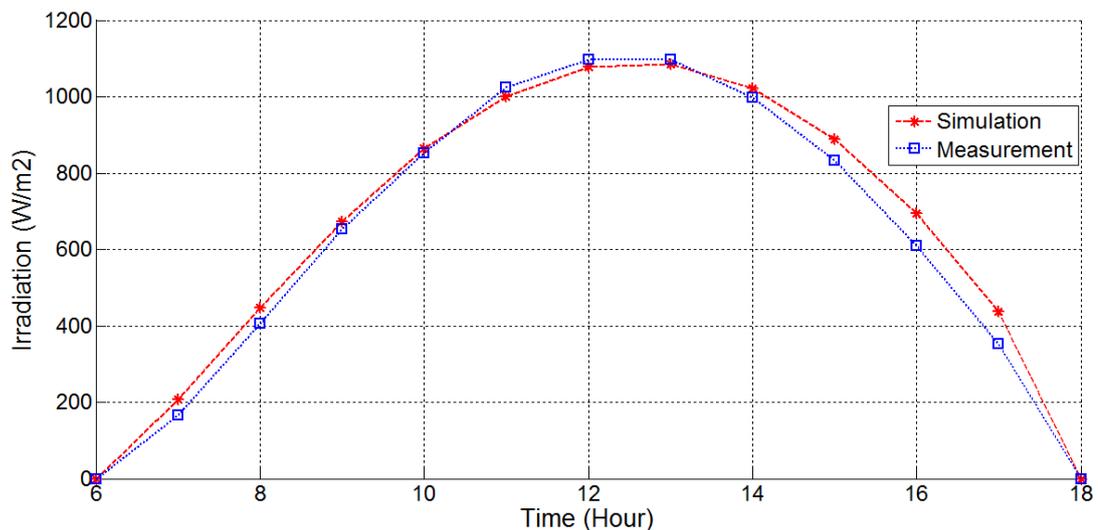
Figure 5.50. Comparison solar irradiance between simulation and measurement

The error between simulation and measurement solar irradiance is smallest at 10:00, 11:00, 12:00, 13:00 and 14:00 and errors are 1.32%, -2.33%, -1.94%, -1.10% and 2.27%, respectively.

❖ Solar irradiance on August
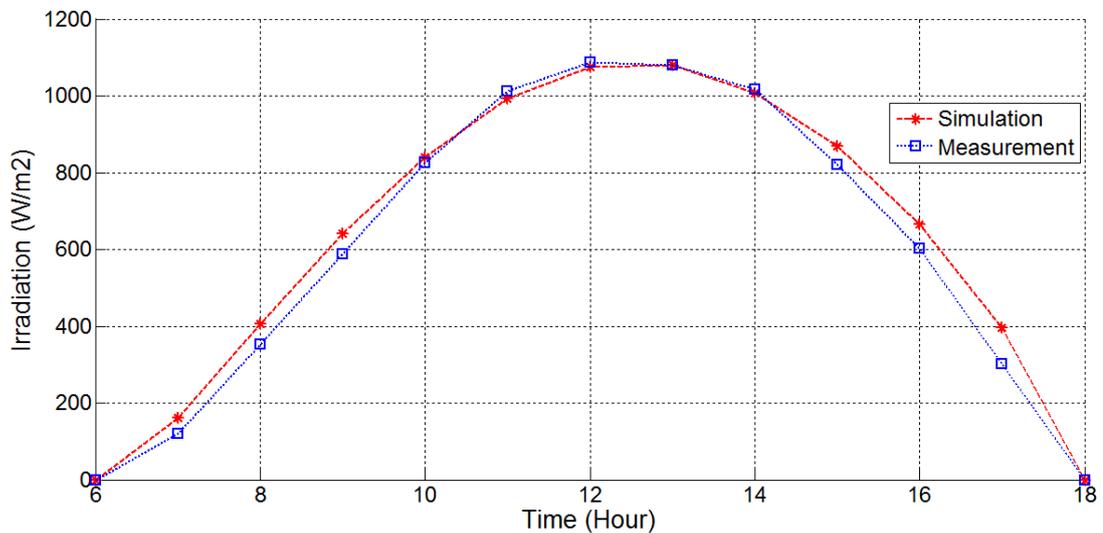
Figure 5.51. Comparison solar irradiance between simulation and measurement

The error between simulation and measurement solar irradiance is smallest at 10:00, 11:00, 12:00, 13:00 and 14:00 are errors are 1.76%, -1.89%, -1.13%, -0.08% and -1.03%, respectively.

❖ Solar irradiance on September
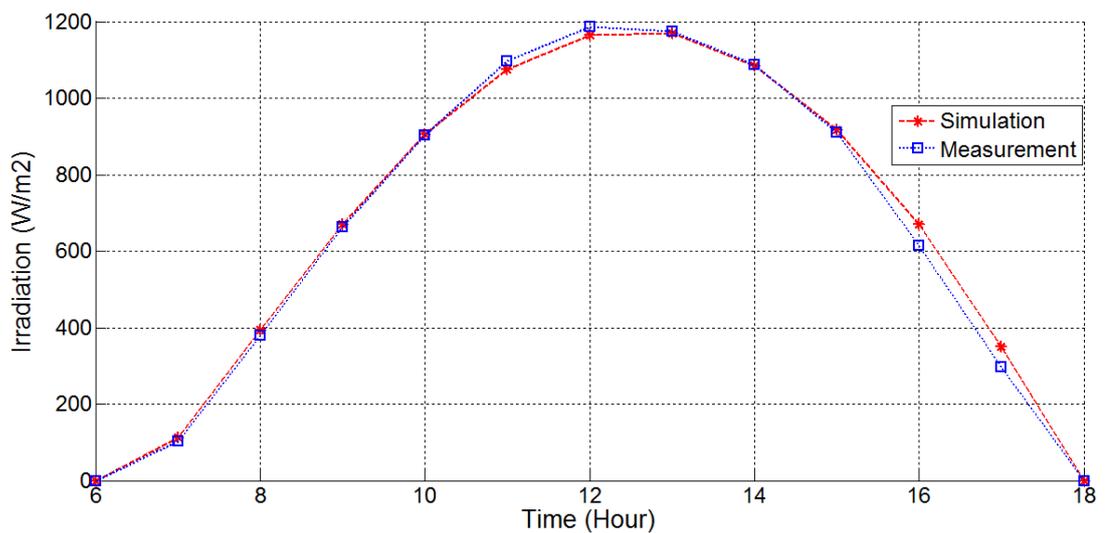
Figure 5.52. Comparison solar irradiance between simulation and measurement

The error between simulation and measurement solar irradiance is smallest at 10:00, 11:00, 12:00, 13:00 and 14:00 and errors are 0.19%, -2.06%, -1.83%, -0.44% and -0.20%, respectively.
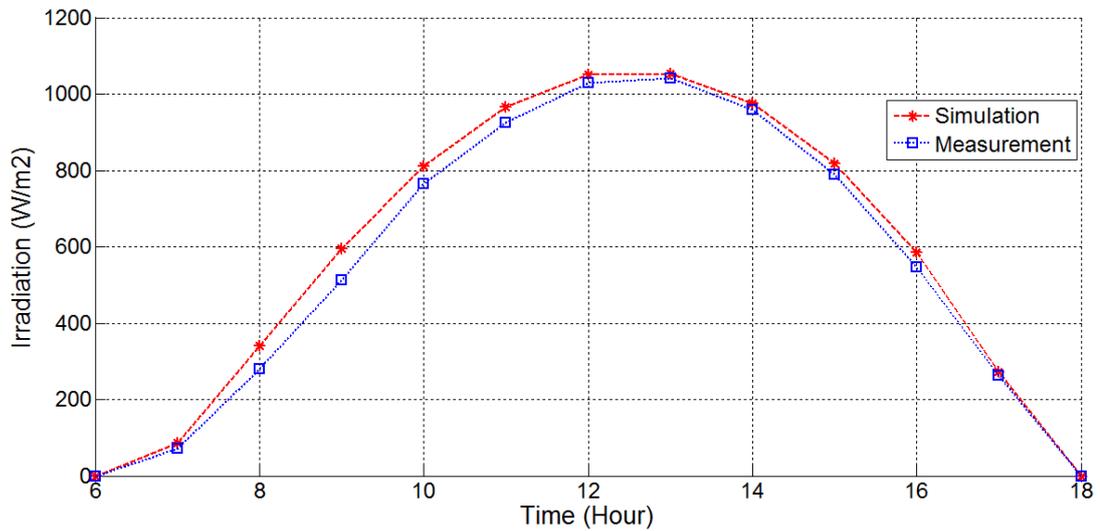
❖ Solar irradiance on October
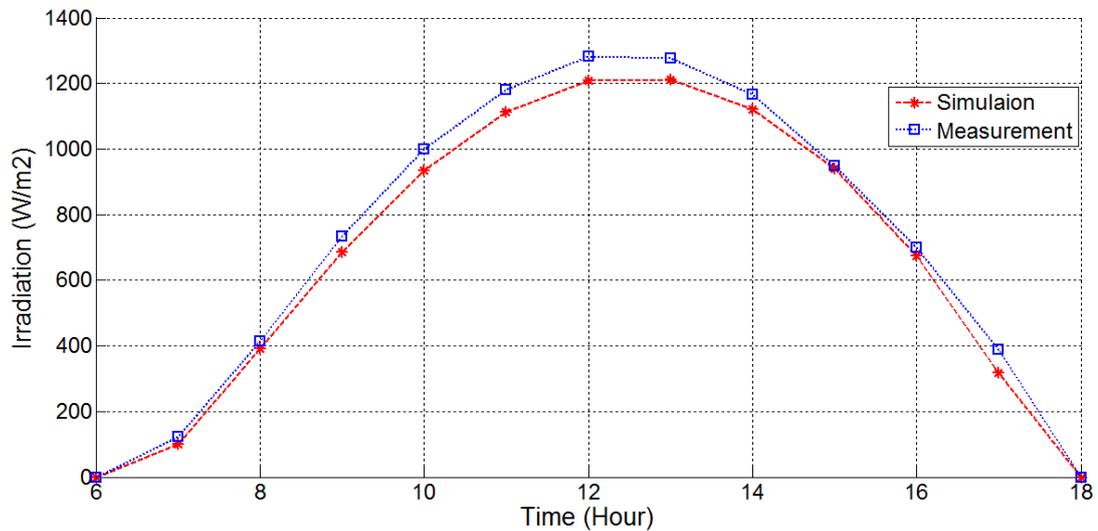
Figure 5.53. Comparison solar irradiance between simulation and measurement

The error between simulation and measurement solar irradiance is smallest at 10:00, 11:00, 12:00, 13:00 and 14:00 and errors are -6.66%, -5.74%, -5.93%, -5.18% and -3.87%, respectively.
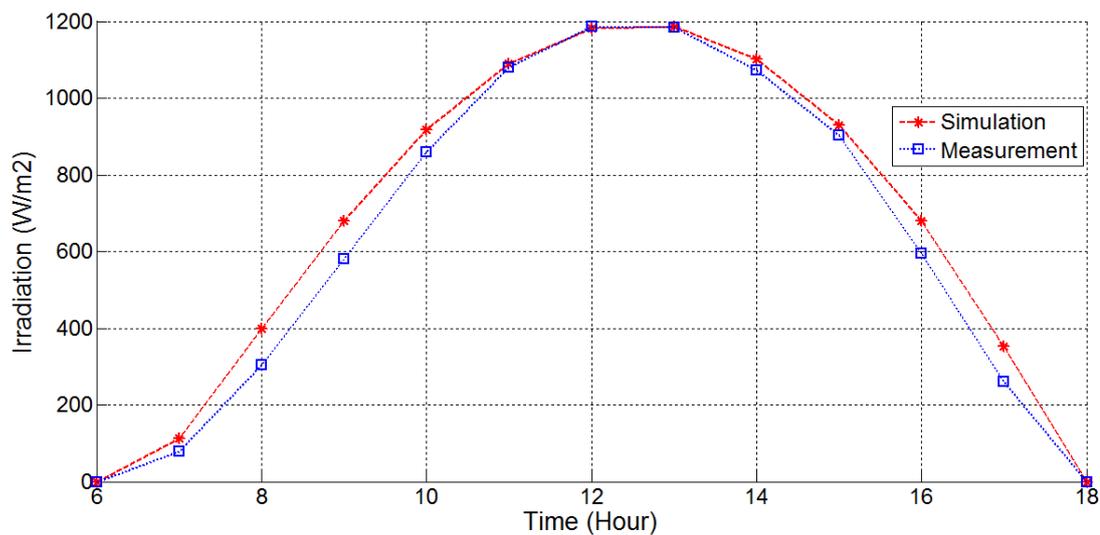
❖ Solar irradiance on November
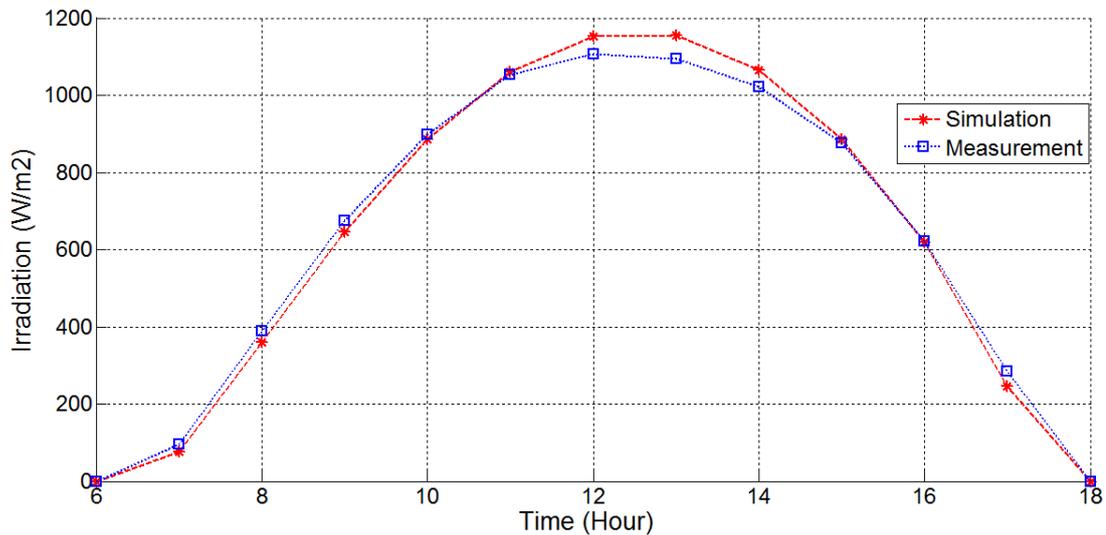
Figure 5.54. Comparison solar irradiance between simulation and measurement

The error between simulation and measurement solar irradiance is smallest at 10:00, 11:00, 12:00, 13:00 and 14:00 and errors are -1.20%, 0.85%, 4.20%, 5.60% and 4.20%, respectively.
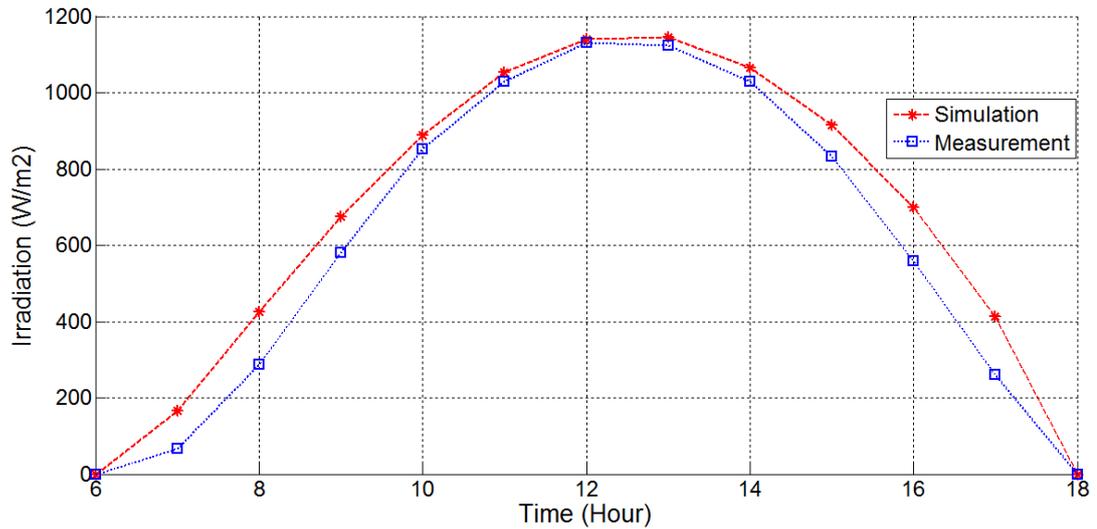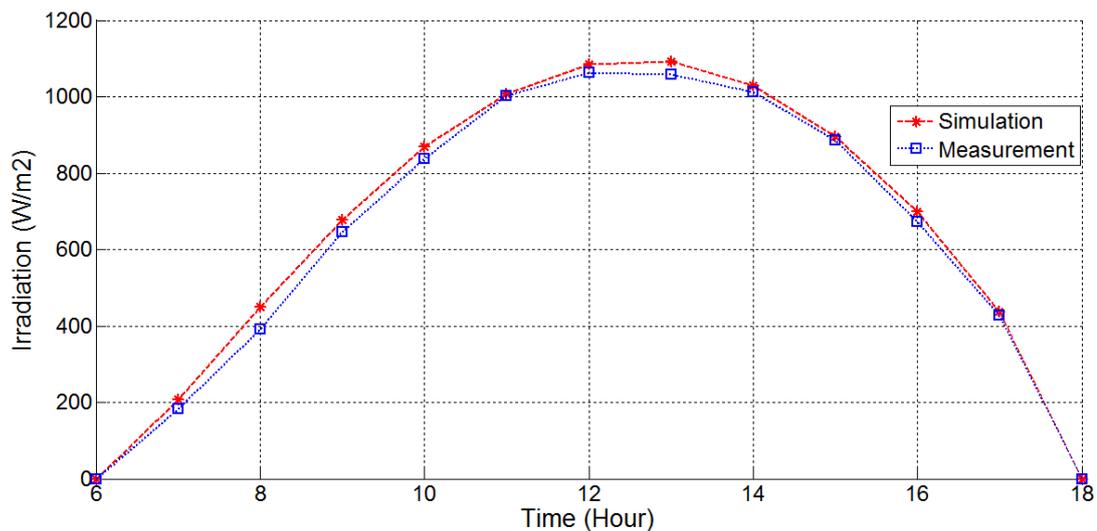
❖ Solar irradiance on December
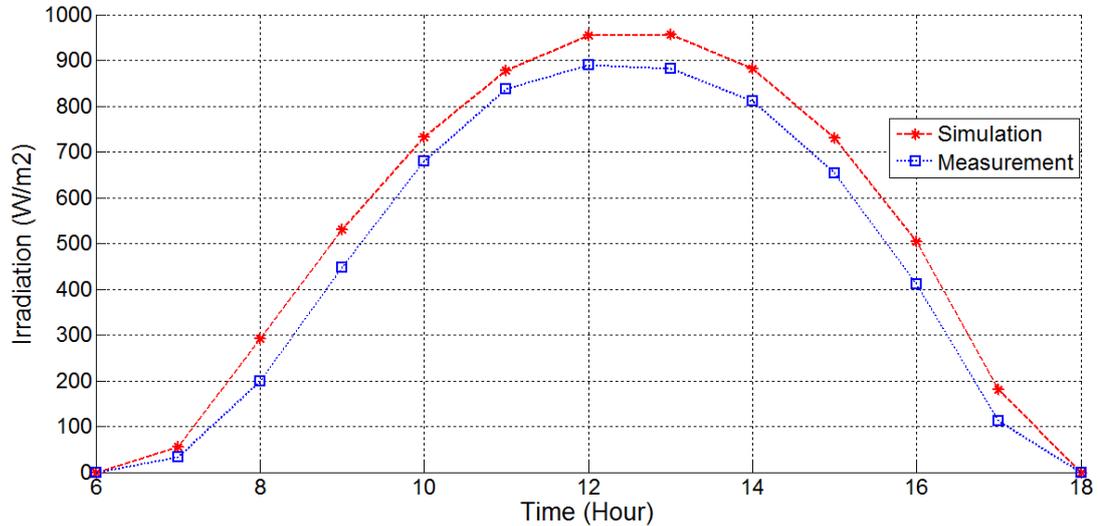
Figure 5.55. Comparison solar irradiance between simulation and measurement

The error between simulation and measurement solar irradiance is smallest at 10:00, 11:00, 12:00, 13:00 and 14:00 and errors are 7.85%, 4.72%, 7.26%, 8.44% and 8.50%, respectively.

It can be seen that the errors between simulation and measurement are not greater than 10%. Hence the forecasting solar irradiance can be used in simulation.

5.7.1 Tilted angle and Azimuth Angle Surface

In the simulation, tilted angle is tested at 5°, 10°, 15°, 20°, 25°, 30°, 35°, 40°, 45° and azimuth angle surface is at 0°, -15°, -30 until -180. Azimuth angle of 0°, PV modules are directed south-facing whereas negative values PV modules are directed in the East-facing. The irradiance and power can be demonstrated in Figures 5.56 and 5.57, respectively.
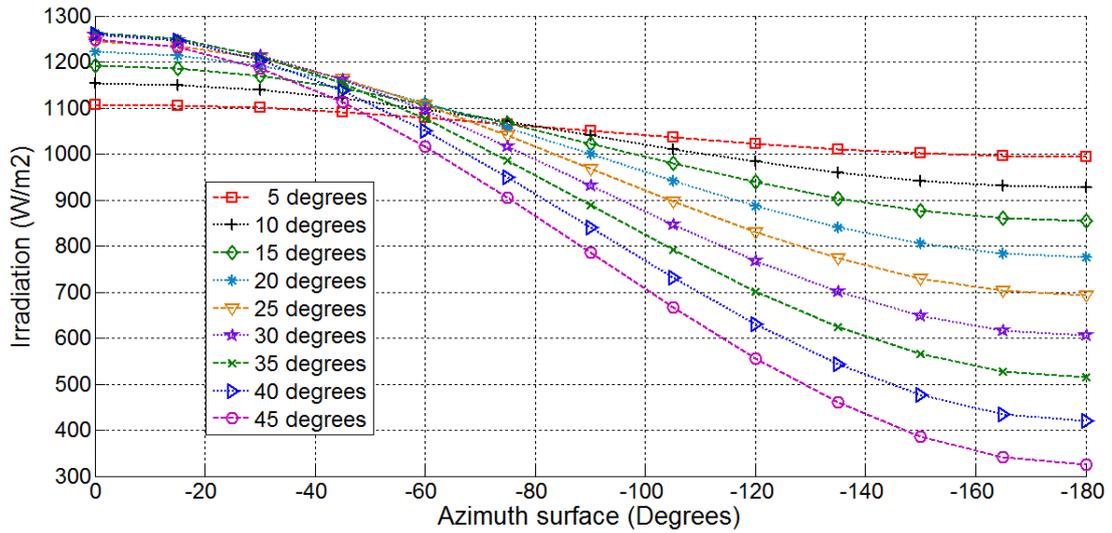
Figure 5.56. Solar irradiance with tilted and azimuth angles
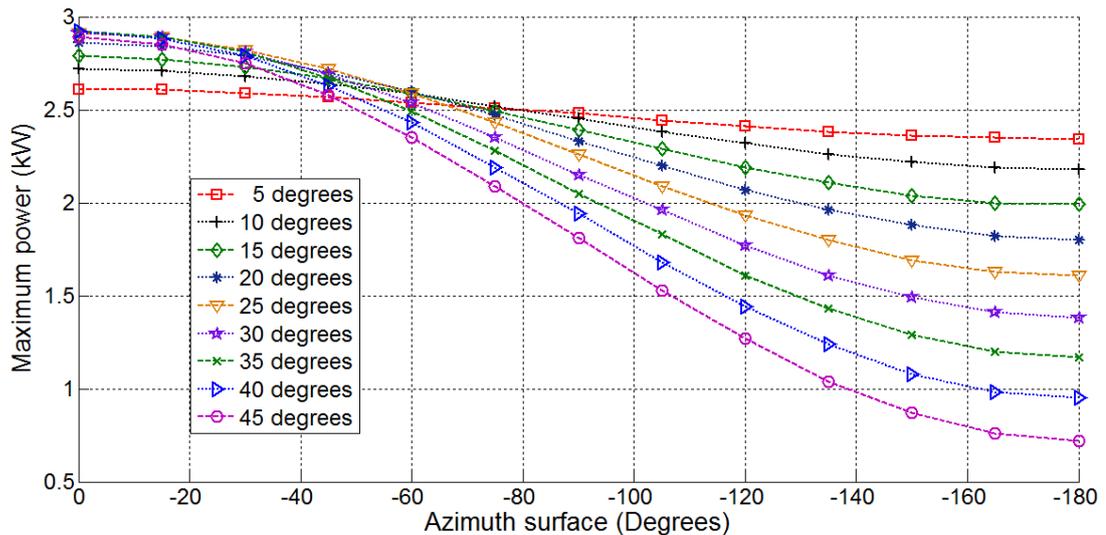
Figure 5.57. Solar irradiance with tilted and azimuth angles

5.7.2 Yearly and Monthly Tilted Angle

The optimal tilted and azimuth angle in each month are modeled. The monthly best tilted angle is shown in Figure 5.58. The tilted angle in January, February, March, September, October, November and December is positive where PV modules are directed in the south-facing. In contrast, the tilted angle in April, May, June, July and August is negative where PV modules are directed in the north-facing. If PV system is fixed, the yearly best tilted angle is 13.48° at which the PV modules are facing to the south.
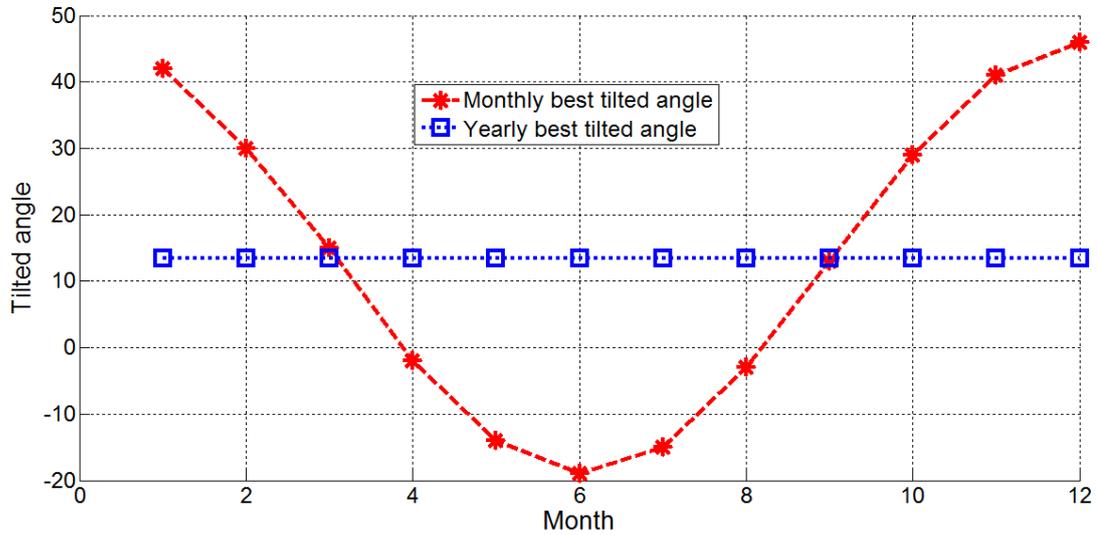
Figure 5.58. Monthly and yearly best tilted angle

5.8 Power Before and After Rearrangement with Approximated Tilted and Azimuth

Firstly, both tilted and azimuth are used in the model for forecasting solar irradiance. Results on 21st March are for compared with the previous real measurement including time instants at 10:00, 11:00, 12:00, 13;00,14:00 as shown in Table 5.28. Secondly, the shaded patterns of 8x20 modules is used to estimate the power generation. Lastly, amounts of power before and after rearrangement are compared at 15° and 40°.

Table 5.28. Forecasting solar irradiance

Duration of time (Hour)	10:00	11:00	12:00	13:00	14:00
Irradiation (W/m²)	1,023.60	1,154.40	1,199.00	1,099.40	1059.65
Ambient temperature (℃)	32.69	33.63	34.76	33.81	34.65
Module temperature (℃)	44.31	50.79	51.35	47.65	49.49

This research considers the approximated tilted angle and azimuth for increasing the amount of sunlight received by the PV modules. The table below shows how much power is increased by rearranging the shaded modules.

❖ Shaded pattern 1

Table 5.29. The percentage of increased power before and after rearrangement when PV modules are installed by best tilted and azimuth angles

Time (hour)		10:00	11:00	12:00	13:00	14:00
Power without shading (kW)		39.39	43.24	44.61	42.44	40.27
Power before rearrangement (kW)	T(15°), A(40°)	36.66	37.34	37.76	35.66	35.18
	T(13.48°), A(0°)	37.89	40.38	41.68	38.05	36.31
Power after rearrangement (kW)	T(15°), A(40°)	37.46	38.23	38.67	36.47	36.00
	T(13.48°), A(0°)	38.71	41.34	42.68	42.45	37.16
Percentage of increased power before rearrangement between T(15°), A(40°) and T(13.48°), A(0°) (%)		3.35	8.14	10.37	6.70	3.22
Percentage of increased power after rearrangement between T(15°), A(40°) and T(13.48°), A(0°) (%)		3.35	8.14	10.37	16.39	3.22
Percentage of increased power before and after rearrangement of T(13.48°), A(0°) (%)		2.16	2.38	2.40	11.57	2.34

❖ Shaded pattern 2

Table 5.30. The percentage of increased power before and after rearrangement when PV modules are installed by best tilted and azimuth angles

Time (hour)		10:00	11:00	12:00	13:00	14:00
Power without shading (kW)		39.39	43.24	44.61	42.44	40.27
Power before rearrangement (kW)	T(15°), A(40°)	30.27	30.53	34.36	32.37	31.94
	T(13.48°), A(0°)	34.38	36.77	37.99	36.22	32.99
Power after rearrangement (kW)	T(15°), A(40°)	37.18	37.91	38.34	36.19	35.71
	T(13.48°), A(0°)	38.43	40.99	42.32	42.12	36.85
Percentage of increased power before rearrangement between T(15°), A(40°) and T(13.48°), A(0°) (%)		13.59	20.45	10.56	11.89	3.27
Percentage of increased power after rearrangement between T(15°), A(40°) and T(13.48°), A(0°) (%)		3.35	8.14	10.37	16.39	3.22
Percentage of increased power before and after rearrangement of T(13.48°), A(0°) (%)		11.76	11.48	11.40	16.28	11.72

❖ Shaded pattern 3

Table 5.31. The percentage of increased power before and after rearrangement when PV modules are installed by best tilted and azimuth angles

Time (hour)		10:00	11:00	12:00	13:00	14:00
Power without shading (kW)		39.39	43.24	44.61	42.44	40.27
Power before rearrangement (kW)	T(15°), A(40°)	32.73	33.38	33.77	31.84	31.41
	T(13.48°), A(0°)	33.84	36.14	37.33	37.14	32.43
Power after rearrangement (kW)	T(15°), A(40°)	36.92	37.61	38.04	35.92	35.43
	T(13.48°), A(0°)	38.15	40.68	41.98	41.80	40.32
Percentage of increased power before rearrangement between T(15°), A(40°) and T(13.48°), A(0°) (%)		3.40	8.28	10.55	16.67	3.27
Percentage of increased power after rearrangement between T(15°), A(40°) and T(13.48°), A(0°) (%)		3.35	8.14	10.36	16.39	13.80
Percentage of increased power before and after rearrangement of T(13.48°), A(0°) (%)		12.74	12.54	12.46	12.54	24.31

❖ Shaded pattern 4

Table 5.32. The percentage of increased power before and after rearrangement when PV modules are installed by best tilted and azimuth angles

Time (hour)		10:00	11:00	12:00	13:00	14:00
Power without shading (kW)		39.39	43.24	44.61	42.44	40.27
Power before rearrangement (kW)	T(15°), A(40°)	32.40	35.70	36.13	34.02	33.59
	T(13.48°), A(0°)	32.96	38.65	39.92	39.66	34.68
Power after rearrangement (kW)	T(15°), A(40°)	35.48	36.07	36.48	34.48	33.99
	T(13.48°), A(0°)	36.67	39.02	40.27	40.14	35.09
Percentage of increased power before rearrangement between T(15°), A(40°) and T(13.48°), A(0°) (%)		1.74	8.25	10.49	16.59	3.26
Percentage of increased power after rearrangement between T(15°), A(40°) and T(13.48°), A(0°) (%)		3.36	8.16	10.40	16.44	3.23
Percentage of increased power before and after rearrangement of T(13.48°), A(0°) (%)		11.25	0.97	0.89	1.21	1.17

❖ Shaded pattern 5

Table 5.33. The percentage of increased power before and after rearrangement when PV modules are installed by best tilted and azimuth angles

Time (hour)		10:00	11:00	12:00	13:00	14:00
Power without shading (kW)		39.39	43.24	44.61	42.44	40.27
Power before rearrangement (kW)	T(15°), A(40°)	34.16	34.75	35.29	33.26	32.82
	T(13.48°), A(0°)	35.32	37.76	39.00	38.78	33.89
Power after rearrangement (kW)	T(15°), A(40°)	35.48	36.07	36.48	36.48	33.99
	T(13.48°), A(0°)	36.67	39.02	40.27	40.14	35.09
Percentage of increased power before rearrangement between T(15°), A(40°) and T(13.48°), A(0°) (%)		3.38	8.67	10.51	16.60	3.26
Percentage of increased power after rearrangement between T(15°), A(40°) and T(13.48°), A(0°) (%)		3.36	8.16	10.40	10.04	3.23
Percentage of increased power before and after rearrangement of T(13.48°), A(0°) (%)		3.84	3.33	3.25	3.52	3.53

❖ Shaded pattern 6

Table 5.34. The percentage of increased power before and after rearrangement when PV modules are installed by best tilted and azimuth angles

Time (hour)		10:00	11:00	12:00	13:00	14:00
Power without shading (kW)		39.39	43.24	44.61	42.44	40.27
Power before rearrangement (kW)	T(15°), A(40°)	32.15	32.76	32.90	31.26	31.15
	T(13.48°), A(0°)	33.24	35.47	36.64	36.47	36.21
Power after rearrangement (kW)	T(15°), A(40°)	36.66	37.34	37.76	35.66	35.18
	T(13.48°), A(0°)	37.89	40.38	41.68	41.51	36.31
Percentage of increased power before rearrangement between T(15°), A(40°) and T(13.48°), A(0°) (%)		3.40	8.29	11.36	16.67	16.24
Percentage of increased power after rearrangement between T(15°), A(40°) and T(13.48°), A(0°) (%)		3.35	8.14	10.37	16.39	3.22
Percentage of increased power before and after rearrangement of T(13.48°), A(0°) (%)		13.98	13.83	13.76	13.80	0.27

Results show that the highest power was generated by PV modules at the tilted and azimuth angle 13.48° and 0°, respectively. In addition, the increased power depends on shaded patterns, number of shaded modules, and shaded level.

5.9 Conclusion

The power generation of PV array can be significantly influenced by changes of irradiation, temperature, and shading pattern. The simulation on a string of 1x10 PV modules shows that the different shading levels and shaded modules affect the output MPP. In addition, if the pattern of moving clouds or shading can be predicted, the PV modules in an array can be arranged in advance so that the number of MPPs is reduced and the PV array can provide the higher single MPP. From the simulation, with the proposed electrical wiring of PV modules, the PV system can generate more active power. However, the yearly best tilted and azimuth angle of PV modules can help increase power generation despite the shaded modules. Importantly, the rearrangement of shaded modules can improve the efficiency and mitigate impacts of partial shading.

This thesis can be resulted by two term of advantage and disadvantage.

5.9.1 Advantage

This thesis provides the understanding of the impacts of partial shading on the photovoltaic generation system and proposes an appropriate tilted and azimuth angle for installing of PV modules. Firstly, the rearrangement of PV modules in an array can alleviate the power decrease when shading is occurred by moving cloud. Secondly, the optimal power is tracked by inverter in maximum power point (MPP) because the multiple maximum power point (MPPs) is improved to be only one MPP. Thirdly, if shaded pattern can be predicted, the rearrangement of PV modules in array can generate the higher MPP. Finally, the installation of PV modules can obtain the best angle and azimuth angle. PV modules receive the higher amount of irradiation and the power can be generated more efficiently.

5.9.2 Disadvantage

In contrast, there are some disadvantages. First, the controlling of switches is difficult because cloud moving is difficult to predict .In addition, it is difficult to know the shaded PV modules. Finally, the rearrangement needs high investment cost, e.g. for rewiring and new protection system.

REFERENCES

[1]   N. K. Sharma, P. K. Tiwari, and Y. R. Sood, "Environmental friendly solar energy in restructured Indian power sector," in *Sustainable Energy and Intelligent Systems (SEISCON 2011), International Conference on*, 2011, pp. 104-109.

[2]   C. Woei-Luen, I. L. Su, and L. Jian-Der, "Design of a gain scheduling photovoltaic energy conversion system," in *Industrial Electronics & Applications, 2009. ISIEA 2009. IEEE Symposium on*, 2009, pp. 813-817.

[3]   A. T. Russell and E. M. A. Oliveira, "Sine Amplitude Converters for efficient datacenter power distribution," in *Renewable Energy Research and Applications (ICRERA), 2012 International Conference on*, 2012, pp. 1-6.

[4]   S. Chowdhury, M. Al-Amin, and M. Ahmad, "Performance variation of Building integrated photovoltaic application with tilt and azimuth angle in Bangladesh," in *Electrical & Computer Engineering (ICECE), 2012 7th International Conference on*, 2012, pp. 896-899.

[5]   A. Mraoui, M. Khelif, and B. Benyoucef, "Optimum tilt angle of a photovoltaic system: Case study of Algiers and Ghardaia," in *Renewable Energy Congress (IREC), 2014 5th International*, 2014, pp. 1-6.

[6]   A. H. Alqahtani, M. S. Abuhamdeh, and Y. M. Alsmadi, "A simplified and comprehensive approach to characterize photovoltaic system performance," in *Energytech, 2012 IEEE*, 2012, pp. 1-6.

[7]   E. I. Batzelis, I. A. Routsolias, and S. A. Papathanassiou, "An Explicit PV String Model Based on the Lambert W Function and Simplified MPP Expressions for Operation Under Partial Shading," *Sustainable Energy, IEEE Transactions on,* vol. 5, pp. 301-312, 2014.

[8]   S. Lineykin, M. Averbukh, and A. Kuperman, "Five-parameter model of photovoltaic cell based on STC data and dimensionless," in *Electrical & Electronics Engineers in Israel (IEEEI), 2012 IEEE 27th Convention of*, 2012, pp. 1-5.

[9]   N. Seddaoui, L. Rahmani, A. Chauder, and A. Kessal, "Parameters extraction of photovoltaic module at reference and real conditions," in *Universities' Power Engineering Conference (UPEC), Proceedings of 2011 46th International*, 2011, pp. 1-6.

[10]   A. Maoucha, F. Djeffal, D. Arar, N. Lakhdar, T. Bendib, and M. A. Abdi, "An accurate organic solar cell parameters extraction approach based on the illuminated I-V characteristics for double diode modeling," in *Renewable Energies and Vehicular Technology (REVET), 2012 First International Conference on*, 2012, pp. 74-77.

[11]   P. Junsangsri and F. Lombardi, "Double diode modeling of time/temperature induced degradation of solar cells," in *Circuits and Systems (MWSCAS), 2010 53rd IEEE International Midwest Symposium on*, 2010, pp. 1005-1008.

[12]   M. A. Yaklin, D. A. Schneider, K. Norman, J. E. Granata, and C. L. Staiger, "Impacts of Humidity and Temperature on the Performance of Transparent Conducting Zinc Oxide," in *Photovoltaic Specialists Conference (PVSC), 2010 35th IEEE*, 2010, pp. 002493-002496.

[13]   M. F. Basquera, R. D. de O Reiter, F. H. Dupont, and L. Michels, "Impacts of local climate conditions onphotovoltaic module efficiency," in *Power Electronics Conference (COBEP), 2013 Brazilian*, 2013, pp. 533-537.

[14]   M. Suthar, G. K. Singh, and R. P. Saini, "Comparison of mathematical models of photo-voltaic (PV) module and effect of various parameters on its performance," in *Energy Efficient Technologies for Sustainability (ICEETS), 2013 International Conference on*, 2013, pp. 1354-1359.

[15]   N. Mutoh, T. Matuo, K. Okada, and M. Sakai, "Prediction-data-based maximum-power-point-tracking method for photovoltaic power generation systems," in *Power Electronics Specialists Conference, 2002. pesc 02. 2002 IEEE 33rd Annual*, 2002, pp. 1489-1494 vol.3.

[16]   A. Kovach, "Effects of inhomogeneous irradiation distribution on a PV array in an urban environment," in *Photovoltaic Energy Conversion, 1994., Conference Record of the Twenty Fourth. IEEE Photovoltaic Specialists Conference - 1994, 1994 IEEE First World Conference on*, 1994, pp. 994-997 vol.1.

[17]   V. Mummadi, "Maximum Power Point Tracking Algorithm For Non-Linear DC Sources," in *Industrial and Information Systems, 2008. ICIIS 2008. IEEE Region 10 and the Third international Conference on*, 2008, pp. 1-6.

[18]   C. Chia Seet, P. Neelakantan, Y. Hou Pin, Y. Soo Siang, and K. T. K. Teo, "Maximum Power Point Tracking for PV Array Under Partially Shaded Conditions," in *Computational Intelligence, Communication Systems and Networks (CICSyN), 2011 Third International Conference on*, 2011, pp. 72-77.

[19]   S. Vemuru, P. Singh, and M. Niamat, "Analysis of photovoltaic array with reconfigurable modules under partial shading," in *Photovoltaic Specialists Conference (PVSC), 2012 38th IEEE*, 2012, pp. 001437-001441.

[20]   R. Ramaprabha and B. L. Mathur, "Modelling and simulation of Solar PV Array under partial shaded conditions," in *Sustainable Energy Technologies, 2008. ICSET 2008. IEEE International Conference on*, 2008, pp. 7-11.

[21]   J. Young-Hyok, J. Doo-Yong, K. Jun-Gu, K. Jae-Hyung, L. Tae-Won, and W. Chung-Yuen, "A Real Maximum Power Point Tracking Method for Mismatching Compensation in PV Array Under Partially Shaded Conditions," *Power Electronics, IEEE Transactions on,* vol. 26, pp. 1001-1009, 2011.

[22]   A. Bidram, A. Davoudi, and R. S. Balog, "Control and Circuit Techniques to Mitigate Partial Shading Effects in Photovoltaic Arrays," *Photovoltaics, IEEE Journal of,* vol. 2, pp. 532-546, 2012.

[23]   R. G. Wandhare, V. Agarwal, and S. Jain, "Novel multi-input solar PV topologies for 1 phase and 3 phase stand alone applications to mitigate the effects of partial shading," in *Applied Power Electronics Conference and Exposition (APEC), 2013 Twenty-Eighth Annual IEEE*, 2013, pp. 76-83.

[24]   P. Sharma and V. Agarwal, "Maximum Power Extraction From a Partially Shaded PV Array Using Shunt-Series Compensation," *Photovoltaics, IEEE Journal of,* vol. 4, pp. 1128-1137, 2014.

[25]   N. Rebei, R. Gammoudi, A. Hmidet, and O. Hasnaoui, "Experimental implementation techniques of P&O MPPT algorithm for PV pumping

system," in *Multi-Conference on Systems, Signals & Devices (SSD), 2014 11th International*, 2014, pp. 1-6.

[26] G. Siyu, T. M. Walsh, A. G. Aberle, and M. Peters, "Analysing partial shading of PV modules by circuit modelling," in *Photovoltaic Specialists Conference (PVSC), 2012 38th IEEE*, 2012, pp. 002957-002960.

[27] S. Essakiappan, H. S. Krishnamoorthy, P. Enjeti, R. S. Balog, and S. Ahmed, "A new control strategy for megawatt scale multilevel photovoltaic inverters under partial shading," in *Power Electronics for Distributed Generation Systems (PEDG), 2012 3rd IEEE International Symposium on*, 2012, pp. 336-343.

[28] *Growth of photovoltaics*. Available: http://en.wikipedia.org/wiki/Growth_of_photovoltaics#Worldwide

[29] S. Jing Jun, L. Kay-Soon, and G. Shu Ting, "Multi-dimension diode photovoltaic (PV) model for different PV cell technologies," in *Industrial Electronics (ISIE), 2014 IEEE 23rd International Symposium on*, 2014, pp. 2496-2501.

[30] T. T. Yetayew and T. R. Jyothsna, "Improved single-diode modeling approach for photovoltaic modules using data sheet," in *India Conference (INDICON), 2013 Annual IEEE*, 2013, pp. 1-6.

[31] P. Hyeonah and K. Hyosung, "PV cell modeling on single-diode equivalent circuit," in *Industrial Electronics Society, IECON 2013 - 39th Annual Conference of the IEEE*, 2013, pp. 1845-1849.

[32] *Multi crystalline silicon solar modules 130 watt*. Available: http://www.solartron.co.th/Catalog/SP130_TH.pdf

[33] *Poly crystalline silicon solar modules 285-295 watt STP285-24/Vd, TTP290-24/Vd*. Available: http://www.redasolar.nl/bestanden/documenten/Suntech/STP_Vd_285-295_156-72_EN.pdf

[34] C. S. Solanki, *Solar Photovoltaics : Fundamentals, Technologies and Applications*, Second Edition ed. Sonepat,Haryana: Asoke K. Ghosh, 2011.

[35] W. A. B. John A. Duffie, *Solar engineering of thermal processes*, Fourth edition ed., 2013.

[36] F. K. D. Yogi Goswami, Jan F.Kreider, *Principles of solar engineering*, 1999.

[37] W. W. a. J. L. Serm Janjai, "The Determination of Surface Albedo of Thailand Using Satellite Data," presented at the The 2nd Joint International Conference on Sustainable Energy and Environment, 2006.

[38] *Poly crystalline silicon solar cells*. Available: http://en.wikipedia.org/wiki/Polycrystalline_silicon

[39] *SMA solar technology, Sunny boy 2100TL*. Available: http://files.sma.de/dl/1348/CEI0-21_B-IA-it-en-de-20.pdf

[40] *SMA solar technology, Sunny sensor box* Available: http://www.sma-america.com/products/monitoring-control/sunny-sensorbox.html

[41] S. R. Best, J. A. Rodiek, and H. W. Brandhorst, "Comparison of solar modeling data to actual PV installations: Power predictions and optimal tilt angles," in *Photovoltaic Specialists Conference (PVSC), 2011 37th IEEE*, 2011, pp. 001994-001999.

[42]   B. Mather and R. Neal, "Integrating high penetrations of PV into Southern California: Year 2 project update," in *Photovoltaic Specialists Conference (PVSC), 2012 38th IEEE*, 2012, pp. 000737-000741.

[43]   *SMA solar technology, Sunny webbox*. Available: http://www.sma-america.com/products/monitoring-control/sunny-webbox.html

[44]   *SMA solar technology, Sunny central 630HE*. Available: http://www.proinso.net/pub/doc/File/ingl/sc630he.pdf

[45]   A. Q. Malik and M. Asghar, "Estimation of atmospheric ozone for Association of South East Asian Nations (ASEAN) countries," *Renewable Energy,* vol. 12, pp. 193-202, 10// 1997.

VITA

Santisouk Phiouthonekham was born in Pakse district, Champasack province of Laos, in 1986. He has been awarded B.Eng in Electrical Engineering from National University of Laos (NUOL) in the academic year 2009-2010. He has been receiving the AUN/SEED-Net scholarship to study at Chulalongkorn University, in Thailand of year 2013. He has been awarded M.Eng in Electrical engineering from Power System Research Laboratory (PSRL) in 2015.

In the years of master study, he has submitted 3 international conference papers: (1) "Concept of PV Array Arrangement for Alleviating the Impact of Partial Shading: An Experiment and Simulations", The 37th Electrical Engineering Conference (EECON37), at 19-21 November 2014, pp. 337-340. (2) "The Impact of Mitigation of Partial Shading on PV Array Power Generation", The 2015 International Electrical Engineering Congress (iEECON2015), at 18-20 March 2015, pp. 267-271. (3) "Mitigating Impact of Partial Shading on Photovoltaic Array Configuration by Using Rearrangement", 12th International Conference on Electrical Engineering/Electronics, Computer, Telecommunications and Information Technology (ECTI-CON2015), at 24-27 June 2015.